

Alma Mater Studiorum – Università di Bologna

DOTTORATO DI RICERCA IN

Scienze ambientali: tutela e gestione delle risorse naturali

Ciclo XXII

settore scientifico: CHIM/12

TITOLO TESI

**Chemical characterization of atmospheric secondary organic aerosol
of biogenic and anthropogenic origin**

Presentata da : **Dott.ssa EMANUELA FINESSI**

Coordinatore dottorato:
Prof.ssa ELENA FABBRI

Tutore:
Prof. EMILIO TAGLIAVINI

Relatore:
Dott.ssa MARIA CRISTINA FACCHINI

Correlatore:
Dott. STEFANO DECESARI

Esame finale anno 2010

Acknowledgements

This doctoral thesis is based on the experimental work carried out at the Institute of Atmospheric Sciences and Climate of the National Research Council (ISAC-CNR) in Bologna, within the Atmospheric Chemistry group headed by Dr. Sandro Fuzzi. I would like to express my appreciation to him for having had the opportunity of this invaluable experience.

I gratefully acknowledge financial supports from the University of Bologna, ISAC-CNR, the Atmospheric Composition Change European Network of Excellence (ACCENT) and the European projects EUCAARI, MAP and PolySOA.

I am most grateful to Dr. Maria Cristina Facchini and Dr. Stefano Decesari for supervision and support during the preparation of this thesis. My work would not have been successful without their help and patience. I would like to thank them for always believing in me and encouraging me to push the limits.

I am very grateful to Prof. Emilio Tagliavini for believing in me from the beginning and for the helpful suggestions.

I warmly thanks present and past fellow colleagues which all contributed substantially to this work and in creating a cheerful atmosphere. My special thanks to Lara Giulianelli, Lorenza Emblico, Valeriana Mancinelli, Claudio Carbone, Fabio Moretti, Marco Paglione and Matteo Rinaldi.

I very much appreciate the unfailing help of Francesca Pollini and Francescopiero Calzolari.

I would like also to acknowledge all the people I worked with during the various field campaigns.

Finally, I warmly thanks my parents for having always support me!

Table of contents

Abstract.....	1
List of original publications	3
Introduction.....	5
Objectives of the study.....	8
1 Literature review	10
1.1 Aerosol particles	10
1.1.1 Size distribution	11
1.1.2 Chemical composition.....	13
1.2 Secondary organic aerosol	15
1.2.1 Organic aerosol source apportionment	17
1.2.2 Gas-to-particle partitioning and volatility basis set	18
1.2.3 Heterogeneous reactions	20
2 Experimental	21
2.1 Laboratory experiments	21
2.1.1 Laboratory-biogenic SOA production	24
2.1.2 Laboratory-anthropogenic SOA production	27
2.1.3 Organics loading in the chamber experiments.....	29
2.2 Field data.....	30
2.2.1 Mace Head	31
2.2.2 Hyytiälä.....	31
2.2.3 K-Pusztta.....	32
2.2.4 Cabauw.....	32
2.2.5 San Pietro Capofiume	33
2.2.6 Melpitz	33
2.3 Samples handling and analysis	35
2.3.1 Sampling methods.....	35
2.3.2 Analytical methods	36
3 Results.....	42
3.1 Terrestrial biogenic SOA	42
3.1.1 Alpha-pinene SOA.....	42
3.1.2 Low-concentration experiments.....	47
3.1.3 SOA generated from mixtures of terpenes.....	49
3.1.4 Effect of ageing on biogenic laboratory-SOA	53

3.2 Anthropogenic SOA.....	56
3.2.1 SOA formed by 1,3,5-trimethylbenzene.....	56
3.2.2 Comparison with TMB-SOA composition as predicted by models	61
3.2.3 Oligomerization reactions with methyl glyoxal.....	63
3.3 Comparison between ambient organic aerosol and laboratory-SOA.....	65
3.3.1 Ambient organic aerosol	65
3.3.2 Clusters analysis applied to ¹ H-NMR spectra of ambient organic aerosol.....	68
3.3.3 Relationship between functional group distribution and WSOC sources.....	72
3.3.4 Identification of biogenic SOA based on NMR spectral signatures observed in chamber experiments and at pristine forest sites	76
3.3.5 Ambient organic aerosol vs anthropogenic laboratory-SOA.....	81
3.3.6 Chemical classes of WSOCs.....	88
4 Conclusions.....	91
4.1 Terrestrial biogenic SOA	91
4.2 Anthropogenic SOA.....	92
Bibliography.....	94
List of frequently used abbreviations.....	106

Abstract

Atmospheric aerosols play a key role in many environmental processes at local and global scale affecting human health, visibility, air quality and the climate system. Worldwide, a major component of the total particulate mass is constituted by organic compounds. Primary organic aerosols are directly emitted in the atmosphere by combustion sources (e.g. fossil fuel combustion, biomass burning) or by wind-driven processes such as re-suspension of soil particles and sea-spray. Conversely, secondary organic aerosols (SOA) form by chemical reactions occurring in the atmosphere, including the oxidation of volatile organic compounds (VOCs) leading to less volatiles species which can condense onto pre-existing particles or form new particles, and as well by the chemical transformations of primary components in the particulate phase (ageing).

State-of-the-art global models estimate that SOA account for a significant fraction of atmospheric aerosol nevertheless these data remain extremely uncertain due to the lack of observations capable to discern natural and anthropogenic SOA from other aged organic aerosol types. A major limitation is given by the complex chemical composition, encompassing myriads of individual compounds, of atmospheric particulate organic matter.

In the present study, nuclear magnetic resonance (NMR) spectroscopy and liquid chromatographic methods were employed to investigate the chemical composition of SOA produced in simulation chambers by photo-oxidation and ozonolysis of atmospherically relevant biogenic and anthropogenic VOCs. The resulting spectroscopic and chromatographic data were then used to interpret the composition of ambient samples of atmospheric fine particulate matter collected at several sites in Europe, in order to determine the fraction of ambient aerosol organic mass accounted for by biogenic and anthropogenic SOA.

Laboratory biogenic SOA analyzed in this thesis were generated from terpene mixtures, including α/β -pinene, limonene, Δ^3 -carene, ocimene, β -caryophyllene and α -farnesene, as representative for VOCs emitted by conifer tree species, whereas one aromatic hydrocarbon having a high SOA formation yield (1,3,5-trimethylbenzene) was used as model anthropogenic SOA precursor.

Ambient samples containing SOA were collected in both unperturbed environments (Finnish boreal forest, Atlantic coast of Ireland) and polluted rural areas (Po Valley, Hungarian plain, Netherlands, Saxony)..

Among the employed analytical techniques, NMR spectroscopy provided “spectral fingerprints” for biogenic and anthropogenic SOA, which accounted for by the variability of the complex fraction of aerosol organic matter not resolvable at the molecular level. These fingerprints were obtained for

the samples of SOA generated in the reaction chambers, and were then compared to spectral types characterizing the ambient samples. The great variability of the ambient sample NMR composition was processed using multivariate statistical methods such as clusters analyses, positive matrix factorization (PMF) and non-negative matrix factorization (NMF), allowing to extract few spectral types (profiles). Based on the comparison with the fingerprints of SOA provided by the lab experiments, on the occurrence of tracer compounds and on ancillary informations, the spectral profiles extracted from the ambient samples were tentatively assigned to SOA and to other oxidized organic aerosol types, such as biomass burning products.

PMF analysis applied to a collection of NMR spectra of aerosol samples from the boreal forest provided one factor fitting unambiguously the NMR fingerprint obtained for biogenic SOA during reaction chamber experiments. Therefore the contribution of biogenic SOA to total organic particulate matter could be estimated for this environment.

By contrast, the comparison of the spectral profiles characteristic of polluted continental areas with the fingerprints of anthropogenic SOA obtained in lab experiments proved to be less successful, indicating that the reaction chamber experiments in this case were not fully representative of the atmospheric system.

These results suggest that NMR spectroscopy combined to statistical multivariate analysis can be profitably employed in source apportionment studies of atmospheric particulate organic matter into its source contributions.

List of original publications

- 2010 > **Primary and secondary organic marine aerosol and oceanic biological activity: recent results and new perspectives for future studies.** Rinaldi, M., S. Decesari, E. Finessi, L. Giulianelli, C. Carbone, S. Fuzzi, C. D. O'Dowd, D. Ceburnis and M.C. Facchini.
Submitted to Advances in Meteorology.
- 2009 > **Chemical composition of PM10 and PM1 at the high-altitude Himalayan station Nepal Climate Observatory - Pyramid (NCO-P) (5079 m a.s.l.).** Decesari, S., M. C. Facchini, C. Carbone, L. Giulianelli, M. Rinaldi, E. Finessi, S. Fuzzi, A. Marinoni, P. Cristofanelli, R. Duchi, P. Bonasoni, E. Vuillermoz, J. Cozic, J. L. Jaffrezo and P. Laj.
Accepted for publication on Atmospheric Chemistry & Physics Discussions.
- > **On the representativeness of coastal aerosol studies to open ocean studies: Mace Head – a case study.** Rinaldi, M., M. C. Facchini, S. Decesari, C. Carbone, E. Finessi, M. Mircea, S. Fuzzi, D. Ceburnis, M. Ehn, M. Kulmala, G. de Leeuw and C. D. O'Dowd.
Atmospheric Chemistry & Physics, 9, 9635-9646, 2009.
- > **Significant variations of trace gas composition and aerosol properties at Mt. Cimone during air mass transport from North Africa - contributions from wildfire emissions and mineral dust.** Cristofanelli, P., A. Marinoni, J. Arduini, U. Bonafè, F. Calzolari, T. Colombo, S. Decesari, R. Duchi, M. C. Facchini, F. Fierli, E. Finessi, M. Maione, M. Chiari, G. Calzolari, P. Messina, E. Orlandi, F. Roccatò, and P. Bonasoni.
Atmospheric Chemistry & Physics, 9, 4603-4619, 2009.
- 2008 > **Coastal and open ocean aerosol characteristics: investigating the representativeness of coastal aerosol sampling over the North-East Atlantic Ocean.** Rinaldi, M., M. C. Facchini, S. Decesari, C. Carbone, E. Finessi, M. Mircea, S. Fuzzi, D. Ceburnis, M. Ehn, M. Kulmala, G. de Leeuw and C. D. O'Dowd.
Atmospheric Chemistry & Physics. Discussions, 8, 19035-19062, 2008.
- > **An important source of marine secondary organic aerosol from biogenic amines.** Facchini, M. C., S. Decesari, M. Rinaldi, C. Carbone, E. Finessi, M. Mircea, S. Fuzzi, F. Moretti, E. Tagliavini, D. Ceburnis and C. D. O'Dowd.
Environmental Science & Technology, 42, 9116-9121, 2008.
- > **Primary submicron marine aerosol dominated by insoluble organic colloids and aggregates.** Facchini, M. C., M. Rinaldi, S. Decesari, C. Carbone, E. Finessi, M. Mircea, S. Fuzzi, D. Ceburnis, R. Flanagan, E. D. Nilsson, G. de Leeuw, M. Martino, J. woeltjen and C. D. O'Dowd.
Geophysical Research Letters, 35, L17814, doi:10.1029/2008GL034210, 2008.
- > **Combined Determination of the Chemical Composition and of Health Effects of Secondary Organic Aerosols: The POLYSOA Project.** Baltensperger, U., J. Dommen, M.R. Alfarra, J. Duplissy, K. Gaeggeler, A. Metzger, M.C. Facchini, S. Decesari, E. Finessi, C. Reinnig, M. Schott, J. Warnke, T. Hoffmann, B. Klatzer, H. Puxbaum, M. Geiser, M. Savi, D. Lang, M. Kalberer and T. Geiser.

Journal of Aerosol Medicine and Pulmonary Drug Delivery, 21, 1, 145-154, 2008.

- 2007 > **An anion-exchange high-performance liquid chromatography method coupled to total organic carbon determination for the analysis of water-soluble organic aerosols.** Mancinelli, V., M. Rinaldi, E. Finessi, L. Emblico, M. Mircea, S. Fuzzi, M. C. Facchini, S. Decesari.
Journal of Chromatography A, 1149, 2, 385-389, 2007.

Introduction

Atmospheric aerosol particles play a significant role in a variety of environmental issues at both regional and global scales, influencing health, air quality and climate. Aerosols scatter and absorb solar and terrestrial radiation, and influence cloud formation thus affecting the radiative balance in Earth's atmosphere (IPCC, 2007; Ravishankara, 2005). Moreover it is now well established that the exposure to submicron aerosol particles is associated to damaging effects on respiratory and cardiovascular systems (Pope and Dockery, 2006, Davidson et al., 2005).

Worldwide organic compounds are a major component of atmospheric submicron particulate matter, accounting for up to 90% of aerosol mass (Kanakidou et al., 2005). Despite much efforts dedicated in the last two decades, only a minor fraction of the organic aerosol mass has been identified at molecular level due to its extreme chemical complexity. Consequently the effects of organic particulate matter remain highly uncertain as highlighted by several reviews (Poschl, 2005; Fuzzi et al., 2006; Goldstein and Galbally, 2007; Rudich et al., 2007).

Organic aerosols are either emitted directly into the atmosphere as primary organic aerosol (POA) or form in the atmosphere as secondary organic aerosol (SOA) due to the photochemical conversion of gaseous precursors (Pankow, 1994; Kroll and Seinfeld, 2008). SOA have recently gained much attention because current models estimate that they account for a dominant fraction of the total organic particulate mass (Baltensperger et al., 2005; Lanz et al., 2007). Nevertheless current estimates of global SOA production remain extremely approximate due to the lack of observations capable to discern between the various SOA sources.

SOA is formed in the atmosphere by transformations of gaseous precursors emitted from both biogenic and anthropogenic activities. On a worldwide basis volatile organic compounds (VOCs) emitted from biogenic sources exceed up to ten times those from anthropogenic sources, however in urban areas anthropogenic VOCs often dominate (Calvert, 2002; Atkinson and Arey, 2003). Alkanes, alkenes, aromatic hydrocarbons and oxygenated compounds are the major classes of the non-methane VOCs typically released from vehicle exhausts, industrial scale combustion, solvents usage, refineries and petrochemical facilities (Lewis et al., 2000). In polluted urban environments anthropogenic emissions include up to 40% of aromatic hydrocarbons (Smith et al., 1999; Molina et al., 2007). Thus the photochemical processing of primary aromatic hydrocarbons can contribute significantly to the production of secondary pollutants in these areas, most notably tropospheric ozone and SOA (Derwent et al., 2003; Derwent et al., 2007a).

Although major efforts have been made in identifying key biogenic and anthropogenic SOA precursors, significant gaps still remain in understanding the formation mechanisms, composition and properties of SOA (Hallquist et al., 2009).

Recent combined experimental and modelling studies have investigated the formation of SOA from the photo-oxidation of several simple aromatic hydrocarbons (e.g. alkyl benzenes such as toluene, xylenes, trimethylbenzenes and their analogues) and of terpenoids (e.g. isoprene, α/β -pinene, limonene, etc.), obtaining a considerable amount of new data (Cao et al., 2007; Cao et al., 2008; Johnson et al., 2004; Ng et al., 2007; Song et al., 2007; Metzger et al., 2008; Rickard et al., 2009). Moreover, the aromatic degradation as represented in the Master Chemical Mechanism (MCM) was recently updated to better fit against smog chamber data (Bloss et al., 2005; EXACT project and references therein). Although the research has been quite active so far significant deficiencies still remain. It was shown for example that models strongly under-estimate the observed production of SOA unless to increase the absorptive partitioning coefficients and these observations were generally interpreted in terms of significant occurrence of condensed-phase association reactions (Johnson et al., 2005). Conclusions from such works have inferred an important role for addition processes involving reactive aldehydes (e.g. formation of peroxyhemiacetals from the reaction of aldehydes with organic hydroperoxides). Few years before Jang (2002) had presented the first evidence that small volatile organic compounds increase the mass of acidic particles by forming low-volatility condensation products and after that several authors showed that high-molecular-weight compounds (with masses up to 1000 Da) are present in laboratory SOA generated from both biogenic as well anthropogenic precursors (Kalberer et al., 2004; Gross et al., 2006; Surratt et al., 2006; Tolocka et al., 2004; Iinuma et al., 2004; Gao et al., 2004; Reinhart et al., 2007). On the basis of the proposed formation pathways (i.e. heterogeneous hydration and polymerisation of low-molecular-weight aldehydes following their transfer from the gas phase) oligomeric structures have been hypothesized for these high-molecular-weight compounds. Kalberer et al. (2004) found that up to 50% of the total SOA mass formed during the photooxidation of 1,3,5-trimethylbenzene can be attributed to oligomers.

In ambient aerosol samples macromolecular substances with spectral characteristics similar to those of humic and fulvic acids (and thus named HULIS, humic-like substances) were first detected by Havers (1998). Hulis were found to be the major contributors (20-50%) to the water-soluble organic aerosol at urban and rural sites in Europe (Facchini et al., 1999a; Zappoli et al., 1999; Krivácsy et al., 2001; Kiss et al., 2003; Limbeck et al., 2005). The origin of these macromolecular substances was tentatively assigned to biomass burning (Facchini et al., 1999a; Hoffer et al., 2004) although their structures and the mechanisms of their formation are still highly speculative (Graber and

Rudich, 2006). Thus exists an urgent need to know how the structures of HULIS found in ambient compare with those of oligomers found in laboratory-generated particles.

Elucidation of SOA chemical composition challenges in many way the analytical techniques currently adopted and a number of reviews has been published in recent years (McMurry, 2000; Rudich et al., 2007; Hoffmann and Warnke, 2007).

Attempts to clarify SOA composition at molecular level (with GC-MS analysis often providing the foundation) supplied no more than 15-30% of the total SOA mass (Forstner et al., 1997; Cocker III et al., 2001; Hamilton et al., 2003; Edney et al., 2005; Surratt et al., 2006). Moreover, with much research geared to evaluate how different experimental conditions affect the physical properties of the laboratory-generated aerosol (e.g. yields, hygroscopicity, etc.), to date few studies have reported the corresponding aerosol chemical composition (Cocker III et al., 2001; Kleindienst et al., 2003; Sax et al., 2005).

Spectroscopic techniques such as aerosol mass spectrometry (AMS), nuclear magnetic resonance (NMR) spectroscopy and Fourier transform infrared (FT-IR) spectroscopy, bypass the constraints of molecular speciation looking to the integral chemical features of the unresolved mixtures of myriads of oxidized compounds which characterise processed aerosol particles.

Nuclear magnetic resonance (NMR) spectroscopy techniques has been profitably used to gain information on the average functional distribution of SOA (Decesari et al., 2001; Fuzzi et al., 2001; Tagliavini et al., 2006; Moretti et al., 2008). This technique has been used in numerous studies, including source apportionment (Decesari et al., 2007), having the potential to separate biomass burning from marine and secondary organic aerosol.

Aerosol mass spectrometry is now widely used for on-line measurements of the aerosol chemical composition and data are generally reported as sulfate, nitrate, ammonium, chloride and organic contents (Allan et al., 2003; Jimenez et al., 2003). Moreover statistical multivariate techniques combined to AMS data can be used to identify components in the total OA spectra (Zhang et al., 2005a, b; Lanz et al., 2007, 2008, Jimenez et al., 2009).

Objectives of the study

In this work has been investigated the chemical composition of SOA produced in smog chambers by photo-oxidation and ozonolysis of atmospherically relevant biogenic and anthropogenic volatile organic compounds (VOCs). Ambient samples containing SOA and collected in both pristine forested and polluted environments were also analyzed with the aim of comparison with the smog chamber data. Ambient sampling sites were mainly selected on the basis of their different environmental typology in order to possibly use them as surrogates for different sources of carbonaceous aerosol present in polluted and natural background in Europe.

Laboratory-SOA analyzed within this thesis were generated from terpene mixtures, including α/β -pinene, limonene, Δ^3 -carene, ocimene, β -caryophyllene and α -farnesene, as representative for VOCs emitted by conifer tree species, whereas a single aromatic hydrocarbon (1,3,5-trimethylbenzene) was used as model of anthropogenic gaseous pollutants. Laboratory-SOA composition was investigated in different ranges of precursor concentration and in different photochemical conditions. Moreover in order to investigate the laboratory-SOA chemical composition in parallel with their photochemical aging, two samplings were generally performed in subsequent moments of each chamber experiment.

A suite of spectroscopic and chromatographic methods were employed to chemically characterize the laboratory-SOA and the ambient organic aerosol samples.

The analytical methods included determination of Total Carbon (TC) and Water-Soluble Organic Carbon (WSOC), the speciation of WSOC into main chemical classes on the basis of their acidic properties and characterization of WSOC by Proton Nuclear Magnetic Resonance ($^1\text{H-NMR}$) spectroscopy for functional group analysis.

A recently set up anion exchange HPLC method was employed for quantitatively resolving WSOC into the following main chemical classes: neutral compounds (N), mono- and di-acids (MDA) and polyacids (PA), the latter including HULIS.

$^1\text{H-NMR}$ spectroscopy in D_2O solution was exploited for functional group characterization of the water soluble organics. The resulting series of $^1\text{H-NMR}$ spectra was further processed by a variety of multivariate statistical methods such as clusters analyses, positive matrix factorization (PMF) and non-negative matrix factorization (NMF), with the aim to identify spectral profiles featuring the different SOA sources through the comparison with the reference spectra provided by laboratory experiments.

In summary, the laboratory experiments provided the spectral fingerprints for biogenic and anthropogenic SOA that were eventually used for the interpretation of field data.

1 Literature review

This section provides a survey of the sources and nature of tropospheric aerosols with a focus on secondary organic aerosols. Primary sources of organic aerosols are described first, followed by an overview of atmospheric processes responsible for the formation and transformation of secondary organic aerosols starting from gaseous compounds.

1.1 Aerosol particles

Aerosols are defined as colloidal systems of liquid or solid particles suspended in gas phase, with particles diameters in the range of 10^{-9} - 10^{-4} m. The lower size limit is represented by molecules or clusters of molecules, while the upper limit corresponds to particles or droplets with a high settling rate (Seinfeld and Pandis, 1998). In atmospheric sciences, the term aerosol refers usually to solid particles whereas cloud droplets are considered a distinct system.

Aerosol particles are made of a large number of chemical compounds originating from both natural and anthropogenic sources. which consequently determine their chemical composition, size and shape characteristics (fig. 1). Natural sources include wind-driven processes such as re-suspension of soil particles and sea-spray, combustion processes such as forest fires, volcanic eruptions and finally emissions from vegetation. Several human activities, such as, e.g., combustion of fossil fuels, domestic heating, traffic-related suspension of road-dust, represent significant sources of atmospheric particulate matter.

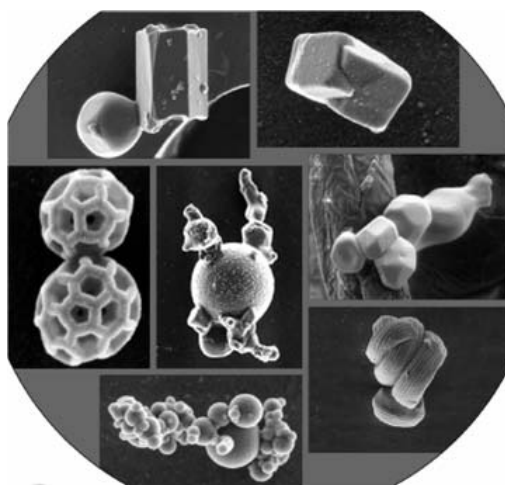


Figure 1. Examples of common aerosol shapes and compositions as observed by scanning electron microscopy, SEM (figure taken by Poschl, 2005).

1.1.1 Size distribution

The atmosphere, either in urban or in remote areas, contains significant amount of aerosol particles, with concentrations sometimes as high as 10^7 - 10^8 cm^{-3} . The diameters of these aerosol particles spans from few nanometers to tens of micrometers. Nevertheless, particles having aerodynamic diameters smaller than $10 \mu\text{m}$ dominate the size spectrum, accounting for most of the total aerosol particles (on either number and mass basis).

As a result of particle formation and removal processes, the atmospheric aerosol size distribution is characterized by a number of modes, i.e. different populations of particles (Fig. 2).

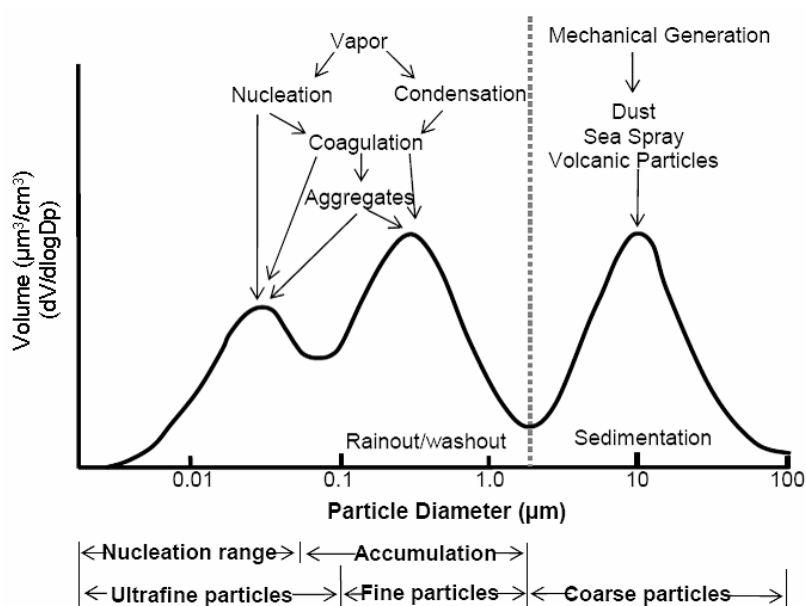


Figure 2. Schematic representation of tropospheric aerosol size distribution on number concentration basis. (adapted from Seinfeld and Pandis, 2006)

These modes are approximated to log normal distributions and are generally found in to the following size ranges (Whitby, 1978):

Nucleation mode ($D < 0.01 \mu\text{m}$);

Aitken mode ($0.01 < D < 0.1 \mu\text{m}$);

Accumulation mode ($0.1 < D < 1 \mu\text{m}$);

Coarse mode ($D > 1 \mu\text{m}$).

Nucleation and Aitken particles are also referred as ultrafine particles. Even if the ultrafine aerosols dominate the number concentration, they contribute to a small fraction of total particle mass concentration.

Most of the mass of fine particles, defined as aerosols with aerodynamic diameter lower than 2.5 μm , is accounted for by the accumulation mode. Coarse particles are defined as those having aerodynamic diameter larger than 1 μm and most of their mass is generally measured below 10 μm .

Fine and coarse particles differ in respect to production mechanisms and sinks.

Coarse particles are the result of mechanical processes such as erosion or re-suspension of mineral dust, and of biological material, such as plant debris, pollen, spores, etc.. Other sources of coarse aerosols include traffic emissions, resuspension of road dust, and the natural production of seasalt particles due to sea spray over oceanic regions. Coarse aerosols are removed from the atmosphere essentially by sedimentation.

Conversely, fine particles are mainly produced by secondary processes such as gas-to-particle conversion mechanisms and by primary combustion sources. The nucleation mode is the result of nucleation of new particles from rapid gas condensation. This occurs during the rapid cooling of an exhaust upon dilution in the background air, but may happen also at ambient temperature through photochemical reactions. The Aitken mode results from condensation of vapors onto nucleation mode particles and from their coagulation, as well as from primary combustion emissions. In turns, the accumulation mode typically results from prolonged condensation of vapors on Aitken particles and from the formation of particle mass by chemical reactions in non-precipitating cloud droplets. Since sedimentation is not effective for fine aerosols and coagulation is too slow for aerosol $> 0.1 \mu\text{m}$, particles in the accumulation mode tend to accumulate in the atmosphere.

Since this thesis deals with organic aerosols of secondary origin, the chemical analyses have been focussed on fine particles.

1.1.2 Chemical composition

Tropospheric aerosol chemical composition is characterized by a great spatial and temporal variability, reflecting the variety of sources and transformation processes. In general, aerosol particles consist of complex mixtures of inorganic and carbonaceous species, the most important classes being inorganic water-soluble salts such as sulfates, nitrates, ammonium salts and sea salt, soluble and insoluble carbonaceous material, and insoluble inorganic compounds from soil particles and combustion ash.

Carbonaceous particles are found in the troposphere as elemental (black) carbon (EC), organic carbon (OC) and carbonate carbon, the latter being negligible in the submicron size range. Produced solely by combustion processes, elemental carbon is a typical primary aerosol component. EC strongly absorbs light and has been associated with poor visibility (Bond and Bergstrom, 2006). Organic carbon is formed by both primary sources and gas-to-particle conversion (Castro et al., 1999).

Aerosol compounds derived from combustion or from gas-to-particle conversion, such as sulphate, ammonium, elemental and organic carbon, are found predominantly in fine particles whereas coarse particles are generally associated with sea salt and crustal species emitted by mechanical processes at the Earth surface. However, heterogeneous chemical reactions at particle surface may lead some compounds, like nitrate, to condense on both fine and coarse modes. An overview of the average chemical composition of European tropospheric aerosols in the different size ranges has been published by Putaud and co-workers (2003) and more recent studies have provided detailed phenomenologies of the aerosol chemical composition for many specific European sites.

Organic compounds are widespread in all areas and represent a large, sometimes even dominant, fraction of atmospheric fine particles accounting for 20-90% of aerosol mass in the lower troposphere (Kanakidou et al., 2005; Zhang et al., 2005; Jimenez, 2009).

Although a substantial amount of new data on organic aerosol has been provided in the last decade, the current understanding of OA chemical composition, sources and formation mechanisms remains very limited (Fuzzi et al., 2006).

Organics in the fine fraction can result either from primary emissions due to combustion processes at high temperature or from VOC oxidation and gas to particle conversion mechanisms (Kroll and Seinfeld, 2008; Zhang et al., 2007), while in the coarse fraction it can originate also from biological debris (Jacobson et al., 2000; Jaenicke et al., 2005). Spray of organic-rich liquid surfaces may inject primary organic particles also in the submicron mode. Such mechanism can contribute to the

formation of fine organic particles over high-biologically productive oceanic waters (O'Dowd et al., 2004).

1.2 Secondary organic aerosol

Ambient organic aerosols (OA) comprise either primary organic aerosol (POA, particle mass directly emitted into the atmosphere from the sources) and secondary organic aerosol (SOA, particle mass formed in the atmosphere due to the photochemical conversion of gaseous precursors) (Pankow, 1994; Seinfeld and Pankow, 2003; Kroll and Seinfeld, 2008).

SOA mass is generated in the atmosphere in various ways: a) low-volatility compounds can be formed in the gas phase and condense onto pre-existing particles or lead to the formation of new particles; b) it can also be formed by chemical transformation of primary components in the condensed phase; and c) as well chemical aging (transformation) of atmospheric aerosols can lead to the formation of multiple generations of secondary chemical components.

Organic aerosol originate from a wide range of both natural and anthropogenic sources including combustion of fossil fuels, direct injection of un-burnt fuel and lubricants, industrial emissions, plant matter, biomass burning, and biogenic emissions (Jacobson et al., 2000).

Current models estimate that secondary organic aerosol account for a dominant fraction of the total organic particulate mass (Baltensperger et al., 2005; Lanz et al., 2007; Robinson et al., 2007).

Recent estimations of primary and secondary, biogenic and anthropogenic emissions are reported in the table below (tab. 1). Nevertheless the relative contribution of POA and SOA to the overall OA budget remains controversial due to the persistent discrepancies between measured OA concentrations and predictions of atmospheric chemistry models.

In particular, the chemical and physical processes associated with SOA formation and evolution are complex.

	Mass emission			Mass Burden	Number Prod.	Number Burden
	"Best guess"	Min	Max			
		Tg a ⁻¹		Tg	a ⁻¹	
<i>Carbonaceous aerosols</i>						
Primary organic (0–2 µm)	95	40	150	1.2	–	310 · 10 ²⁴
Biomass burning	54	26	70	–	7 · 10 ²⁷	–
Fossil fuel	4	3	9	–	–	–
Biogenic	35	15	70	0.2	–	–
Black carbon (0–2 µm)	10	8	14	0.1	–	270 · 10 ²⁴
Open burning and biofuel	6	5	7	–	–	–
Fossil fuel	4.5	3	6	–	–	–
Secondary organic	28	2.5	83	0.8	–	–
Biogenic	25	2.5	79	0.7	–	–
Anthropogenic	3.5	0.05	4.0	0.08	–	–
<i>Sulfates</i>	200	107	374	2.8	2 · 10 ²⁸	–
Biogenic	57	28	118	1.2	–	–
Volcanic	21	9	48	0.2	–	–
Anthropogenic	122	69	214	1.4	–	–
<i>Nitrates</i>	18	12	27	0.49	–	–
<i>Industrial dust, etc.</i>	100	40	130	1.1	–	–
<i>Sea salt</i>						
<i>d</i> < 1 µm	180	60	500	3.5	7.4 · 10 ²⁶	–
<i>d</i> = 1–16 µm	9940	3000	20,000	12	4.6 · 10 ²⁶	–
Total	10,130	3000	20,000	15	1.2 · 10 ²⁷	27 · 10 ²⁴
<i>Mineral (soil) dust</i>						
< 1 µm	165	–	–	4.7	4.1 · 10 ²⁵	–
1–2.5 µm	496	–	–	12.5	9.6 · 10 ²⁵	–
2.5–10 µm	992	–	–	6	–	–
Total	1600	1000	2150	18 ± 5	1.4 · 10 ²⁶	11 · 10 ²⁴

Table 1. Particles emission/production burdens estimated for the year 2000 (taken from Andreae and Rosenfeld, 2008)

1.2.1 Organic aerosol source apportionment

The organic source apportionment problem has been approached by numerous techniques.

A frequently adopted method to estimate primary and secondary OA has been to use the ratio between elemental and organic carbon (EC/OC) measured on aerosol filter samples (Turpin and Huntzicker, 1991).

An other widely adopted approach to apportion OA is the use of molecular markers, e. g. detected by GC-MS, with a chemical mass balance (Schauer et al., 1996). Several sources with unique markers can be identified, but source profiles must be known a priori and in general only primary OA sources are accounted for by this method.

Recently have received much attention techniques based on carbon isotopic ratios ($^{14}\text{C}/^{12}\text{C}$) but they have very low time resolution (many hours to several days to collect enough material for the analyses) and overall can identify only few categories of sources (Szidat et al., 2006).

The last years have seen the development of a new generation of real-time aerosol chemical instrumentation based on mass spectrometry or ion chromatography, noticeably aerosol mass spectrometers (AMS) and particle in to liquid sampler (PILS) (Sullivan et al., 2004; DeCarlo et al., 2006; Canagaratna et al., 2007; Murphy et al., 2007). AMS produce ensemble average spectra for organic species and several methods (PCA, PMF) have been applied to deconvolve them into their principal components. The resulting main factors were commonly identified as hydrocarbon-like organic aerosol (HOA) and oxygenated organic aerosol (OOA) and were strongly linked to primary and secondary organic aerosol (POA and SOA). More advanced source apportionment methods further separate OOA in different types.

Other spectroscopic techniques such as nuclear magnetic resonance and infrared spectroscopies (NMR and FTIR) have been used aiming to OA source apportionment. In particular NMR spectroscopy allowed to separate biomass burning from marine and secondary organic aerosol (Decesari et al., 2007)

1.2.2 Gas-to-particle partitioning and volatility basis set

The most commonly studied mechanism of SOA formation is the oxidation of volatile organic compounds (VOCs), forming products with lower volatility that subsequently partition onto the condensed phase. Nevertheless temperature reduction, as well as reactive uptake via heterogeneous reactions and adsorption of chemical species, also shift species from the gas to particle phase.

A fundamental concept underlying the current SOA modelling concerns the treatment of the volatility of its components, including those present entirely in the condensed phase (non-volatile organics), as well as those that may be present in both the gas and the particle phase (semi-volatiles organics). The adopted definition of semi-volatile organic is quite broad involving saturation vapour pressures spanning seven orders of magnitude (Donahue et al., 2006).

Basically, SOA is thought as composed predominantly by semi-volatile organics and consequently SOA formation can be described by gas-particle partitioning. The theoretical foundations on partitioning have been developed by Pankow in the 1990s (Pankow, 1994a, 1994b). In the Pankow's partitioning theory each compound is described by an equilibrium partitioning coefficient $K_{p,i}$ ($\text{m}^3/\mu\text{g}$), or equivalently by its inverse, the saturation vapour concentration C_i^* ($\mu\text{g}/\text{m}^3$):

$$\frac{C_i^p}{C_i^g} = K_{p,i} C_{OA} = \frac{C_{OA}}{C_i^*}$$

in which C_i^p is the mass concentration of the semi-volatile species in the gas phase, C_i^g is the mass concentration of the semi-volatile species in the particle phase, and C_{OA} is the mass concentration of the total absorbing particle phase. Odum et al. (1996) extended for the first time this model to SOA formation, showing that SOA yield (the mass of aerosol formed per mass of hydrocarbon reacted) can be expressed in terms of the formation of a collection of semi-volatile compounds:

$$F_{OA} = \frac{\Delta M_{OA}}{\Delta M_{HC}} = C_{OA} \sum_i \frac{\alpha_i K_{p,i}}{1 + C_{OA} K_{p,i}} \equiv \sum_i \frac{\alpha_i}{1 + C_i^*/C_{OA}}$$

In principle SOA formation can be calculated by carrying out the summation over all the semi-volatile compounds formed within a given reaction but such degree of details is unfeasible due to the large number of unknown compounds. Instead two surrogate products ($i=2$) have been traditionally used to represent the SOA formation (fig.) (Seinfeld and Pankow, 2003; Keywood et al., 2004; Kanakidou et al., 2005; Chan et al., 2007).

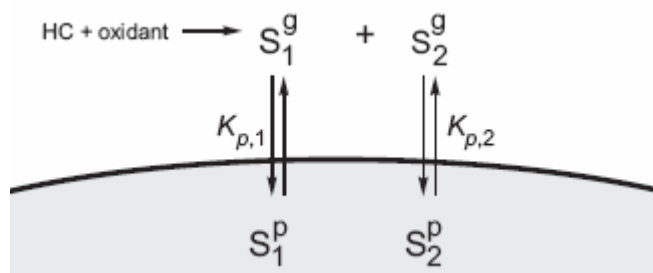


Figure 3. Schematic representation of the two-product model of SOA formation (taken by Odum et al., 1996)

Recently Donahue and co-workers has proposed the use of a volatility basis set (VBS) to address this issue. The VBS approach is similar, though with a larger number of lumped semi-volatiles which span a wider range of prescribed vapour pressures (fig.4) (Donahue et al., 2006; Presto and Donahue, 2006; Pathak et al., 2007).

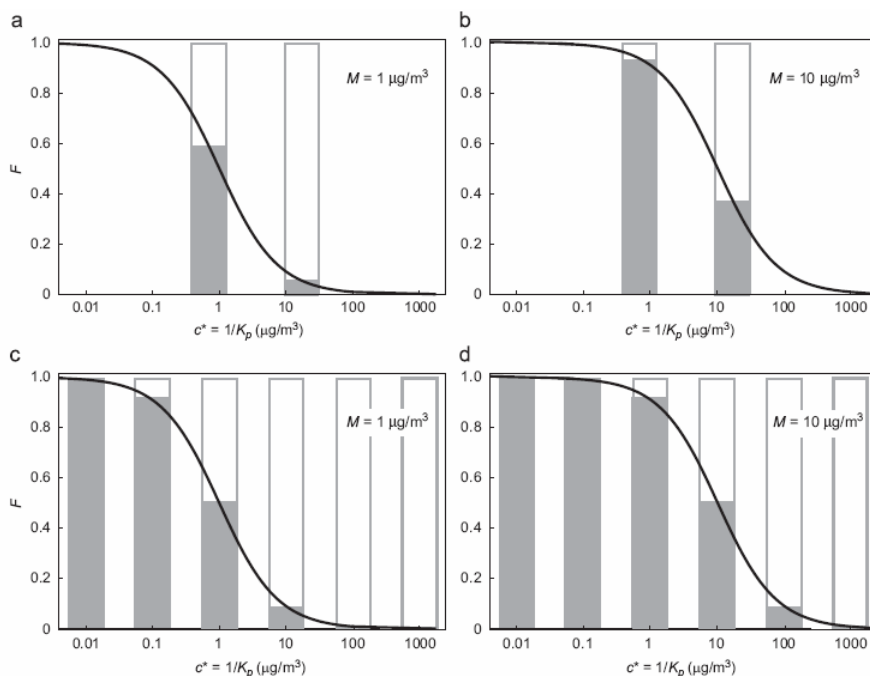


Figure 4. Representation of gas–particle partitioning for a complex mixture of semi-volatiles using (a–b) the two-product model, in which the semivolatiles are represented by two model compounds with experimentally determined vapor pressures, and (c–d) the volatility basis set, which employs a larger number of lumped compounds with prescribed vapor pressures. Partitioning at two mass loadings of organic aerosol is shown for each (figure taken from Kroll and Seinfeld, 2008)

1.2.3 Heterogeneous reactions

The occurrence of polymeric material has been observed in SOA generated by aromatic compounds such as trimethylbenzene (Karlberer et al., 2004). Furthermore measurements performed on TMB-SOA by laser desorption ionization-mass spectrometry (LDI-MS) have shown that a substantial fraction of TMB-SOA mass is composed of polymers (fig. 5).

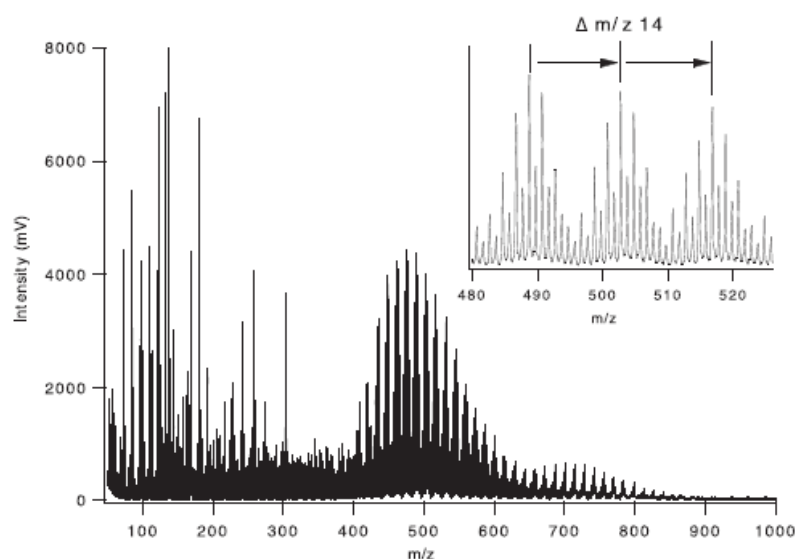


Figure 5. Figure taken from Karlberer et al., 2004. LDI-mass spectrum of TMB-SOA. In the inset is a detail from $480 < m/z < 625$ where the regular repetitive structure typical of polymers is visible.

In that study an acetal polymerization mechanism with methylglyoxal as the main monomer unit has been proposed to explain the formation of these high molecular mass compounds in the particle phase (fig. 6).

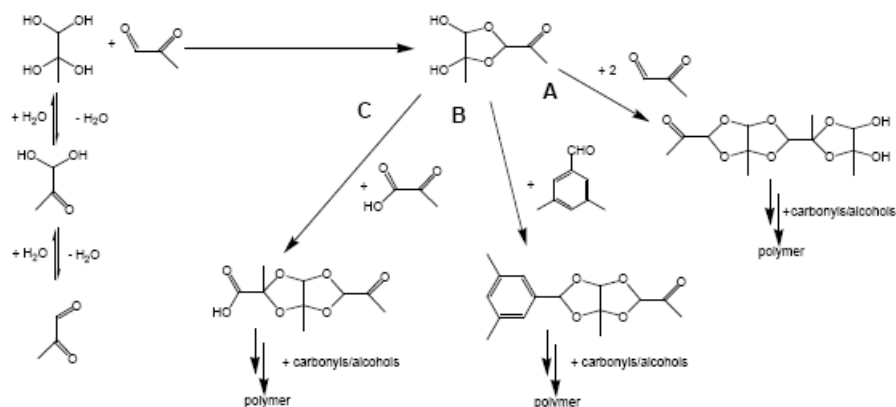


Figure 6. Chemical structure and formation reactions of the acetal polymerization mechanism proposed to explain the occurrence of polymers in TMB-SOA. Routes A, B and C include the incorporation into the polymer of: pure methylglyoxal, 3,5-dimethylbenzaldehyde and pyruvic acid, respectively. (figure taken from Karlberer et al., 2004).

2 Experimental

2.1 Laboratory experiments

Laboratory experiments are performed to study the chemistry and the physical properties of model systems representative of atmospheric aerosols. Most of the studies about SOA formation from VOCs oxidation are conducted in simulation chambers (i. e. static reactors or smog chambers), ranging in volume from 1 up to 300 m³ and designed to mimic atmospheric conditions as closely as possible. In order to generate SOA in controlled experimental conditions, the chambers are equipped with various instruments monitoring fundamental parameters such as gaseous precursors concentration, overall oxidant levels, temperature, relative humidity, light intensity and wavelength, etc.

Laboratory SOA characterized within the present work were produced in two different facilities, namely in the SAPHIR and PSI smog chambers. Technical data and instrumentations of the SAPHIR and PSI chambers are described in detail by Bohn and Paulsen papers respectively (Bohn et al., 2005 and Paulsen et al., 2005). A basic technical description of them follows in the table below.

	<i>chamber</i>	
	SAPHIR	PSI
<i>institute</i>	ICG-Jülich Forschungszentrum, Jülich, Germany	LAC-Paul Scherrer Institut , Villigen (Switzerland)
<i>volume (m³)</i>	270	27
<i>wall material</i>	Teflon-FEP, double wall	Teflon-FEP
<i>lighting</i>	sun	xenon arc lamps
<i>temperature range (°C)</i>	outside temperature	15-30

The SAPHIR facility is a very large outdoor chamber which uses the sun as natural light source (see picture SAPHIR). The wall material is chemically inert and UV transparent (80% of the outside actinic flux (290–420 nm) is generally available inside the chamber. It is also equipped with a louvre system which permits to modulate the radiation reaching the chamber up to dark conditions. In the indoor PSI facility, four xenon arc lamps mimic the sun's UV radiation supplying the energy required for the chemical reactions taking place in the chamber (see picture PSI chamber).

Synthetic SOA particles are generated in the chambers oxidizing a variety of organic gases by species such as the hydroxyl radical (OH), ozone (O₃) and nitrate radical (NO₃). OH is a universal oxidizing agent in the troposphere, being capable to react with all volatile organic compounds. Photolytical OH radical sources typically used in chambers are listed below:

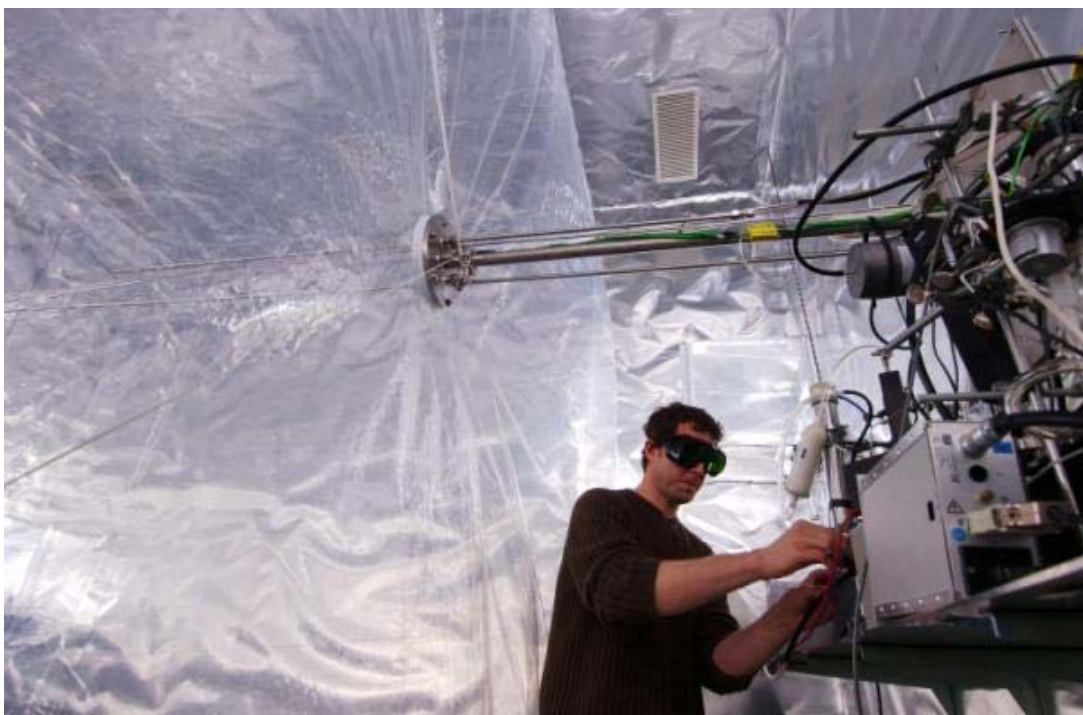


Laboratory-SOA characterized within the present work were mostly produced in NO_x photo-oxidation experiments, nevertheless few nitrous acid photo-oxidation and ozonolysis experiments were also performed.

Terpenes and aromatic hydrocarbons are respectively regarded as the main biogenic and anthropogenic compounds contributing to SOA mass, thus volatile precursors for the laboratory experiments were chosen among these chemical classes.



The outdoor chamber SAPHIR in Jülich, Germany.



The indoor chamber at the Paul Scherrer Institut in Villigen, Switzerland.

2.1.1 Laboratory-biogenic SOA production

The contribution of a given volatile compound to produce SOA in the atmosphere depends concurrently on its emission rate (atmospheric abundance), its chemical reactivity and on the volatility of its oxidation products. Among the hydrocarbons emitted by terrestrial vegetation, isoprene, monoterpenes (MT) and sesquiterpenes (SQT) are estimated to be the major source of secondary organic particulate matter on the basis of the three above-mentioned features (Kanakidou et al., 2005; Goldstein and Galbally, 2007).

Biogenic SOA analyzed in the present study were produced by photo-oxidation of α -pinene (α -pin), mixtures of monoterpenes, and mixtures of monoterpenes and sesquiterpenes. The laboratory experiments were performed at the PSI and SAPHIR facilities in the framework of the PolySOA and EUCAARI projects. The mixtures employed to generate biogenic SOA are representative for VOCs emitted typically by European boreal forests where conifers such as pine and spruce are the most dominant tree species with few contributes from broadleaf deciduous trees such as birch and larch (table 1). Biogenic SOA were mostly produced in NO_x photo-oxidation experiments, nevertheless few ozonolysis experiments were also conducted (table 2).

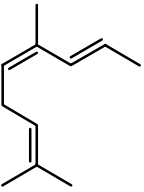
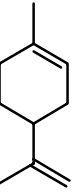
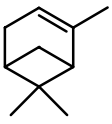
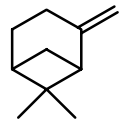
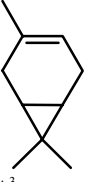
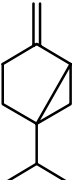
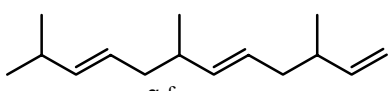
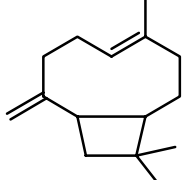
Table 1. Chemical structures of VOCs employed to generate biogenic SOA					
	ACYCLIC	MONOCYCLIC	BICYCLIC		
double bonds	n=3	n=2	n=1	n=2	
MT Monoterpenes C ₁₀	 cis-ocimene	 limonene	 α -pinene	 β -pinene	
			 Δ^3 -carene		
				 sabinene	
SQT Sesquiterpenes C ₁₅	 α -farnesene			 β -caryophyllene	

Table 2. Experimental conditions during the biogenic SOA particles generation experiments

date	VOCs	Oxidation conditions			VOC/NO _x
	α -pin (ppb)	NO _x =NO+NO ₂ (ppb)	HONO ^(a) (ppb)	O ₃ (ppb)	
09/10/2006	160	80		How much?	2
23/10/2006	160	80			2
24/09/2007	240	240			1
26/09/2007	240	240			1
28/09/2007	3 ^(b)		1.5		2
01/10/2007	240		1.5		160
03/10/2007	240		1.5		160
05/10/2007	3 ^(b)		1.5		2
MT mix wo Ocimene (ppb)					
06/06/2008	50	1.5		40	33
16/06/2008	100	0.95		43	105
MT mix (ppb)					
06/10/2007	50	1.7		75	29
04/06/2008	50	1.3		55	38
09/06/2008	100	1.8		40	56
13/06/2008	100	0.8		43	125
20/06/2008	100	0.15		180 ^(c)	
MT+ SQT mix (ppb)					
04/10/2007	55	1.05		60	52
31/10/2007	55	0.4		60	138
11/06/2008	55	1.5		35	37
18/06/2008	110	0.9		40	122
29/10/2007	55	1.70		80 ^(c)	

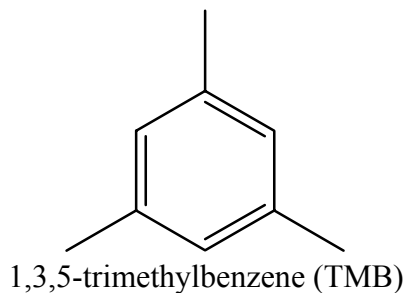
(a) concentration pumped continuously into the chamber at 2.0 lpm

(b) concentration kept constant throughout the experiment

(c) ozonolysis experiment (dark conditions)

2.1.2 Laboratory-anthropogenic SOA production

1,3,5-trimethylbenzene (TMB) was employed in laboratory experiments as single gaseous precursor representative for aromatic VOCs emitted by anthropogenic sources.



All the experiments performed to produce anthropogenic SOA were carried out at the PSI smog chamber in the frame of the EU-funded project PolySOA (web reference). In a typical photo-oxidation experiment, the humidification of the chamber to the desired humidity value (~50% relative humidity, RH) was achieved before the injection of the other components and after that, they were let to diffuse and mix for at least 30 min before the experiment was started by turning on the lights. The initial TMB concentration was almost always pretty high (1200 ppb) as well the NO_x level (600 ppb), except for few experiments where TMB initial level was 600 ppb and NO_x was 300 ppb. Hence most of the photo-oxidation experiments were carried out under high NO_x conditions with an initial VOC/NO_x ratio of 2 (table 3). The temperature in the smog chamber was kept constant at 20 ± C°.

Table 3. Experimental conditions during the anthropogenic SOA particles formation experiments.

exp.	date (dd/mm/yy)	TMB (ppb)	NO _x (ppb)	SO ₂ (ppb)	mean aerosol mass conc. ^a (µg/m ³)	
					initial stage	final stage
1	04/10/06	600	300	0.4	54	
2	06/10/06	1200	600	0.8	128	
3	11/10/06	1200	600	2	135	155
4	13/10/06	1200	600	2	162	159
5	18/10/06	1200	600	2	142	135
6	20/10/06	1200	600	2	160	160
7	19/10/07	1200	300	2	103	101
8	21/10/07	1200	300	2	108	101

^a Aerosol mass concentration from SMPS data assuming a density of 1 g cm⁻³ and spherical particles. Two averaged values are respectively given for the initial and final stages of the aerosol growth, corresponding to the filter sampling times in each experiment.

2.1.3 Organics loading in the chamber experiments

Over the last two decades, several laboratory experiments have been conducted to study the formation of SOA, constituting the basis to parameterize SOA formation and evolution in the real atmosphere. Laboratory studies must mimic the ambient conditions with specific attention to key parameters. For instance, the organics loading, i.e., the concentration of SOA inside the chamber, has been proved to be very important. In fact, it has been shown that laboratory loadings higher than those present in atmosphere favour the partitioning of slightly oxidized species which would otherwise remain in gas phase under atmospheric conditions (Duplissy et al., 2008). At the same time, the limited volume of the reaction chambers imply a minimum concentration of SOA inside to guarantee a sufficient amount of sample for the chemical analyses.

The organics loadings reached during the laboratory experiments considered in this thesis are shown in the graphic below. Different lines in the graph refer to distinct VOCs. Starting from the bottom are encountered values for TMB, α -pin, MT and SQT photo-oxidation experiments respectively. The three values in the upper line belong to the ozonolysis experiments. The organics loadings observed in ambient exceed very rarely $25 \mu\text{g}/\text{m}^3$ as reported by worldwide AMS data (Jimenez et al., 2009).

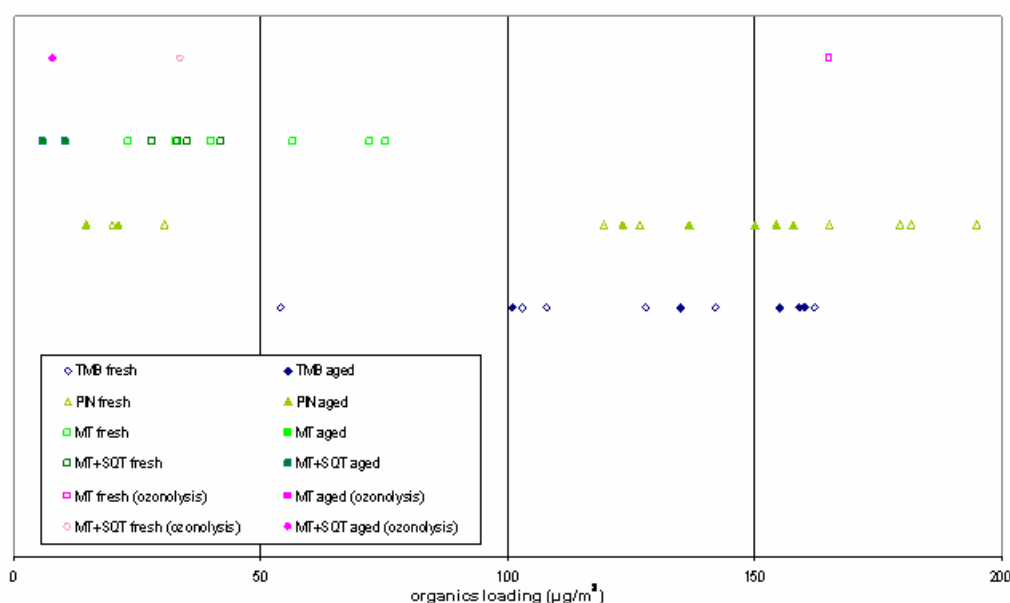


Figure 5. Mean aerosol mass concentrations calculated from SMPS data (assuming a density of 1 g cm^{-3} and spherical particles) and averaged upon the filter sampling times. The values are lumped in different lines depending on the precursors employed: starting from the bottom are listed TMB, α -PIN, MT and SQT photo-oxidation experiments. In the upper line are those of ozonolysis experiments. Empty and filled symbols stand respectively for the organics loading present in the initial and final part of each experiment.

2.2 Field data

Ambient aerosol samples analyzed within this thesis were mostly collected during various intensive field experiments set up in the frame of the EU-funded EUCAARI project. The joint-measurements campaigns were carried out at six European sites selected on the basis of their different typology of aerosol emission patterns and pollution levels. Referring to the criteria used by Van Dingenen and coworkers for Europe (Van Dingenen et al., 2004), e.g. the distance from pollution sources, the sites can be classified into: marine background, natural continental background, rural background, near-city background or urban background (table 4).

ID	site	position	altitude (m asl)	typology	operated by
MHD	Mace Head, Ireland	53° 19' N, 9° 53' W	5	marine background	National University of Ireland, Galway
HYY	Hyytiälä, Finland	61° 51' N, 24° 17' E	181	natural continental background	University of Helsinki
KPO	K-Pusztá, Hungary	46° 58' N, 19° 33' E	125	rural background	Hungarian Meteorological Service and ACUV
CBW	Cabauw, Netherlands	51° 18' N, 04° 55' E	60	rural background	KNMI
SPC	San Pietro Capofiume, Italy	44° 39' N, 11° 37' E	11	near-city background	ISAC-CNR and regional environmental protection agency
MPZ	Melpitz, Germany	51° 32' N, 12° 54' E	87	near-city background	Leibniz Institute for Tropospheric Research

Table 4. Synthetic description of the sites.

Intensive observing periods (IOP) of the field measurement campaigns are reported in the table 2 along with number and type of the collected samples.

site (year)	IOP		samples n°	aerosol type
	start exp. date	stop exp. date		
HYY (2007)	29/03/2007	18/04/2007	22	PM ₁
SPC (2008)	31/03/2008	20/04/2008	34	PM ₁ and PM ₁₋₁₀
CBW (2008)	08/05/2008	26/05/2008	30	PM ₁ and PM ₁₋₁₀
MPZ (2008)	01/05/2008	31/05/2008	15	PM _{2.5} -PM _{2.5-10}
MHD (2008)	17/05/2008	10/06/2008	7	PM _{1.5} -PM _{1.5-10}
KPO (2008)	26/05/2008	14/08/2008	10	PM _{2.5}
SPC (2009)	27/06/2009	15/07/2009	100 (29+71)	PM ₁ and PM ₁₋₁₀

Table 2. Sampling periods.

A more detailed description of the sites is reported in the following paragraphs.

2.2.1 Mace Head

The atmospheric research station of Mace Head is located on the west coast of Ireland, offering a westerly exposure to the North Atlantic ocean. The climate is prevalently dominated by maritime air masses: on average over 60% of air masses arrive to the site from a *clean sector* (180° through west to 300°). In fact, it has been shown that this site can be representative of clean background marine air (Rinaldi et al., 2009). By contrast, when easterly air masses reach the station, aerosols characteristic of the European pollution background are observed. More details on the station are available on the official web site (<http://macehead.nuigalway.ie/>).



Figure 2. Mace Head Atmospheric Research Station. Department of Experimental Physics National University of Ireland, Galway.

2.2.2 Hyytiälä

The Finnish Station for Measuring Forest Ecosystem-Atmosphere Relations (SMEAR II) is located in Hyytiälä, Finland. This forestry station is situated in the middle of a more than 40-years old Scots pine stand (*Pinus Sylvetris L.*) which surrounds homogeneously the site for about 200 m in all directions and it extends up to 1.2 km towards the North. Tampere is the largest city nearby and it is situated more than 60 km S-SW far. In fact, it has been shown that this site can be representative of the boreal coniferous forest. More details on the station are available on the official web site (http://www.mm.helsinki.fi/hyytiala/english/eng_index.htm).



Figure 3. Landscape surrounding the Hyytiälä forestry field station (SMEAR II). Faculty of Agriculture and Forestry, Helsinki University.

2.2.3 K-Puszt

K-Puszt is a central European site located in the middle of the Hungarian plain. The station is surrounded by coniferous forests spaced out with clearings. The station resides at 80 km south-east far from Budapest. The largest nearby town (Kecskemét, 110,000 inhabitants) is 15 km far from the station, S-E direction. Thus the site can be representative of the European rural background as well as more polluted air masses depending on the meteorological conditions.

2.2.4 Cabauw

The Cabauw Experimental Site for Atmospheric Research (CESAR) is located in flat rural area in the western part of The Netherlands. The North Sea is more than 50 km away from the site in the N-W direction. The region nearby the site is predominantly agricultural although the station is not very far from large cities such as Amsterdam and Utrecht. Hence the site offers the opportunity to study a variety of air masses from clean maritime to continental polluted ones. More details on the station are available on the official web site (<http://www.cesar-database.nl/About.do>).



Figure 4. Landscape surrounding the CESAR observatory. The Royal Netherlands Meteorological Institute.

2.2.5 San Pietro Capofiume

The Italian field station is located at San Pietro Capofiume in a flat rural area in the river Po Valley region. The Adriatic Sea is more than 60 km away from the site in the east direction. The closest large cities are Bologna and Ferrara which are each roughly 40 km far from the site. This region is overall characterized by a high population density and by intensive agricultural as well industrial activities. Moreover major highways cross this area. Hence according to EMEP (European Monitoring and Evaluation Programme under the Convention on Long-range Transboundary Air Pollution) conventions this site can be representative even for urban background air.



Figure 5. Atmospheric research station “G. Fea”, San Pietro Capofiume. ISAC-CNR.

2.2.6 Melpitz

The IFT-Melpitz ground-based research station is located in the river Elbe Valley in Germany. Melpitz is a small village surrounded by agricultural land interspersed by edges of forest and it is far from the city of Leipzig about 40 km in the southwest direction. Nevertheless major highways cross the region at a minimum distance of 1.5 km. Moreover during high pressure conditions dry air masses are transported from the north-east area where coal heated power plants and old industries with poor exhaust treatments still operate. Anyway air masses reaching the station come

predominantly from the south-west direction after crossing part of western Europe. Hence Melpitz can be described as a rural polluted continental site.



Figure 6. IFT-Melpitz atmospheric research station.

2.3 Samples handling and analysis

2.3.1 Sampling methods

Within this work aerosol samples have been prevalently collected on quartz micro fiber filters (QMA grade purchased by Whatman or Pall), except for few chamber experiments where Teflon substrates have been used, and then analyzed off-line. The quartz fiber filters were washed with Milli-Q water and fired for 1h at 800 °C before sampling in order to reduce their blank values. The Teflon substrates were as well cleaned with Milli-Q water but left to dry in a clean room for 24 h before sampling.

Atmospheric aerosols have been sampled by various high volume samplers depending on the instrument available on the site. During the intensive observing periods held in the SPC and CBW stations was employed a Dichotomous high volume sampler from MSP Corporation (Universal Air Sampler, model 310) working at a constant nominal air flow rate of 300 L/min. The Dichotomous sampler allowed to collect atmospheric aerosols in their PM₁ and PM₁₋₁₀ fractions. A Sierra Andersen high volume sampler, segregating PM_{1.5} and PM_{1.5-10} particles, was used in the MHD station. PM_{2.5} and PM_{2.5-10} fractions of atmospheric aerosol were obtained in the MPZ station using a Digital high volume sampler. In the HYY and KPO stations were employed two high volume samplers working at 600 and 850 L/min and configured to remove particles with aerodynamic diameter larger than 1 and 2.5 µm respectively.

Synthetic SOA particles formed in the chamber experiments were simply pumped to the filters sucking up the air inside the chamber at a flow rate of 10 or 20 L/min. Sampling times lasted typically two hours. Denuders (charcoal or XAD resins) upstream the filter holders were employed to remove gaseous organic compounds from the sampled air stream to prevent positive artefacts. A sampling tandem configuration consisting in the use two piled filters, one front (F) and one back up (BU) filter, in separate filter holders, was adopted when possible in order to assess negative sampling artefacts.

In order to investigate the laboratory-SOA chemical composition in parallel with their photochemical aging, two filters sets were generally collected in subsequent moments of each chamber experiments. Thus obtaining *fresh* SOA from the initial part and *aged* SOA from the final part of each experiment. The experiments conducted at the PSI smog chamber (specifically those

with α -pinene and 1,3,5-trimethylbenzene as gaseous precursors) lasted typically 8 hours: *fresh* SOA was roughly collected between the 4th and the 6th hour while *aged* SOA between the 6th and the 8th hour. In the case of SOA formed in the SAPHIR simulation chamber, typical aging experiments ran up to about 30 hours. A two-hours sampling was performed in the first day of the experiment, during the particles generation, while a second sampling was performed in the day after. In this way the *aged* SOA particles were actually subjected to a long time OH-radical exposure.

After sampling the aerosol samples were stored in a fridge at 4 ° C until the analyses.

2.3.2 Analytical methods

A scheme of the analytical protocol deployed to characterize the aerosol samples collected on quartz fiber filters (or in few cases on Teflon substrates) is reported below (fig.1). Overall a small portion of the samples was directly subjected to high temperature combustion analysis in order to measure their Total Carbon (TC) content, except for samples collected on Teflon substrates on which TC analysis is not feasible. The leftover filter portions underwent extraction with ultrapure mQ water (Millipore, 18.2 mOhm cm water resistivity): about 1 mL of mQ water per filter's cm² has been generally employed. The extraction procedure was performed using a ultrasonic bath on quartz fiber filters and by stirring on Teflon substrates: 60 minutes for the former and 30 minutes for the latter. After sonication, water extracts were filtered on PTFE membranes (pore size 0.45 μ m) in order to remove suspended particles. After filtration the water extract was split into aliquots devoted to the various analyses on the dissolved water soluble organic matter as schematically reported in figure 7. Additional analytical details will be reported in the following sections.

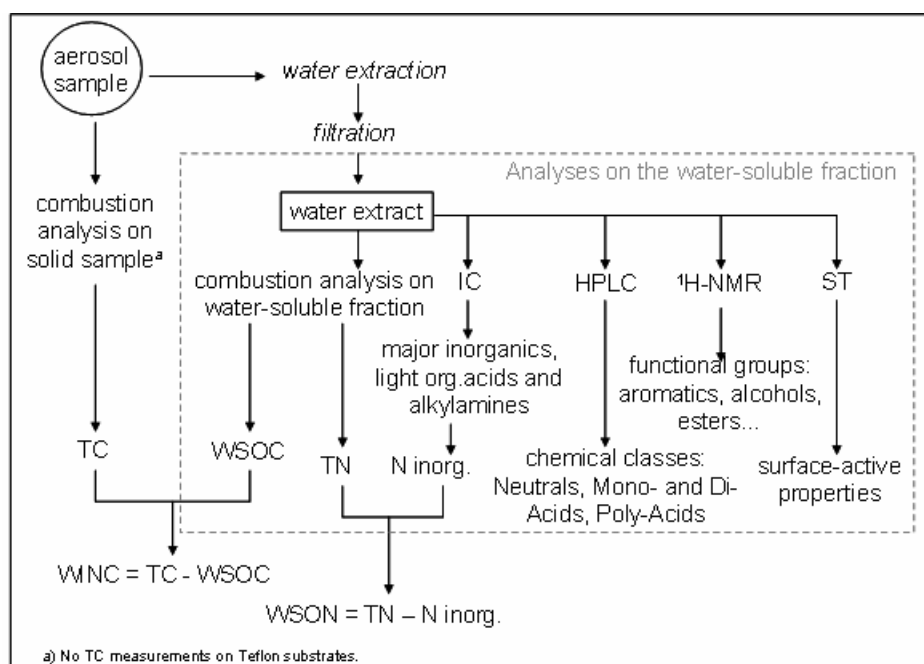


Figure 7. Scheme of the analytical protocol deployed to characterize aerosol samples.

2.3.2.1 Total Carbon (TC) analysis

Total carbon content was directly measured on a small portion of the quartz fiber filters (about 1 cm²) by evolved gas analysis. Measurements were performed by a Multi N/C 2100 elemental analyser (Analytik Jena, Germany) equipped with a furnace suited for solid samples. Inside the furnace samples were exposed to increasing temperature (up to 950 °C) in a pure oxygen carrier gas. Under these conditions all carbonaceous matter (Organic Carbon, Carbonate Carbon and Elemental Carbon) is converted in CO₂ (Gelencser et al., 2000). TC is measured as total evolved CO₂ by a non-dispersive infrared (NDIR) analyser. The instrumental detection limit was 0.2 µgC and the accuracy resulted better than 5% for 1 µgC.

2.3.2.2 Water Soluble Organic Carbon (WSOC) analysis

WSOC content was measured by the liquid module of the above-mentioned Multi N/C 2100 total organic carbon analyser. For each aqueous sample parallel measurements of carbonate carbon (CC) and total soluble carbon (TSC) were carried out. The measure of the TSC is performed by catalytic high temperature combustion in a pure oxygen carrier gas (up to 800 °C in presence of Pt as catalyst) and a NDIR detector. The measure of the CC content is provided by the acidification of the sample before its combustion. The difference between the measured total soluble carbon and inorganic carbon results in WSOC (Rinaldi et al., 2007). Replicate analysis of standard solutions

showed a reproducibility within 5% for both TSC and carbonate carbon at the concentrations typically employed for samples extracts (i.e. between 0.5 and 5 ppmC).

2.3.2.3 Ion Chromatography (IC)

The inorganic water soluble fraction of the ambient aerosol samples has been characterized by means of Ion Chromatography (IC). Inorganic ions (NH_4^+ , Na^+ , K^+ , Mg^{2+} , Ca^{2+} , Cl^- , NO_2^- , NO_3^- , SO_4^{2-}) were identified along with light organic acids ions such as acetate (Ace), formate (For), oxalate (Oxa) and methanesulfonate (MSA). Even light alkyl ammonium ions were identified such as mono-, di- and tri-methyl ammonium ions (MMA^+ , DMA^+ , TMA^+), and mono-, di- and tri-ethyl ammonium ions (MEA^+ , DEA^+ , TEA^+).

A Dionex instrument (ICS-2000) equipped with a conductivity detector, a gradient pump and a self-regenerating suppressor has been used to separate and quantify the above-listed ions. Anions were specifically analyzed by the ion chromatograph, equipped with IonPac AG11 2x50mm Dionex guard column, IonPac AS11 2x250mm Dionex separation column and ASRS ULTRA II self-regenerating suppressor. A solution of KOH was used as eluent. Its concentration increased from 0.1 mM to 38 mM, in a 25 minutes long run (0.1 mM for 8 min, 5 mM reached at 12 min, 10 mM at 17 min and 38 mM at 25 min). The flow rate was 0.25 mL/min. Cations were analyzed with the same ion chromatograph, equipped with IonPac CG16 3x50 mm Dionex guard column, IonPac CS16 3x250mm Dionex separation column and CSRS ULTRA II self-regenerating suppressor. The analysis were performed isocratically with a 30 mM solution of MSA as eluent held for 35 min. The flow rate was 0.36 mL/min.

The detection limit for the analysed inorganic ions corresponds to an average air concentration of 4 ng/m³, except for sodium, nitrite and calcium for which it is 45 ng/m³.

2.3.2.4 Water Soluble Organic Nitrogen (WSON)

The above-mentioned Multi N/C elemental analyser has been even employed to measure also the Total Soluble Nitrogen (TSN) content of the water-soluble fraction of the aerosol. The instrument's module for nitrogen analysis is equipped with a chemiluminescence detector to measure the NO_x evolved from the high temperature combustion (800 ° C, 100% O_2) of the samples. The elemental analyzer resulted sensitive to nitrogen regardless to its chemical form. TSN was quantified against calibration curves obtained using sodium nitrate as standard compound. The instrumental

reproducibility resulted very good (better than 2%) at concentration of 1 ppmN but increases at lower concentrations (8% at 300 ppbN).

Once determined the TSN, the Water Soluble Organic Nitrogen (WSON) content was calculated subtracting the inorganic nitrogen content derived by ion chromatography (i.e. the sum of nitrate, nitrite and ammonium).

2.3.2.5 WSOC separation by High Performance Liquid Chromatography (HPLC)

A new liquid chromatography method has been applied to simplify the initial complex mixture of water soluble organics into few main chemical classes according to their neutral/acidic character (Mancinelli et al., 2007). An anion exchange HPLC method coupled to WSOC analysis was specifically exploited to quantitatively resolving water soluble organics into: neutral compounds (N), mono- and di-acids (MA and DA), and poly-acids (PA, i.e. compounds carrying more than two carboxylic groups).

The analyses were performed on a HPLC instrument from Agilent (Model 1100), equipped with a TSK-GEL® DEAE-5PW column (7.5mm i.d. × 7.5 cm length, Tosoh Bioscience), an autosampler, UV detector and a fractions collector. The selected injection volume, flow rate and wavelength were respectively 1 mL, 0.7 mL/min and 260 nm. The mobile phase consisted of A) mQ water and B) a ClO₄⁻/PO₄³⁻ buffer solution at pH 7 (NaClO₄ 0.5 M, KH₂PO₄ 0.05 M, NaOH 0.044 M) whose composition changed towards an increasing ionic strength within the elution program. The mobile phase composition changed as follows: A 100 % isocratically from 0 to 8 min; first gradient from 8 to 15 min reaching B 10 %; B 10 % isocratically from 15 to 21 min; second gradient from 21 to 26 min reaching B 100 %; final gradient back to A from 26 to 31 min. N, MA, DA and PA compounds were subsequently eluted and collected on the bases of time intervals chosen depending on the minima between the UV peaks in the chromatogram (7-20 min for N, 20-23 min for MA, 23-30 min for DA and 30-37 min for PA). Avoiding organic additives, the mobile phase does not interfere with the measure of the dissolved organic carbon in the HPLC collected fractions thus allowing the direct WSOC analyses after the collection (before the elemental analysis PA fractions were acidified with 50 µL HCl conc. and purged with CO₂ free-air to remove the carbonates due to the mobile phase).

The instrumental detection limits of the NB, MA, DA and PA fractions were 2.2, 1.0, 1.3 and 3.2 µgC, respectively.

2.3.2.6 WSOC characterization by proton-Nuclear Magnetic Resonance ($^1\text{H-NMR}$) spectroscopy

$^1\text{H-NMR}$ spectroscopy in deuterium oxide (D_2O) solution was exploited to functional group characterization of water soluble organics. Aliquots of water extracts were dried under vacuum and re-dissolved in 650 μL D_2O . Sodium 3-trimethylsilyl-(2,2,3,3- d_4) propionate (TSP- d_4) was prevalently used as referred internal standard adding 50 μL of a TSP- d_4 0.05 % (w/w) solution in D_2O (1.455 μmol H belonging to the standard in the probe) following the protocol already tested by Decesari (Decesari et al., 2000; Tagliavini et al., 2006). In some cases methanol (MeOH) was used as alternative internal standard (0.5 μmol H belonging to the standard in the probe). The $^1\text{H-NMR}$ spectra were acquired with a Varian spectrometer working at 400 MHz (Mercury 400) in 5 mm probes. Mono-deuterated water (HDO) signal's pre-saturation was always performed nevertheless residuals were still appearing in few spectra in the region between 4.5-5.5 ppm.

At least 80 μg of carbon content has to be in the sample aliquot destined to $^1\text{H-NMR}$ experiments in order to achieve a good signal to noise ratio. Due to its limited sensitivity, $^1\text{H-NMR}$ spectroscopy has been rarely applied to the analysis of atmospheric aerosols, nevertheless this technique offers several advantages with respect to other techniques such as GC/MS, LC/MS or AMS.

In principle, $^1\text{H-NMR}$ spectroscopy can detect any protons belonging to the organic molecules, but it is mainly sensitive to protons attached to carbon atoms (i.e. H-C bonds) because, in aqueous solutions, the hydrogen atoms attached to oxygen and nitrogen atoms (e.g. H-O of carboxylic acids, alcohols and the H-N bonds of amines) are exchanged with the solvent and cannot be detected.

Then, sensitivity is higher for functional groups carrying more hydrogen atoms, i.e., it is higher for methyls than for methylenes or methynes, and it is higher for aliphatic than for aromatic compounds.

$^1\text{H-NMR}$ spectroscopy thus provides information about both the main structural units as well it is able to identify individual compounds. Moreover, it is not affected by the interference of inorganic compounds.

An important advantage of $^1\text{H-NMR}$ spectroscopy is that quantitative analysis is straightforward: the integrals of the peaks in $^1\text{H-NMR}$ spectra are proportional to the molar concentrations of hydrogen atoms within 15%. Then, a simple a-specific internal standard can be used for calibration (Derome, 1987; Braun et al., 1998).

The different bands of the spectra can be integrated providing molar concentrations of the organic hydrogen atoms associated with the various functional groups. To derive the molar concentrations of the functional groups, their stoichiometry is required, i.e., the H:C ratios.

Most of the signal in spectra of aerosol samples is accounted for unresolved bands rather than narrow peaks attributable to single compounds. On the basis of the range of frequency shifts (the so-called *chemical shift*, *ppm*) in which these bands occur, they can be attributed to different functional groups. Since there are a lot of overlaps between the characteristic chemical shifts of the various functional groups, the functionality that can be resolved unambiguously are limited to:

H-(C=O)R (> 9 ppm): aldehydic protons;

H-Ar (6.5-8.5 ppm): aromatic moieties;

H-C= (4.5-6.5 ppm): vinylic or (hemi)acetalic protons;

H-C-O (3.3-4.5 ppm): protons bound to oxygenated aliphatic carbon atoms such as alcohols and ethers;

H-C-C= (1.9-3.3 ppm): aliphatic groups adjacent to unsaturated carbon atoms such as carbonyls and carboxyls or benzylic protons;

H-C-C< (0.8-1.9 ppm): aliphatic groups bound to saturated carbon atoms.

3 Results

3.1 Terrestrial biogenic SOA

3.1.1 Alpha-pinene SOA

Here are present data on chemical characterization of biogenic SOA formed in photo-oxidation experiments with α -pinene. A complete list of the collected samples is reported in the table below.

exp. date	VOC		oxidants		sample ID		SOA mass. conc. ($\mu\text{g}/\text{m}^3$)	sampling volume (m^3)
	α -pin (ppb)	NO _x (ppb)	HONO (ppb)	front	back up			
09/10/2006	160	80		PIN_091006_F	PIN_091006_BU	195	1.6	
23/10/2006	160	80		PIN_231006_1F_teflon	PIN_231006_1BU	165	0.65	
				PIN_231006_2F_teflon	PIN_231006_2BU	150	0.90	
24/09/2007	240	240		PIN_240907_1F	PIN_240907_1BU	182	0.87	
				PIN_240907_2F	PIN_240907_2BU	158	0.87	
26/09/2007	240	240		PIN_260907_1F_teflon	PIN_260907_1BU	179	0.86	
				PIN_260907_2F_teflon	PIN_260907_2BU	154	0.85	
01/10/2007	240	1.5		PIN_011007_1F_teflon	PIN_011007_1BU	119	0.80	
				PIN_011007_2F_teflon	PIN_011007_2BU	123	0.79	
03/10/2007	240	1.5		PIN_031007_1F	PIN_031007_1BU	127	0.84	
				PIN_031007_2F	PIN_031007_2BU	137	1.0	
28/09/2007	3	1.5		PIN_280907_1F	PIN_280907_1BU	20	4.0	
				PIN_280907_2F	PIN_280907_2BU	15	6.6	
05/10/2007	3	1.5		PIN_051007_1F	PIN_051007_1BU	30	4.8	
				PIN_051007_2F	PIN_051007_2BU	21	6.3	

Table 6. List of SOA samples collected during experiments employing α -pinene as precursor VOC. Two filters sets were sampled each experiment: numbers 1 or 2 in the sample ID stand for sets sampled in the initial or in the final part of the experiment respectively. Only one sampling was done in the first experiment. The sample ID reports as well when Teflon was used as alternative substrate. Grey colour is used for back up filters. The mean aerosol mass concentrations are calculated from SMPS data and averaged upon the filters sampling times.

The experiments lasted roughly 8 hours and two filters sets were typically sampled in subsequent moments in order to obtain *fresh* SOA from the initial part and *aged* SOA from the final part of each experiment: *fresh* SOA was roughly collected between the 4th and the 6th hours while *aged* SOA between the 6th and the 8th hours (fig. 1).

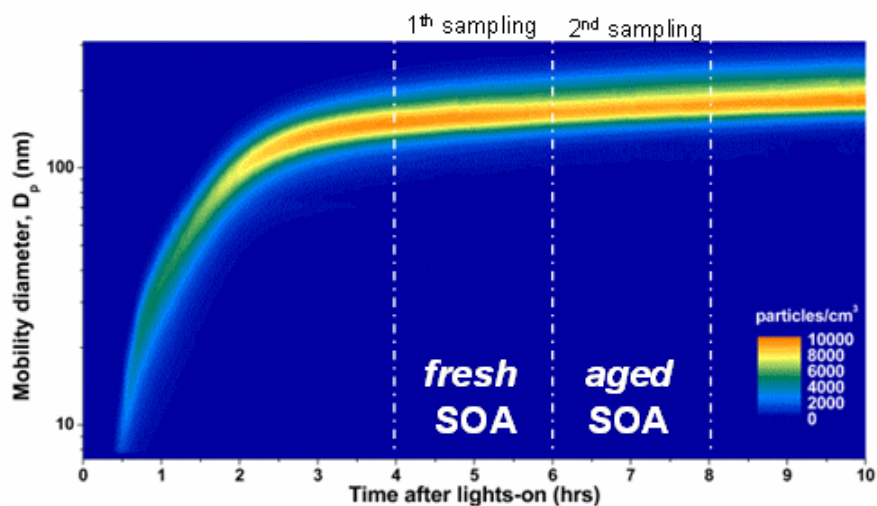


Figure 1. Typical time-resolved number-weighted size distribution from a photo-oxidation experiment. The measured total and water-soluble organic carbon contents are reported in the table 2.

sample ID	front		back up	
	TC ($\mu\text{g C / m}^3$)	WSOC ($\mu\text{g C / m}^3$)	TC ($\mu\text{g C / m}^3$)	WSOC ($\mu\text{g C / m}^3$)
PIN_091006	138	95	25.96	16.99
PIN_231006_1_teflon	n.a.	71	64	41
PIN_231006_2_teflon	n.a.	34	86	35
PIN_240907_1	150	71	7.5	1.6
PIN_240907_2	103	79	7.5	5.3
PIN_260907_1_teflon	n.a.	73	34	1.7
PIN_260907_2_teflon	n.a.	81	44	5.4
PIN_011007_1_teflon	n.a.	20	44	36
PIN_011007_2_teflon	n.a.	16	38	33
PIN_031007_1	135	58	12	4.0
PIN_031007_2	96	78	16	12
PIN_280907_1	20	11	2.9	1.2
PIN_280907_2	11	8.5	2.3	1.5
PIN_051007_1	27	13	6.4	3.4
PIN_051007_2	18	9.9	3.9	2.5

Table 2. Total and water-soluble organic contents of α -pin-SOA. TC analyses are not feasible for Teflon substrates.

The aerosol mass concentrations obtained by off-line measurements on quartz filter samples resulted to fit nicely with those calculated from SMPS data, particularly with values corresponding to experiments conducted at low VOC level (fig. 2). On the contrary, samples collected on Teflon substrates resulted affected by negative artefacts. Since the carbon loadings of such substrates were found systematically in defect with respect to those expected from SMPS data, the hereinafter comments will concern only quartz filter samples.

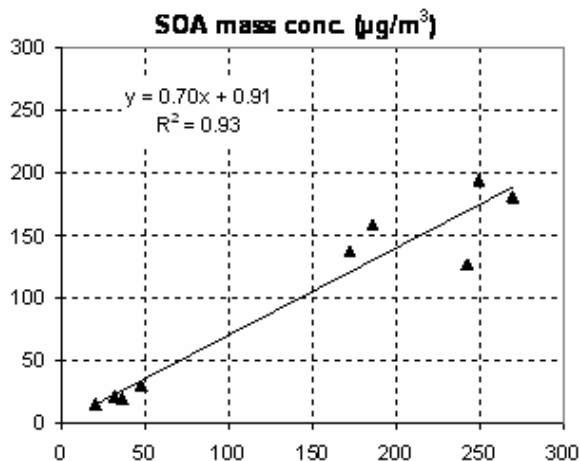


Figure 2. Scatter plot of aerosol mass concentrations ($\mu\text{g}/\text{m}^3$) as derived from SMPS data and calculated from total carbon measurements upon the filters. (TC measured on front filters have been multiplied by 1.8 to be compared with the value obtained by SMPS).

Since SOA are supposed to be composed by fairly oxygenated (polar) compounds, WSOC was expected to approach TC. The measured WSOC resulted to contribute between 50% up to 80% to total carbon of α -pinene SOA. Hence the analyses performed show that α -pinene SOA contain a small but significant amount of water-insoluble organic compounds (fig. 3).

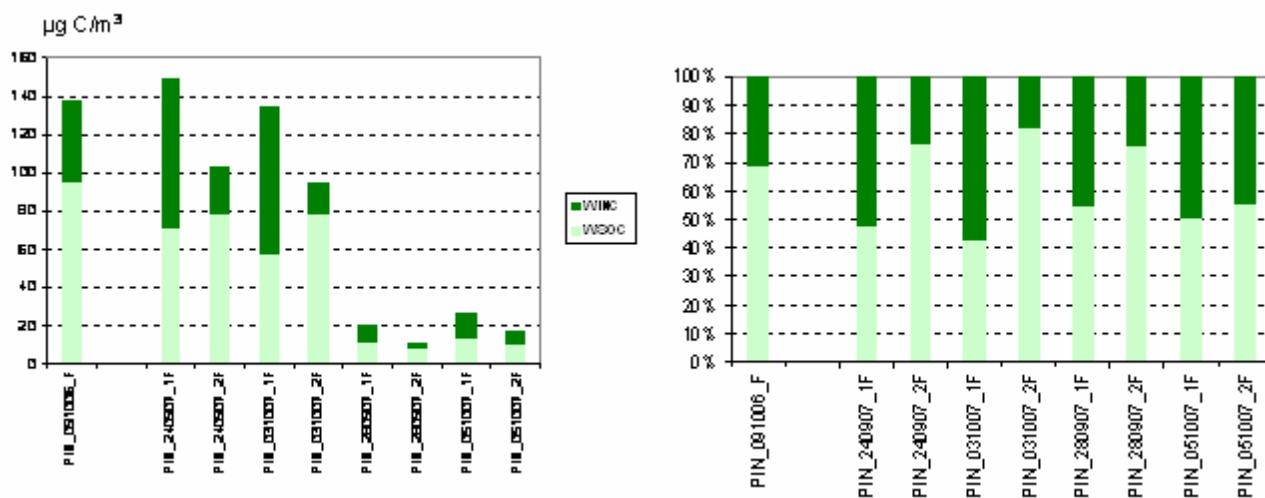


Figure 3. Diagrams showing the water-soluble and insoluble organics concentrations of α -pinene SOA: absolute and relative values are in the left and right side respectively.

As can be seen even in the upper figure (right side), the samples collected in the last parts of the experiments (*aged* SOA) are characterized by WSOC fractions systematically higher with respect to those collected at the beginning (*fresh* SOA). Thus confirming that more oxygenated compounds constitute *aged* with respect to *fresh* α -pinene SOA. Interestingly the WSOC/TC ratios increase concordantly to the initial VOC level: in greater extent (up to 1.8 times) within high-level VOC experiments and in lesser extent (up to 1.3 times) within low-concentration experiments (fig. 4).

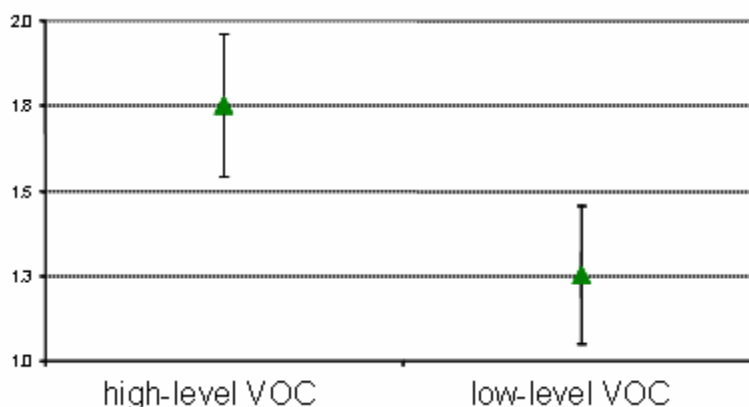


Figure 4. Extent of the increase of the WSOC/TC ratios from *fresh* to *aged* SOA within high- and low-level VOC experiments. The y-axis corresponds to the averaged ratios between the WSOC fraction of *fresh* SOA and the WSOC fraction of *aged* SOA (e.g. for high-level VOC experiments, WSOC/TC in aged SOA is about 1.8 times greater than WSOC/TC in the corresponding fresh SOA). The bars has not to be considered as errors bars but they serve merely to show the observed variability as standard deviation from the mean values.

During the low-concentration experiments, constant low SOA levels were maintained by injecting a constant flow of HONO and α -pinene: steady-state conditions were thus reproduced during these experiments. New SOA particles were continuously generated so that a negligible difference was actually expected between SOA collected in the beginning and in the end of these experiments.

By contrast, the great WSOC fraction enhancement in SOA collected in the end of the high loadings experiments could possibly reflect both an actual oxidizing activity (ageing process) or as well the partitioning of species such as small polar semi-volatile organics (e.g. pinic acid) which otherwise remain in gas phase under low organics loading conditions.

In order to obtain a better insight into the chemical features of the water soluble organic compounds constituting α -pinene SOA, $^1\text{H-NMR}$ spectroscopy has been deployed. A typical $^1\text{H-NMR}$ spectrum of α -pinene SOA is shown in figure 5.

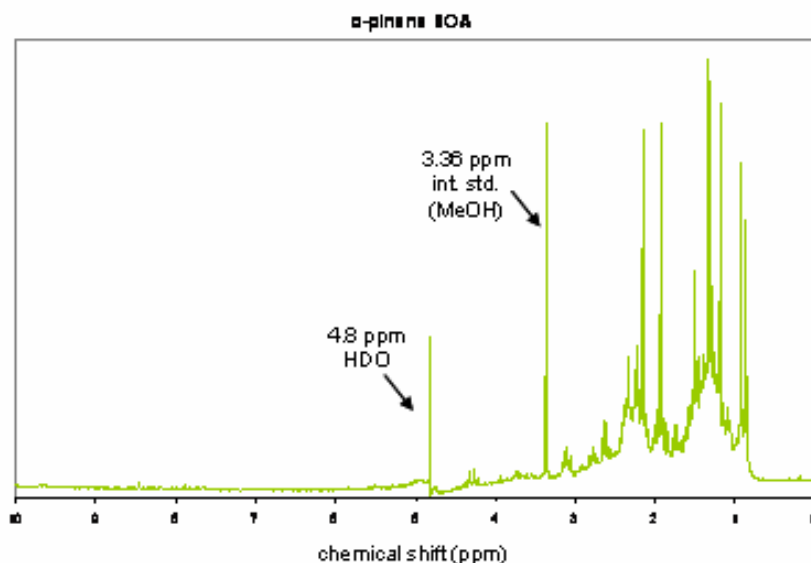


Figure 5. ¹H-NMR spectrum of α -pinene SOA (PIN_091006_F) in D₂O at 400 MHz. The horizontal scale reports the frequency shift (“chemical shift”, ppm). The peaks at 3.36 and 4.8 ppm are the internal standard (methanol) and the residue of the solvent peak (HDO) upon suppression by instrumental methods.

As expected the α -pinene SOA spectra show a functional groups distribution strongly dominated by aliphatic compounds with aromatic signals (6.5-8.5 ppm) completely absent. This profile is consistent with the current knowledge about monoterpenes oxidation mechanism and agree with previous spectroscopic data from chamber experiments (Cavalli et al., 2006).

The spectra also show sharp peaks superimposed to a broad background signal attributable to a complex mixture of α -pinene oxidation products. Among the sharp peaks, the most important are those of well-known species such as pinic acid and pinonic acid (fig. 6).

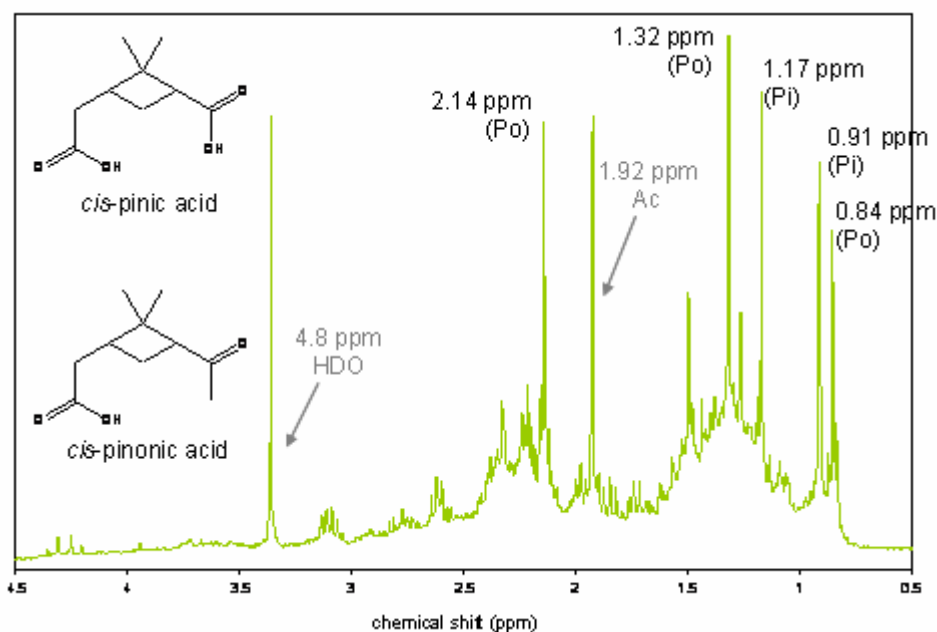


Figure 6. Enlarged version of the spectrum shown in fig. 6. Pi and Po mark the main singlet peaks from methyl groups belonging to pinic and pinonic acid respectively, those chemical structures are also reported in the left side of the figure. The peak at 1.92 ppm is from acetate (Ac).

3.1.2 Low-concentration experiments

The different partitioning of pinic and pinonic acid in the different SOA concentration regimes are clearly reflected in the $^1\text{H-NMR}$ spectra and their signals resulted the main distinguishing feature between SOA produced during high VOC level and steady-state low concentration experiments. Pinonic and pinic acid resulted actually to contribute in much lesser extent to SOA mass of samples collected in low concentration experiments (fig.7, 8). Hence the spectra of SOA produced at low precursor concentration can be interpreted as resulting from compounds with a higher partitioning coefficient (i.e., a lower volatility) than pinonic and pinic acids. Such compounds may include extensively oxidized products, which have lost the original molecular backbone of α -pinene, i. e. a cyclobutane ring with two geminal methyls and also products of accretion reactions (i.e., oligomerization).

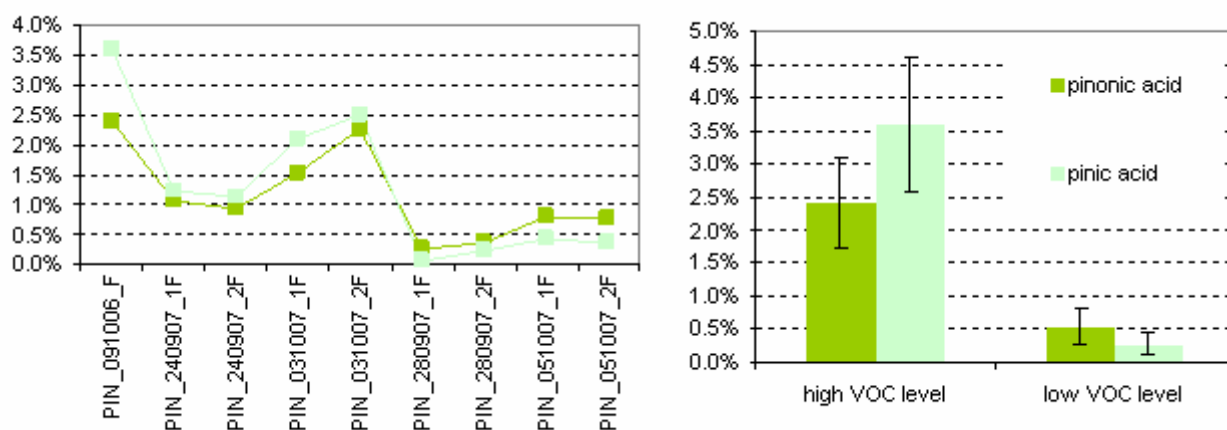


Figure 7. Left side: pinic and pinonic acid relative contributions (percentage) to α -pinene SOA samples. Right side: pinic and pinonic acid relative contributions averaged upon high and low level VOC experiments. The percentages have been calculated using the concentrations ($\mu\text{mol H/m}^3$) derived from the NMR analyses.

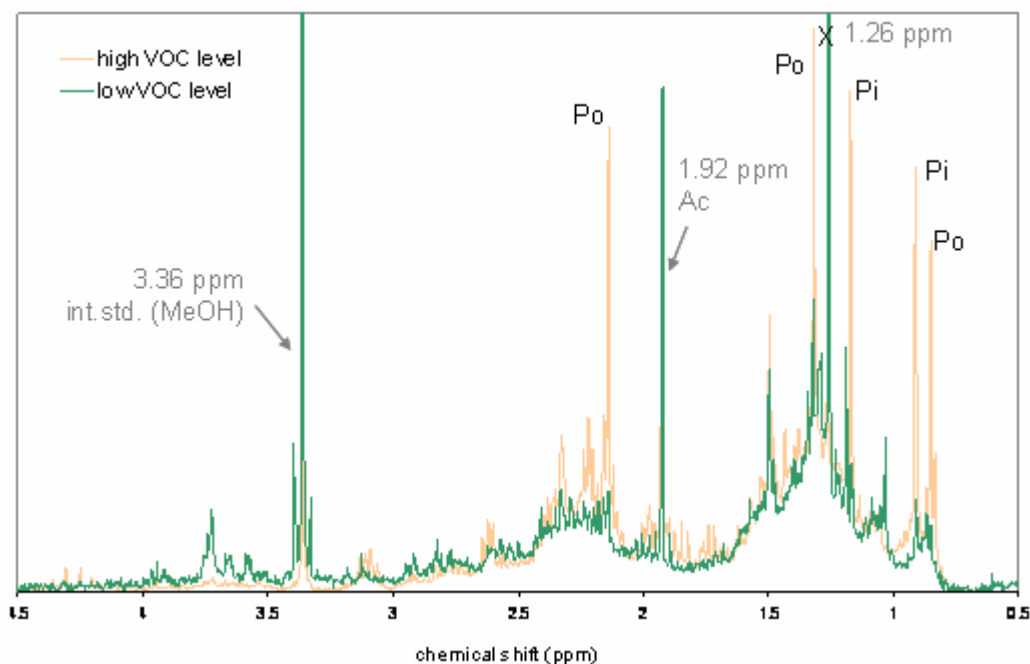


Figure 8. $^1\text{H-NMR}$ spectra of α -pinene SOA generated in high concentration (orange profile) and in low concentration (green profile) experiments (PIN_091006_F and PIN_280907_1F). The vertical scales have been normalized by the total area of the corresponding spectrum. Pi and Po mark the pinic and pinonic acid signals. Peaks at 3.36 ppm and at 1.92 ppm are from the internal standard and from acetate. The peak at 1.26 ppm is ubiquitous among quartz filters extracts and it doesn't belong to the samples.

3.1.3 SOA generated from mixtures of terpenes

Laboratory-SOA samples produced by the photo-oxidation of terpenes mixtures are listed in the table below (tab.3). Two experiments performed in dark conditions (ozonolysis experiments) are also reported at the bottom of the table.

exp. type	oxidants			sample ID	TC ($\mu\text{g C/m}^3$)	WSOC ($\mu\text{g C/m}^3$)
	VOCs (ppb)	NOx (ppb)	O ₃ (ppb)			
MT mix wo ocimene	50	1.5	40	MT_060608_1F	36	26
				MT_060608_2F	n.a.	12
	100	0.9	43	MT_160608_1F	37	n.a.
				MT_160608_2F	22	n.a.
MT mix	50	1.7	75	MT_061007_1F	41	32
				-	-	-
	50	1.3	55	MT_040608_1F	32	n.a.
				MT_040608_2F	12	n.a.
	100	1.8	40	MT_090608_1F	40	35
				MT_090608_2F	n.a.	16
MT + SQT mix	100	0.8	43	MT_130608_1F	65	49
				MT_130608_2F	18	15
	55	1.0	60	MT+SQT_041007_1F	67	45
				MT+SQT_041007_2F	26	24
	55	0.4	60	MT+SQT_311007_1F	59	48
				MT+SQT_311007_2F	13	16
MT + SQT mix	55	1.5	35	MT+SQT_110608_1F	38	37
				MT+SQT_110608_2F	10	n.a.
	110	0.9	40	MT+SQT_180608_1F	48	29
				MT+SQT_180608_2F	16	15
ozonolysis	100	0.2	180	MT+O3_200608_1F	54	44
				-	-	-
	55	1.7	80	MT+SQT+O3_291007_1F	61	59
			MT+SQT+O3_291007_2F	12	15	

Table 3. List of SOA samples produced in laboratory from terpenes mixtures. Two filters sets were sampled each experiment: numbers 1 or 2 in the sample ID stand for sets sampled in the initial or in the final part of the experiment respectively. Measured total and water soluble carbon concentrations are reported in the last columns on the right.

VOCs constituting the employed mixtures are specified in the table below. Equi-molar VOCs concentrations were used for each mixture.

Mixture's ID	Monoterpenes	Sesquiterpenes
MT mix without ocimene	α -pinene, β -pinene, limonene, Δ^3 -carene	
MT mix	α -pinene, β -pinene, limonene, Δ^3 -carene, ocimene	
MT + SQT	α -pinene, β -pinene, limonene, Δ^3 -carene, ocimene	β -caryophyllene, α -farnesene

In the next figure WSOC/TC ratios of laboratory-generated biogenic SOA are reported, lumped by the different experiment types and including the α -pinene SOA formed in the PSI chamber. Experiments employing an increasing complexity of the initial VOC mixture are reported from the left to the right side. At least two trends are clearly visible upon these data: The WSOC fraction increase slightly along with the mixture complexity and, looking at each experiment type, the water soluble fraction increase concordantly with SOA ageing.

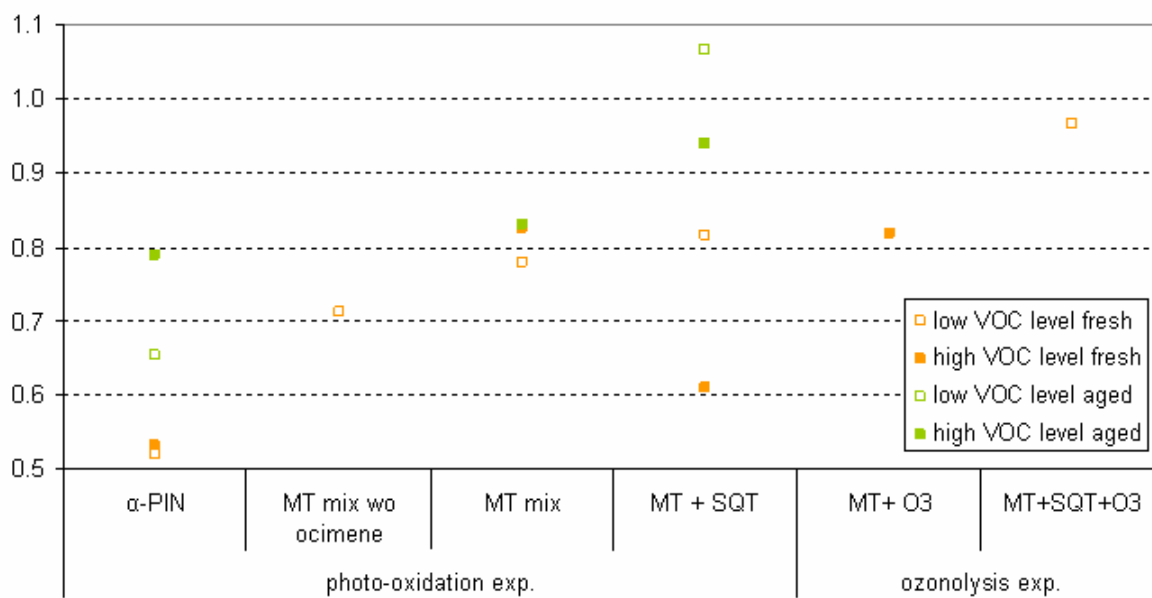


Figure 9. WSOC/TC ratios of biogenic SOA generated in laboratory. Empty symbols represent SOA generated in low VOC concentration experiments (less than 55 ppb) and filled symbols represent those generated in high VOC level experiments (more than 55 ppb). Colours distinguish between *fresh* and *aged* SOA, orange and green respectively.

An overall increase of the water soluble fraction in aged SOA with respect to fresh SOA is also visible in the following histogram where averaged values upon all laboratory-generated biogenic SOA are reported (fig. 10).

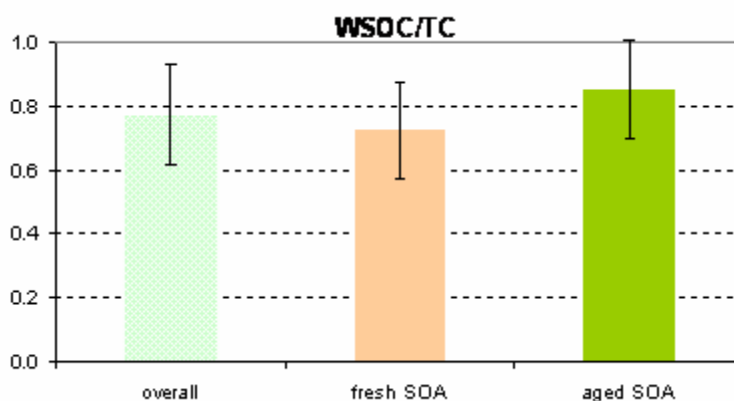


Figure 10. Averaged WSOC/TC ratios upon all laboratory-generated biogenic SOA (overall), upon all biogenic *fresh* SOA and upon all *aged* SOA.

The chemical structures of water soluble compounds constituting SOA generated from mixtures of terpenes have been further investigated by $^1\text{H-NMR}$ spectroscopy. The main spectral features of MT mix- and MT+SQT mix-SOA presented several analogies with those of the above-mentioned spectra of α -pinene-SOA (fig.11). Most of the resonances fall in the aliphatic region, whereas the aromatics region is completely void of signals. Sharp and intense peaks are visible upon unresolved background bands. Some of such distinct peaks have been identified in both α -pinene-SOA as well in MT mix-SOA spectra and have been attributed to pinic and pinonic acid. Signals at 0.94 ppm and 1.08 ppm, found exclusively in MT-mix SOA spectra, have not been yet identified but they come likely from a compound with analogous molecular structure of pinic acid (hereinafter called Pi-like). This Pi-like compound shows concentrations comparable to those of pinic acid in most of the analyzed samples. Other singlets and some doublets from unidentified compounds are systematically seen in the chemical shift range between 0.8 and 1.6 ppm, pointing to several oxidation products often occurring in similar or even higher concentrations with respect to pinic acid. Standards of carboxylic acids expected to form from extensive oxidation of α -pinene SOA were analyzed with aim of comparison with the major unidentified peaks in the HNMR spectra of MT SOA but they did not show an exact match.

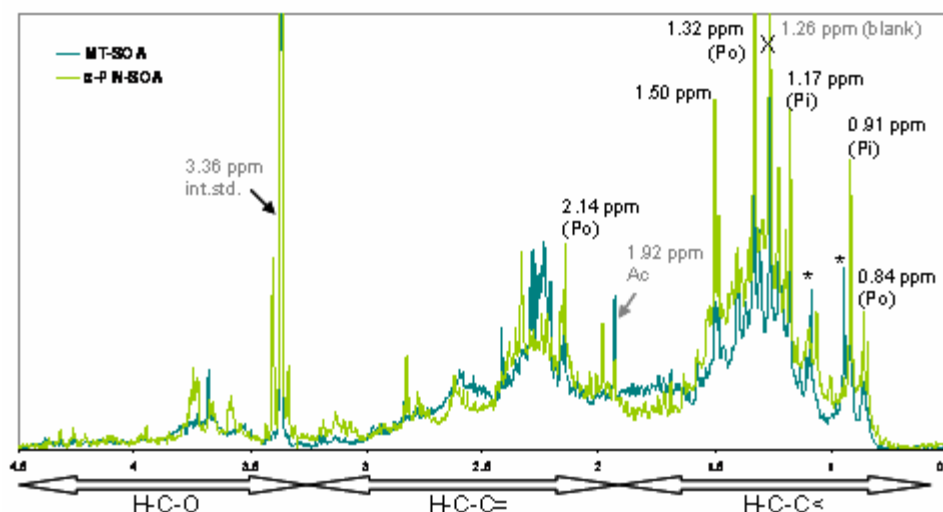


Figure 11. $^1\text{H-NMR}$ spectra of α -pinene SOA (PIN_240907_1F) and MT-SOA (MT_130608_1F). The vertical scales have been normalized by the total area of the corresponding spectrum. Pi and Po mark the pinic and pinonic acid signals identified in both spectra whereas stars mark signals at 0.94 ppm and 1.08 ppm present in MT-SOA spectrum only.

Main functional groups quantified for biogenic laboratory-SOA correspond to: a) primary or secondary alcohols and ethers (H-C-O), b) aliphatic groups adjacent to carbonyls/carboxyls (H-C-C=) and c) alkyl groups (H-C-C<). The measured functional groups concentrations ($\mu\text{mol H/m}^3$),

averaged for each type of experiment, are reported in the figure below (fig. 12, upper panel). Basically, the $^1\text{H-NMR}$ spectra of the SOA samples generated in different photochemical conditions and from different mixtures showed a very low variability in terms of functional groups distributions (fig. 12, lower panel). Overall, aliphatic groups adjacent to carbonyls together with alkyl groups account for most of the detected $^1\text{H-NMR}$ signal, while the aliphatic groups adjacent to hydroxyls are present in much lower amounts (fig. 12, pie-graph).

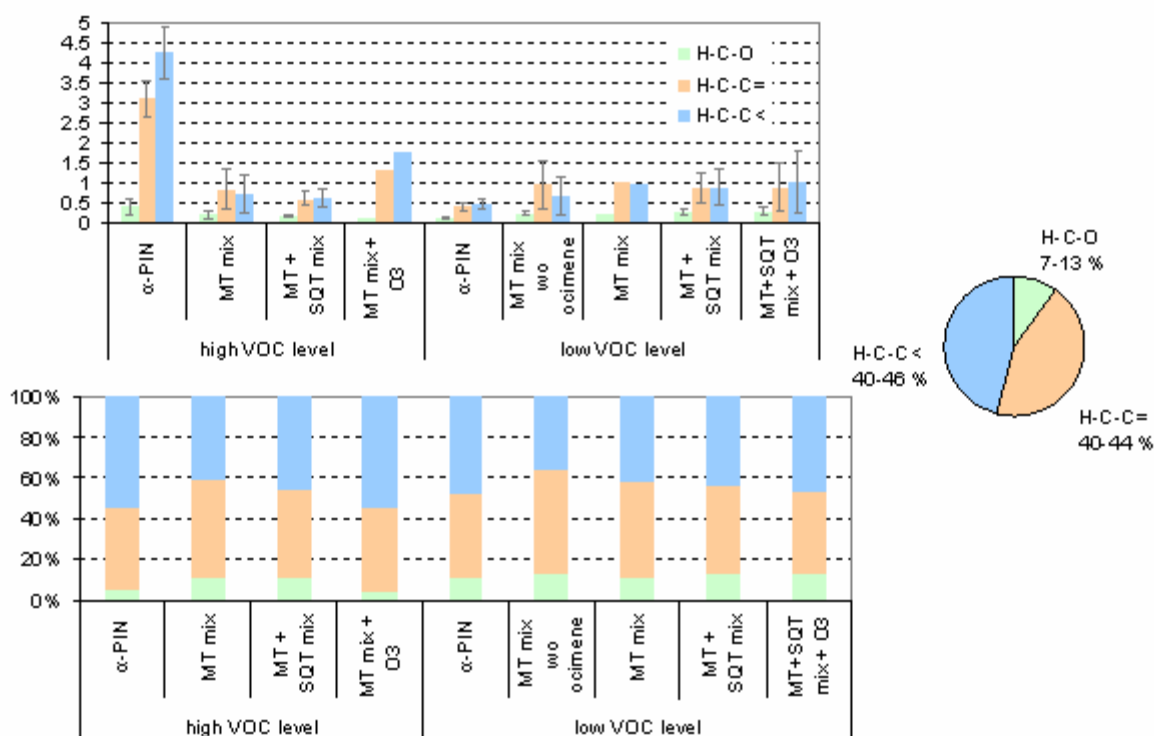


Figure 12. $^1\text{H-NMR}$ functional groups of biogenic laboratory-SOA averaged upon the type of experiment. Upper histogram: functional groups absolute concentrations ($\mu\text{mol H/m}^3$). Deviation standard is given for experiments performed in replicate. Lower panel: functional groups percentage of the total $^1\text{H-NMR}$ signal. The pie-graph in the right side reports the mean percentages averaged upon all the experiments.

3.1.4 Effect of ageing on biogenic laboratory-SOA

The concentrations of *aged* SOA are typically from 1/2 to 1/4 those of the correspondent *fresh* SOA as can be seen in the figure below where WSOC concentrations are reported together with the total $\mu\text{mol H m}^{-3}$ derived by the NMR analysis (fig. 13).

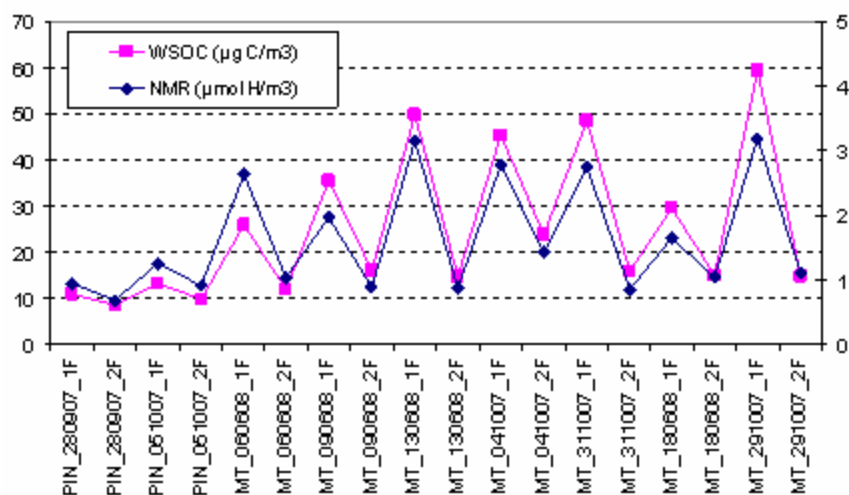


Figure 13. The left vertical axis reports the WSOC concentrations ($\mu\text{g C/m}^3$) and the vertical axis on the right reports the total $\mu\text{mol H/m}^3$ derived by the ^1H -NMR analyses.

In spite of this significant differences in the concentrations, the overall distribution of the various HNMR functional groups resulted very similar between the *fresh* and *aged* samples (fig.14).

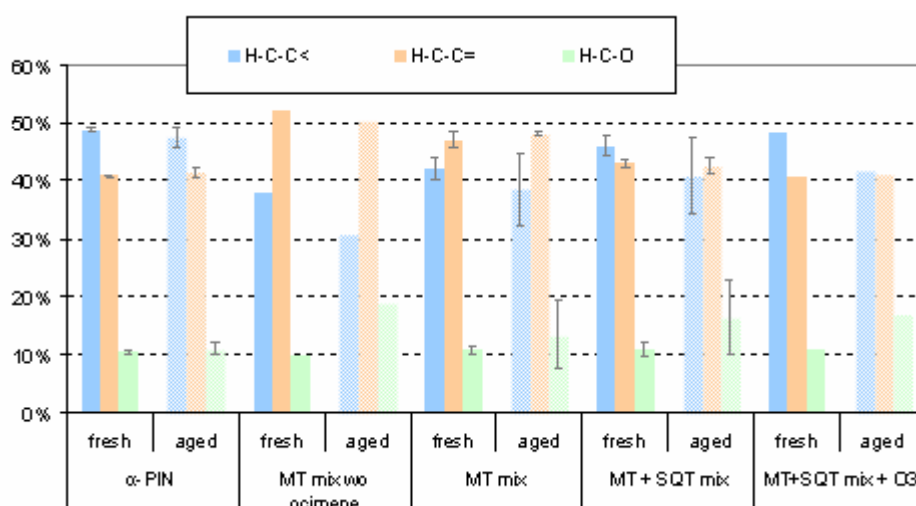


Figure 14. Functional groups percentages averaged separately upon *fresh* and *aged* SOA for each type of experiment. Deviation standard is reported for experiments performed in replicate.

Nevertheless, some changes in the distribution of individual compounds and in minor bands belonging to the background unresolved signal are observable. Multivariate statistical methods were therefore applied to the $^1\text{H-NMR}$ spectra obtained from biogenic laboratory-SOA in order to possibly better quantify such variability. The $^1\text{H-NMR}$ spectra were subjected to Positive Matrix Factorization (PMF) and Non-negative Matrix Factorization (NMF) analyses. Since the results from the two techniques were analogous, here only those of NMF will be discussed.

A total of 16 $^1\text{H-NMR}$ spectra obtained from *fresh* and *aged* MT-SOA were subjected to NMF analysis. In the figure below the profiles are reported resulting with the simplest two-factors solution applied to MT_SOA spectra (fig.15).

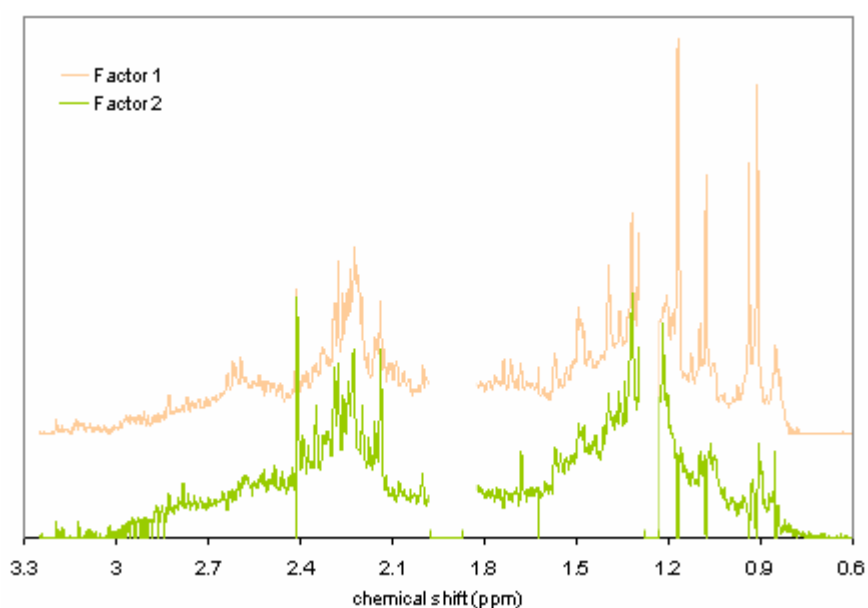


Figure 15. Profiles obtained applying NMF (two-factor solution) to $^1\text{H-NMR}$ spectra of MT-SOA. The profile colors distinguish between factor 1 (orange) and factor 2 (green). The signals at 1.92 ppm (acetate) and at 1.26 ppm (from blank) were cancelled from the spectra subjected to NMF analysis thus they are not visible into the resulted profiles.

The resulted loadings (percentage) of the two factors shown in Fig.16 are reported in the following diagram (fig.16).

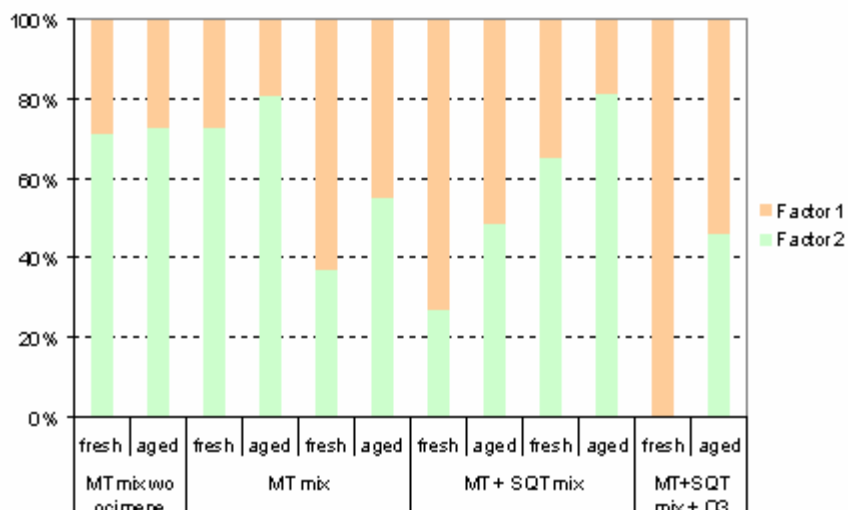


Figure 16. Relative abundances (percentage) of the factors obtained applying NMF analysis to MT-SOA spectra.

Factor 1 (corresponding to the orange profile) accounts for the majority of the spectral signal of MT-SOA generated during ozonolysis experiments. A NMF run using even a two-factors solution but excluding the ozonolysis experiments from the input data matrix was also performed: the same profiles and the same corresponding loadings were found.

Basically, the loadings of factor 1 decrease clearly from *fresh* to *aged* SOA samples. Conversely, the loadings of factor 2 (corresponding to the green profile) looks to increase with ageing, except for the experiment without ocimene in the MT mixture. The main distinguishing feature between the spectral profiles of factor 1 and factor 2 is the intensity of the peaks of pinic acid and of pi-like compound with respect to the background signal: the singles peaks of such early generation oxidation products contribute strongly to the factor 1 signal whereas they disappear among the factor 2 signal. The profiles of factor 1 and factor 2 have been therefore interpreted as the fingerprints of *fresh* and *aged* MT-SOA respectively.

3.2 Anthropogenic SOA

3.2.1 SOA formed by 1,3,5-trimethylbenzene

A series of SOA generation experiments were performed employing 1,3,5-trimethylbenzene (TMB) as gaseous precursor representative for aromatic VOCs emitted by anthropogenic sources (tab.4).

exp. date	TMB (ppb)	NO _x (ppb)	sample ID		SOA mass conc. (µg/m ³)	sampling volume (m ³)
			front	back up		
04/10/2006	600	300	TMB_041006_F	TMB_041006_BU	54	1.8
06/10/2006	1200	600	TMB_061006_F	TMB_061006_BU	128	1.4
11/10/2006	1200	600	TMB_111006_1F_teflon	TMB_111006_1BU	135	1.5
			TMB_111006_2F_teflon	TMB_111006_2BU	155	1.2
13/10/2006	1200	600	TMB_131006_1F	TMB_131006_1BU	162	1.2
			TMB_131006_2F	TMB_131006_2BU	159	1.0
18/10/2006	1200	600	TMB_181006_1F_teflon	TMB_181006_1BU	142	1.2
			TMB_181006_2F_teflon	TMB_181006_2BU	135	1.2
20/10/2006	1200	600	TMB_201006_1F	TMB_201006_1BU	160	1.2
			TMB_201006_2F	TMB_201006_2BU	160	1.0
19/10/2007	1200	300	TMB_191007_1F	TMB_191006_1BU	103	0.9
			TMB_191007_2F	TMB_191006_2BU	101	0.9
21/10/2007	1200	300	TMB_211007_1F	TMB_211007_1BU	108	0.9
			TMB_211007_2F	TMB_211007_2BU	101	0.9

Table 4. List of SOA samples collected during experiments employing 1,3,5-trimethylbenzene as VOC precursor. Two filters sets were sampled each experiment: numbers 1 or 2 in the sample ID stand for sets sampled in the initial or in the final part of the experiment respectively. Only one sampling was done in the first two experiments. The sample ID reports as well when Teflon was used as alternative substrate. Grey colour is used for back up filters. The mean aerosol mass concentrations are calculated from SMPS data and averaged upon the filters sampling times.

The measured total and water-soluble organic carbon contents are reported in the table 5.

sample ID	front		back up	
	TC ($\mu\text{g C/m}^3$)	WSOC ($\mu\text{g C/m}^3$)	TC ($\mu\text{g C/m}^3$)	WSOC ($\mu\text{g C/m}^3$)
TMB_041006	67	35	13	4.8
TMB_061006	79	61	16	6.3
TMB_111006_1_teflon ^(*)	n.a.	8.1	89	35
TMB_111006_2_teflon	n.a.	29	32	21
TMB_131006_1	68	41	33	12
TMB_131006_2	105	98	25	16
TMB_181006_1_teflon	n.a.	48	30	15
TMB_181006_2_teflon	n.a.	19	18	9.5
TMB_201006_1	84	56	14	0.04
TMB_201006_2	97	75	19	4.7
TMB_190907_1	69	n.a.	5.0	n.a.
TMB_190907_2	196	n.a.	6.0	n.a.
TMB_210907_1	76	95	14	6.5
TMB_210907_2	65	83	21	10

Table 5. Total and water-soluble organic contents of TMB-SOA. TC analyses are not feasible for Teflon substrates. (*) Teflon substrate broken during the sampling.

Since the carbon loadings of samples collected on Teflon substrates were found strongly affected by negative artefacts, the following discussion applies only to quartz-fiber filter samples.

The analyses performed show that TMB-SOA are mostly composed by water soluble organic compounds: overall WSOC account for about 75 % of TC on front quartz-fiber filters and this percentage decreases to ca. 43 % on back up filters (fig. 17). The organic compounds found on back up filters represent likely the semi-volatile fraction constituting TMB SOA which is expected to evaporate from the particles trapped on front filters. The lower WSOC/TC ratios found systematically on back up filters with respect to the front filters reflect a less oxygenated nature of the semi-volatile compounds (SVOCs) with respect to the others compounds constituting TMB SOA.

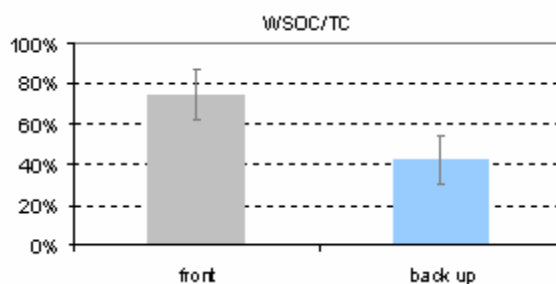


Figure 77. Averaged WSOC/TC ratio of TMB-SOA (front). The reported averaged WSOC/TC ratio found on back up filters (back up) which characterize likely the SVOCs escaped from the particles collected on the front filters. The bars represent the observed variability as standard deviation from the mean values.

The samples collected in the last parts of the experiments are characterized by WSOC fractions slightly higher with respect to those collected at the beginning: WSOC/TC in *aged* SOA is about 1.3 times greater than WSOC/TC in the corresponding *fresh* SOA (fig. 18), thus confirming the more oxygenated state of the particles constituting *aged* with respect to *fresh* TMB-SOA.

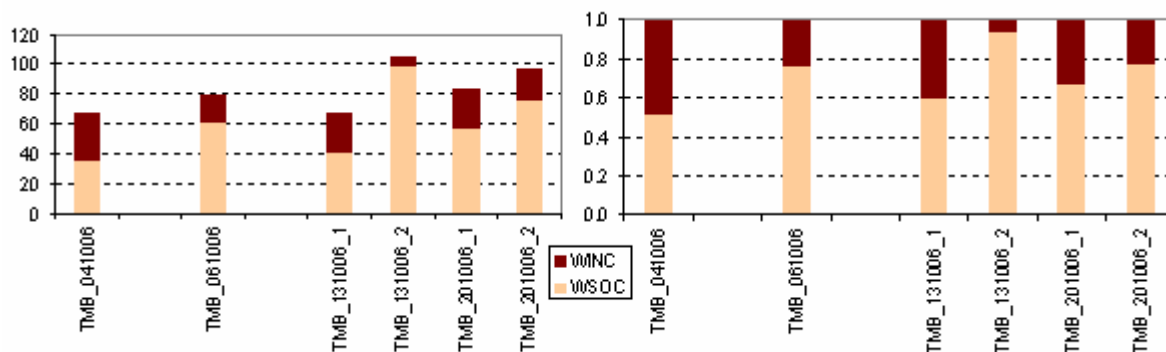


Figure 18. Histograms showing the water-soluble and insoluble organics concentrations of TMB-SOA on front quartz-fiber filters: absolute ($\mu\text{g C/m}^3$) and relative values are in the left and right side respectively.

The chemical features of the water soluble organic compounds constituting TMB-SOA have been further investigated by $^1\text{H-NMR}$ spectroscopy. The resulted $^1\text{H-NMR}$ spectra appear typically as shown in figure 19. Looking to this spectrum it can be noticed that TMB SOA present a chemical composition prevalently aliphatic, being the signal mostly accounted for by alkylic protons bound to sp^3 - and sp^2 -hybridized carbons. Vinylic protons and protons close to hydroxylic groups are found in much lower amounts. Only a weak singlet peak is detectable in the spectral region of the aromatic protons suggesting a very few aromatic ring-retaining products content in TMB SOA. It should be anyway mentioned that completely substituted aromatic structures are not visible by this technique thus they can't be definitively excluded.

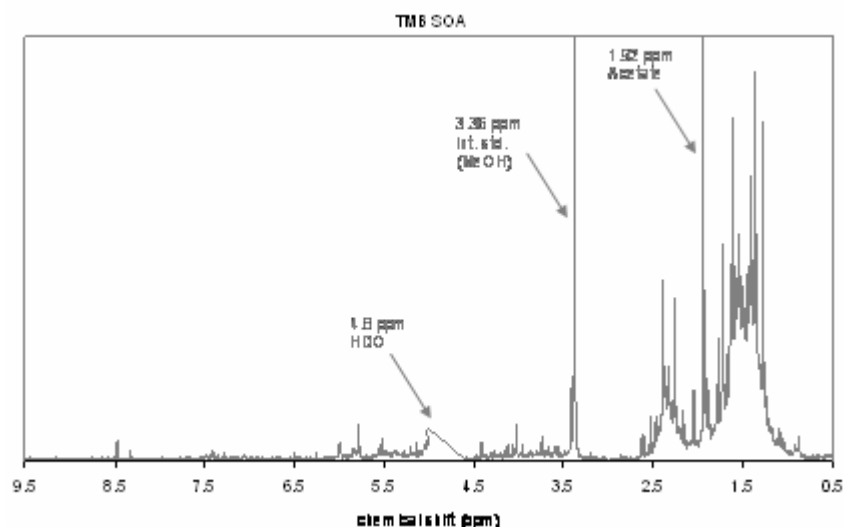


Figure 19. ^1H -NMR spectrum of TMB-SOA (TMB_201006_1F) in D_2O at 400 MHz. The horizontal scale reports the chemical shift (ppm). The peaks at 3.36 and 4.8 ppm are the internal standard (methanol) and the residue of the solvent peak (HDO) upon suppression by instrumental methods. The peak at 1.92 ppm is from acetate.

The mean TMB SOA functional group absolute concentrations ($\mu\text{mol H/m}^3$), obtained by the integration of the bands in the ^1H -NMR spectra, are reported in the figure 20. This figure reports also the corresponding averaged values measured on back up filters, i.e. representing the composition of the semi-volatile fraction of TMB-SOA. It can be noticed that the two series of values differ mostly in the amount of the alkylic groups ($\text{H-C-C}<$).

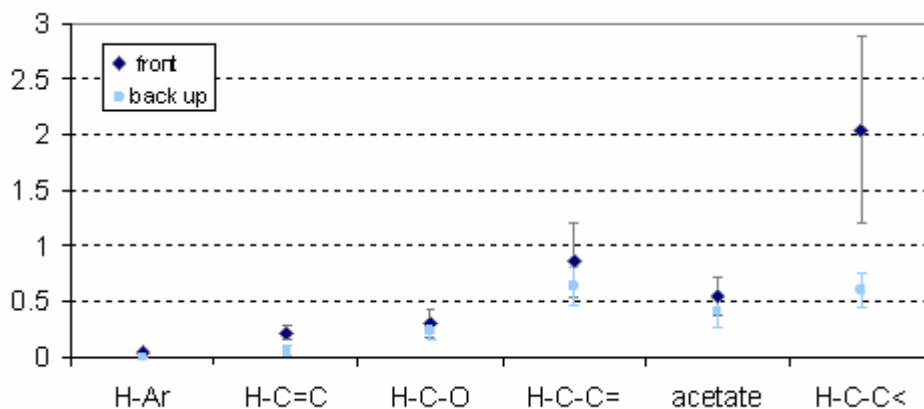


Figure 20. TMB-SOA averaged functional groups absolute concentrations ($\mu\text{mol H/m}^3$). The values measured on back up filters are also reported (light blue symbols) for comparison. The bars represent the observed variability as standard deviation from the mean values.

The figure below concerns on the differences between *fresh* and *aged* TMB SOA functional group composition (fig. 21). A general increasing of the absolute concentrations is recorded for the last sampling stages, having the alkyl protons bound to sp^3 - and sp^2 -hybridized carbons the mostly enhanced values. Conversely, the main spectral features remain unvaried for TMB-SOA sampled at the beginning and those collected in the last part of each experiment: the relative functional groups

distribution is fairly the same in both fresh and aged TMB SOA. This may indicate that the time scales of SOA evolution in the PSI chamber was not long enough to observe an actual ageing of the composition of the particles.

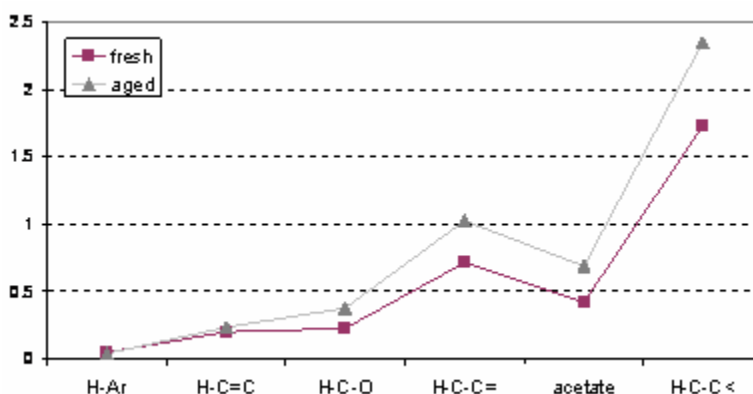


Figure 21. TMB-SOA functional groups absolute concentrations ($\mu\text{mol H/m}^3$) averaged separately upon *fresh* and *aged* TMB-SOA. Solid lines serve merely to help the eyes.

The overall distribution of the various bands in the different chemical shift regions for TMB-SOA is also shown in the following pie-graph (fig. 22).

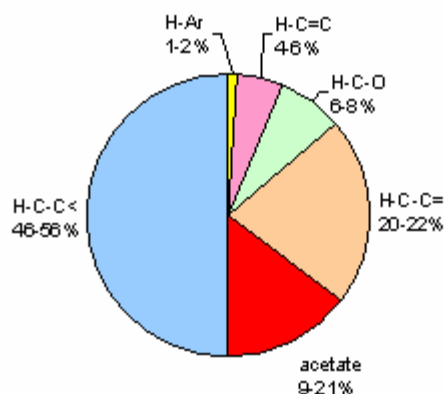


Figure 22. Relative abundances (percentage) of the main functional groups quantified in TMB-SOA.

3.2.2 Comparison with TMB-SOA composition as predicted by models

The formation and composition of secondary organic aerosol generated by the photo-oxidation of 1,3,5-trimethylbenzene has been already simulated using the Master Chemical Mechanism (MCM v3.1) model coupled to a representation of the transfer of organic material from the gas to particle phase (Johnson et al., 2005; Bloss et al., 2005b). A partial schematic representation of the OH-initiated photo-oxidation of TMB as simulated by MCM v3.1 is reported in figure 23. The model indicates specific classes of organic compounds as the best candidates for contributing to SOA mass such as: ring-retaining products including aromatic aldehydes and cyclic peroxides, and ring-opening products (e.g. low-molecular weight carbonyls). The measured $^1\text{H-NMR}$ functionalities of TMB-SOA can then be compared to those predicted by models.

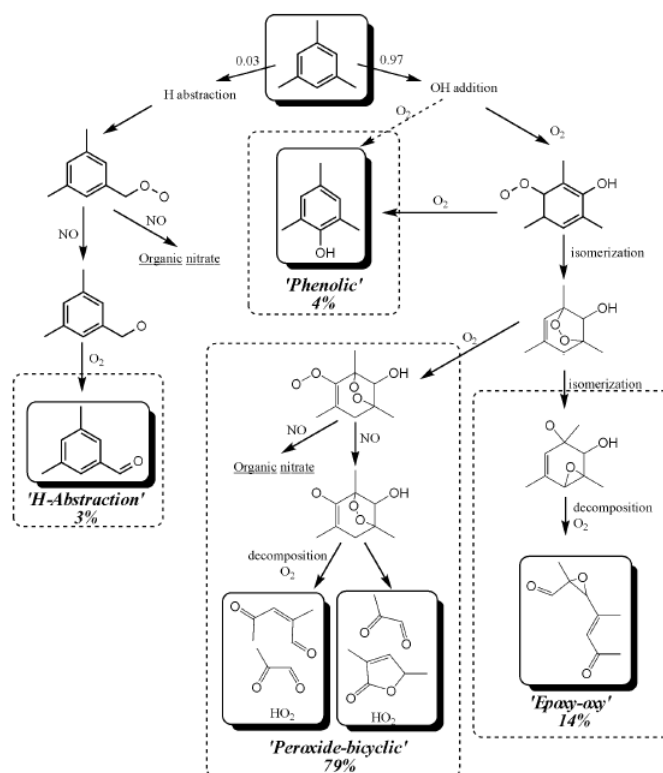


Figure 23. Partial schematic representation of the OH-initiated oxidation of TMB as implemented in the MCM v3.1. The first generation products are shown in boxes and the branching ratio of the respective forming pathway is given in percent (figure taken from Metzger et al., 2008).

Basically, the major degradation pathway for TMB involves the addition of OH to the aromatic ring, followed by further steps leading to the formation of an oxygen-bridged bicyclic peroxy radical structure. Several large multifunctional O_2 -bridged products (both ring-retaining as well ring opening oxygenated and nitrated compounds) are generated by this so called “peroxide-bicyclic

route” and are likely to be sufficiently non-volatile to partition into the organic aerosol phase (fig. 24). Recently such high molecular weight primary products have been actually detected in the gas phase during TMB photo-oxidation experiments and for them an important role in the initiation of the TMB-SOA nucleation process have been inferred (Whyche et al., 2009; Rickard et al., 2009).

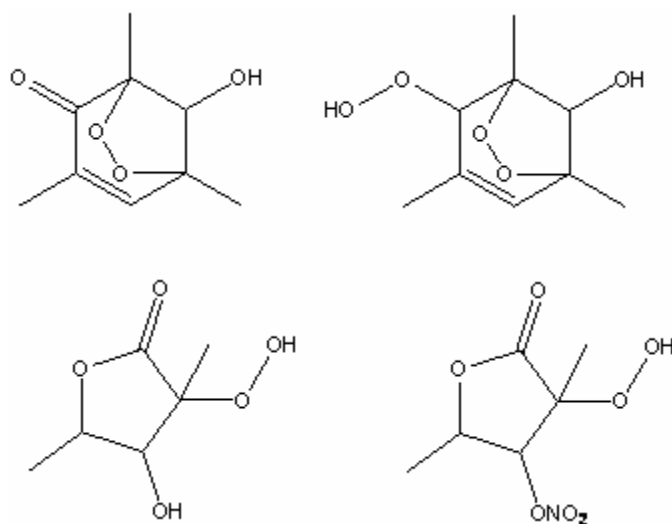


Figure 24. Examples of structures considered to made a significant contribution to the simulated TMB SOA mass.

The presence of methyl groups within these structures which have resonance among the alkyls spectral range are highlighted in the following figure (fig. 9) using light-blue spots for methyl groups in beta position to an oxygen atom (H-C-C-O) and orange spots for methyl groups bound to sp^2 -hybridized carbons (H-C-C=). The same distinctive colours were used for these functional groups in the above pie-graph (fig. 25).

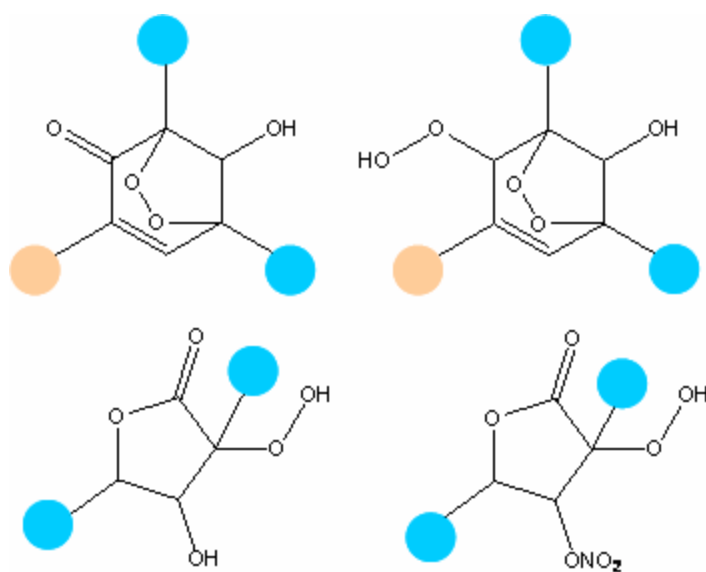


Figure 25. The above figure with coulored spots highlighting HC-C= (orange) and HC-C< (blue) functionalities.

3.2.3 Oligomerization reactions with methyl glyoxal

In the frame of the chemistry of SOA formation and transformation considerable attention has been paid to condensed phase reactions. Even in the Johnson et al. paper, the need to scale the gas-to-particle partitioning coefficients in the simulated SOA mass to fit the measured SOA mass suggested a significant occurrence of association chemistry in the condensed organic phase.

Experimental evidence of accretion reactions (i.e. non-oxidative association reactions occurring in condensed phase) involves the detection of high-MW species in laboratory-generated as well in ambient aerosol (Hallquist et al., 2009). In respect to TMB photo-oxidation experiments, Kelberer et al. (2004) have shown that accretion reactions take place within the particles resulting in oligomers molecules and suggested that the observed oligomers could be formed by the polymerization of methyl glyoxal. Low molecular weight dicarbonyls, particularly aldehydes like methylglyoxal, are expected to occur on mature SOA particles in the form of oligomers.

Methyl glyoxal (MG) is a first generation product of the OH-initiated oxidation of TMB and it is produced in large amounts based on branching ratios predicted by the MCM v3.1 (fig.23).

Moreover, in a recent study on TMB photo-oxidation, MG exhibited experimental gas/particle partitioning coefficient several order of magnitude higher than theoretically expected, based on its vapour pressure (Healy et al., 2008).

The following figure reports only few products (acetals) possibly formed via methylglyoxal uptake and subsequent reactions in particle-phase along with coloured spots highlighting the methyl groups (fig. 26).

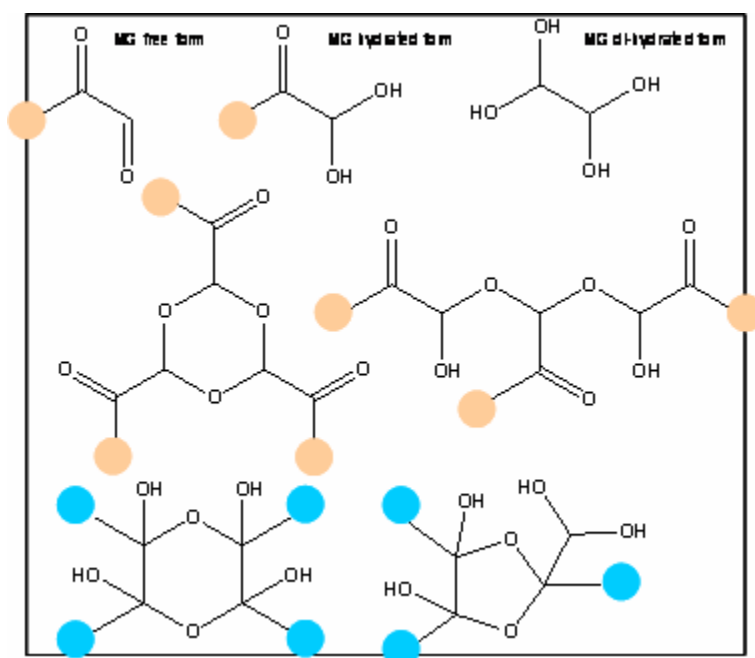


Figure 26. Examples of structures formed via methylglyoxal uptake in condensed phase and (hemi)acetals formation. Light-blue spots stand for methyl groups in beta position to an oxygen atom (H-C-C-O) and orange spots for methyl groups bound to sp²-hybridized carbons (H-C-C=).

The occurrence of H-C-C= and H-C-C-O groups in large amounts in MG condensation products was confirmed by recording ¹H-NMR spectra of MG oligomers synthesized in laboratory (fig. 27).

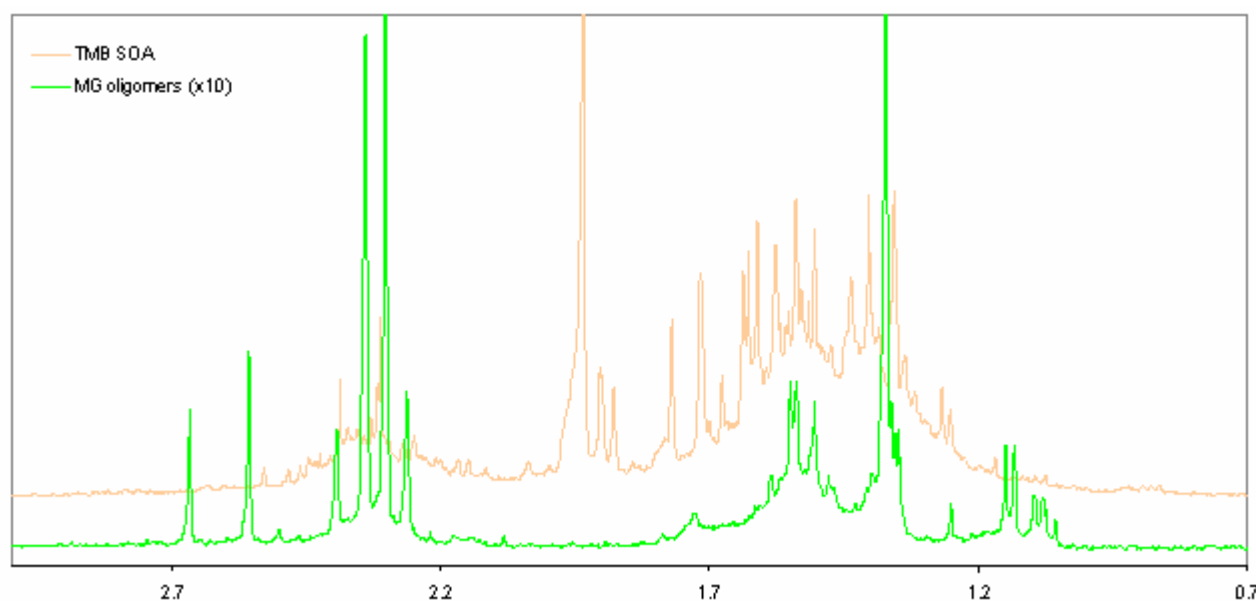


Figure 27. ¹H-NMR spectra in D₂O of methylglyoxal oligomers (green line) and a TMB SOA sample (TMB_##) (orange line). The horizontal scale reports the chemical shift (ppm). Only the alkyl spectral region is shown.

Together with the multifunctional O₂-bridged compounds formed by oxidation reactions (fig. 25), also compounds having chemical structures like those of (hemi)acetal oligomers formed via methylglyoxal uptake in the condensed phase could actually contribute in substantial amount to the TMB SOA composition.

3.3 Comparison between ambient organic aerosol and laboratory-SOA

3.3.1 Ambient organic aerosol

A substantial amount of atmospheric aerosol samples (about 150) has been collected across Europe in the frame of the European EUCAARI project and analyzed within this thesis. As already mentioned in the experimental section, the six sampling sites were mainly selected on the basis of their different characteristics of their environment in respect to the sources of carbonaceous aerosol in Europe. Since most of the intensive measurements campaigns took place between the months of March and July, the data resulted as well in a recent overview of the aerosol chemical composition over Europe in spring seasons.

Night-time and day-time samplings, lasting roughly 12 hours, were generally carried out, except for the clean background sites where longer sampling times were applied to collect enough material for the analyses. The chemical composition of the fine aerosol samples collected on quartz-fiber filters have been investigated off-line following the analytical protocol described in the experimental section, and both organic and inorganic components have been characterized. The latter have been used in this study primarily as supporting information for tracing the origin and type of carbonaceous particles. Indeed, inorganic components can be used as tracers for aerosols being transported at the regional scale (sulphate), or anthropogenic semivolatile (nitrate), originating from biomass burning (potassium), or from sea-spray (seasalt).

The organic composition of the samples showed quite different chemical features depending on both the site as well the atmospheric conditions present during the sampling. As expected, the lowest carbon concentrations were found in the remote areas (Mace Head, Hyytiälä) with respect to those collected at the sites closer to anthropogenic emissions. The following plots show these trends for the measured total and water-soluble carbon concentrations (fig.28).

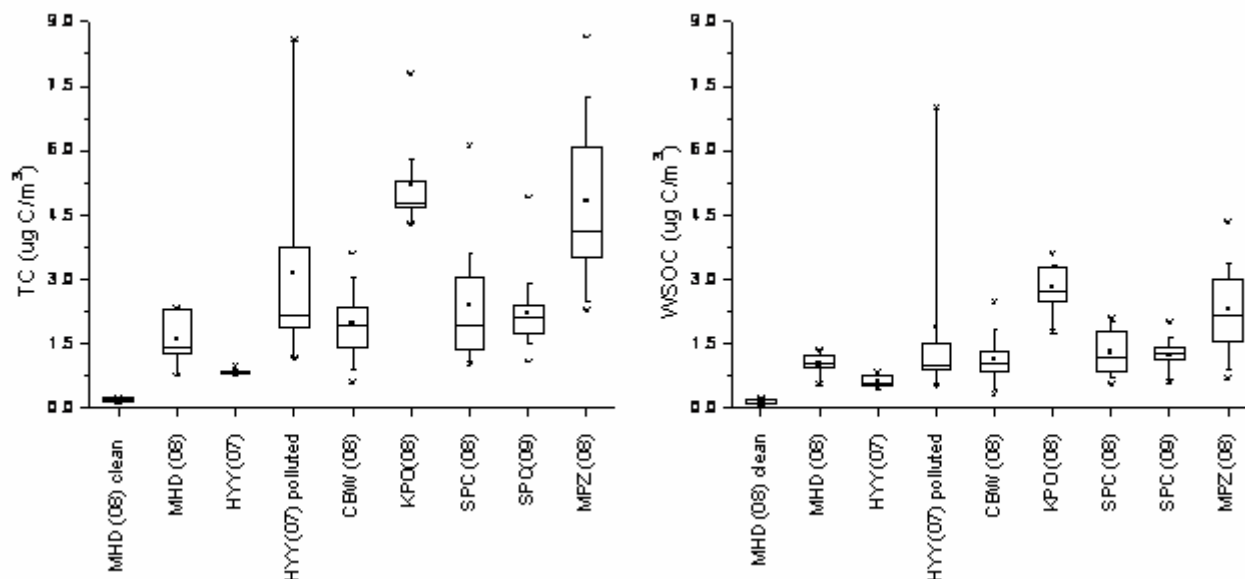


Figure 28. Box-and-whiskers plots for the total and water-soluble carbon averaged concentrations, left and right panel respectively. Box and whiskers denote the 10th, 25th, 50th, 75th, 90th percentiles. Maximum and minimum values are represented by the stars while the squares indicate the mean values.

In these plots are reported the averaged values obtained within each sampling site.

Data resulted from samples collected at Mace Head and Hyytiälä were further classified into “clean” and “polluted” subsets, based on particulate matter and trace gases concentrations and meteorological parameters. In the station of Mace Head, a computer-based sampling system ensured the selective collection of background marine particles coming from the so-called “clean sector”. Air masses were thus defined “clean” according to the following criteria: a) reaching the site from the oceanic sector between 180 and 300 degrees, b) having a total particle number concentration below 700 cm^{-3} , and c) having black carbon concentration below 50 ng m^{-3} . As can be seen from the figure 1, the background marine particles sampled in clean sector regime showed actually the lowest carbonaceous content with respect to the other samples, in terms of both water-soluble as well water-insoluble carbon content.

A rough classification of the samples collected in the Finnish forest station (HYY) was carried out by dividing the series in “clean” and “polluted” subsets on the basis of: a) total carbonaceous concentrations, b) nitrate and sulphate ions contents as derived from the AMS data, and c) air mass backtrajectory analysis (fig.2). A similar approach was adopted by Cavalli et al. (2006) for a previous intensive field campaign in Hyytiälä.

Basically, the average TC and WSOC concentrations of the polluted MHD and HYY series are in the same range of those measured in the other continental sites. Among all sites, the series of samples collected in Melpitz resulted to have in average the highest TC and WSOC contents.

The averaged WSOC/TC ratios are shown for each site in the following plot (fig.29). Two different WSOC/TC ranges can be clearly distinguished: a) the samples collected in continental areas, including those collected in Hyytiälä when the site were impacted by air masses transported from Eastern/Central Europe, and b) the samples collected in marine areas together with HYY samples collected in the “clean” period, having the latter (b-type) higher water-soluble organic fractions with respect to the former (a-type).

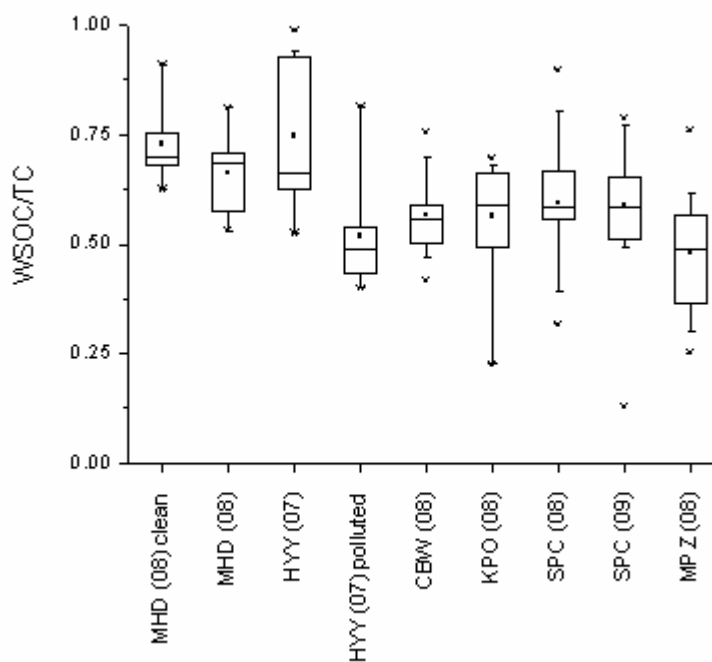


Figure 29. Box-and-whiskers plots for the WSOC/TC averaged ratios. Box and whiskers denote the 10th, 25th, 50th, 75th, 90th percentiles. Maximum and minimum values are represented by the stars while the squares indicate the mean values.

The higher WSOC/TC ratios found in b-type samples reflect likely a major contribution of sources of secondary organic carbon (SOC), or vice versa a minor contribution of primary organic carbon (POC), with respect to the a-type samples. In fact SOC is expected to be mostly comprised in the WSOC fraction, being composed primarily of oxygenated compounds highly water-soluble. Another possible contribution to aerosol WSOC is biomass burning smoke. For this reason, measurements of WSOC has been used in the past as a proxy for secondary organic carbon after correction for the contribution of biomass burning emissions, estimated through EC- or levoglucosan- tracer methods (Snyder et al., AST 2009; Decesari et al. 2001; Szidat et al. 2004; Docherty et al. 2008; Stone et al. 2008).

3.3.2 Clusters analysis applied to $^1\text{H-NMR}$ spectra of ambient organic aerosol

In order to achieve a closer insight to the chemical composition of the water-soluble organic compounds constituting the collected ambient aerosol, $^1\text{H-NMR}$ spectroscopy has been exploited, providing a unique data base of $^1\text{H-NMR}$ spectra of atmospheric particulate matter samples.

The spectral features of the various samples has been found to reflect roughly the distinct patterns just observed on the basis of the WSOC/TC ratios, i.e. showing the marine particles, and particularly those collected in clean sector conditions, the mostly evident distinctive characteristics with respect to the rest of the samples. Clusters analysis has been therefore applied to the $^1\text{H-NMR}$ spectra with the aim to group together samples with similar features obtaining few groups representing the different typologies.

In particular, agglomerative hierarchical clustering has been applied, with a complete linkage method and a Pearson-distance metric, as this method should produce well separated, small and compact clusters. The algorithm starts with each object (i.e. each $^1\text{H-NMR}$ spectrum) in its own cluster and in following steps the spectra with the highest similarity degree are joined. Each step result in one fewer cluster number than the step before, until at the end all objects are in one cluster. The hierarchy of the clusters obtained for the ambient aerosol samples is displayed in the binary tree in the following figure (fig. 30).

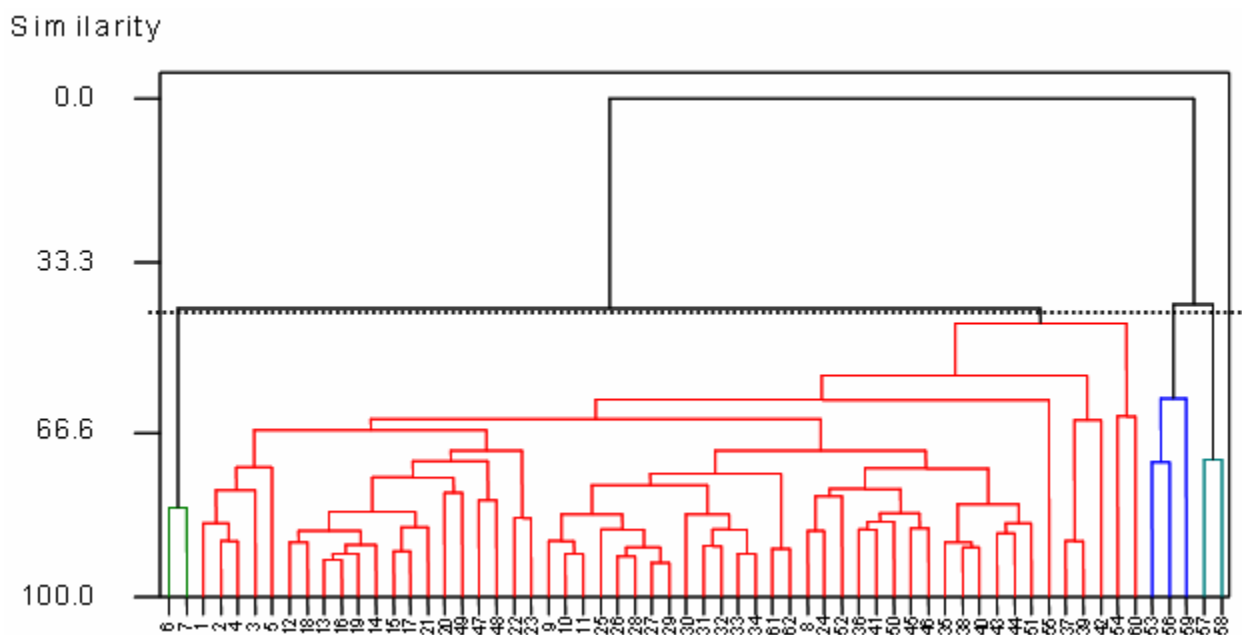


Figure 30. Dendrogram displaying the hierarchy of the clusters obtained from the ambient aerosol samples. The terminal nodes at the bottom of the tree are clusters containing a single spectrum. Numbers were assigned to each samples instead of their extended labels in order to make the horizontal axis less crowded. The vertical axis indicates the similarity level at which the clusters were formed. The horizontal black line cutting the tree at about 50% of similarity level serves merely to better visualize the clusters described in the discussion.

Cutting the tree at a specified similarity level a certain number of clusters is determined. At a similarity level of about 50%, the various spectra merged basically into 3 main groups: 1) one group containing only the two samples collected at Mace Head during clean sector conditions (on the left of the dendrogram), thus linked to a marine biogenic source; 2) one group containing few samples collected at Hyytiälä mostly in clean conditions, thus corresponding to a terrestrial biogenic source on the right of the dendrogram), and 3) one very crowded cluster including the samples collected in the continental areas plus the samples collected at Mace Head and in Hyytiälä under polluted conditions.

The resulted three cluster centroid spectral profiles representing the above-listed three source typologies are shown in the figure below (fig. 31).

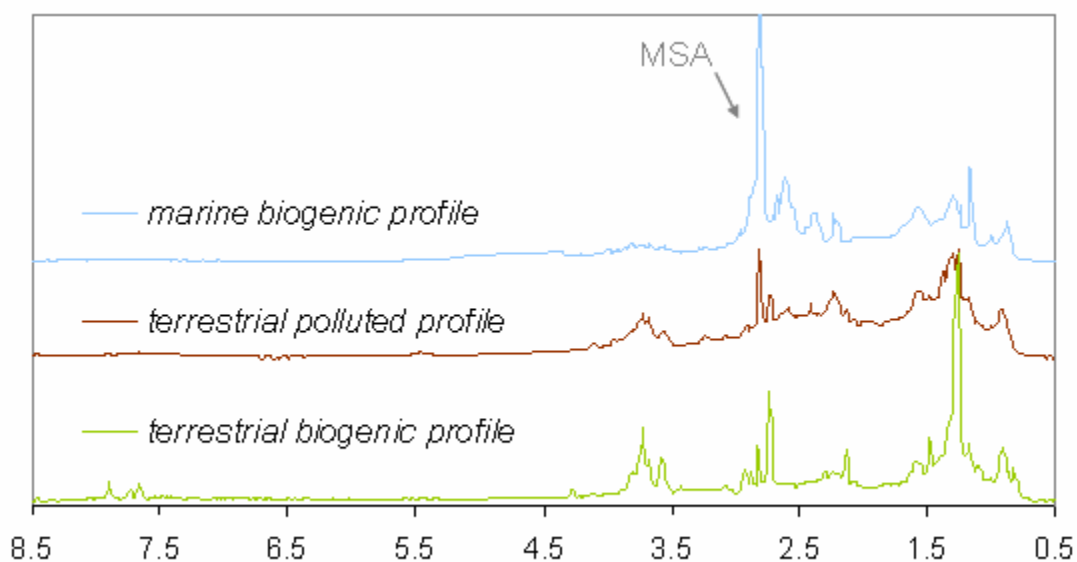


Figure 31. Cluster centroid spectral profiles resulting applying hierarchical clustering to the series of ^1H -NMR spectra of ambient aerosols and cutting the clustering at 50% similarity level. At 2.82 ppm is indicated the peak of methanesulfonic acid (MSA).

It is worth to notice that these three cluster centroids correspond to the averaged spectral profiles of samples belonging to clusters which have together a very low similarity degree, nevertheless cutting the tree at increased similarity levels (e.g. 66%), the same basic pattern is still recognizable, being these three main clusters just divided in smaller subgroups.

Interestingly, applying a further cluster analysis to the samples of group 3, i.e. selecting only the samples having a polluted continental source profile, they resulted split into other two main subgroups, with one tracing biomass burning products (fig.32).

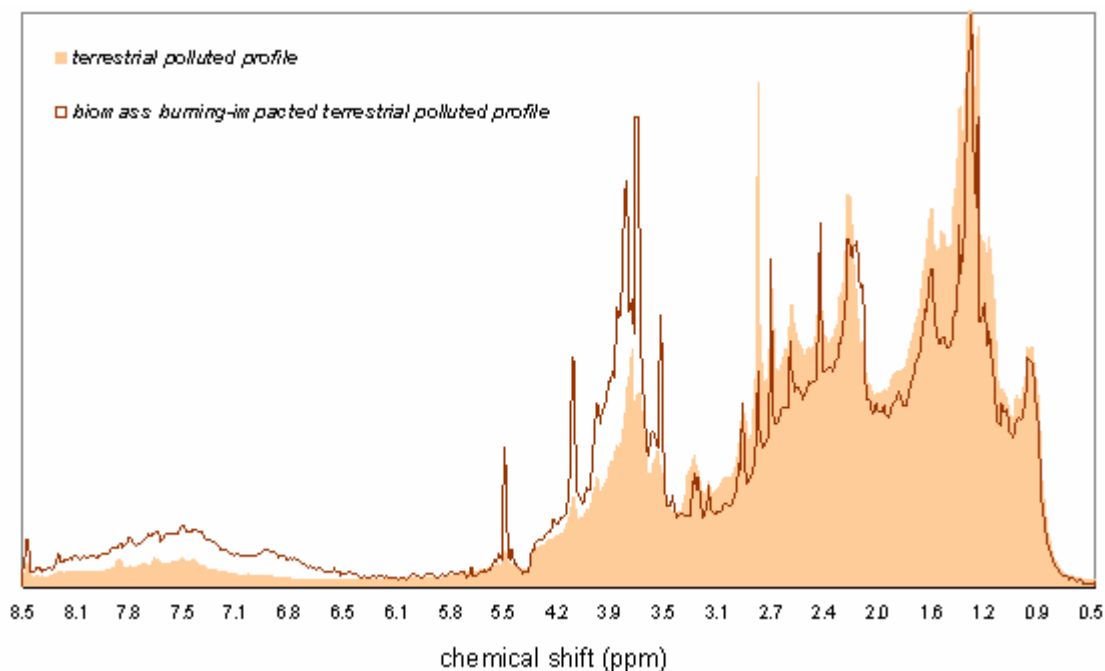


Figure 32. Cluster centroid spectral profiles resulting applying hierarchical clustering to the series of $^1\text{H-NMR}$ spectra of samples included in group 3, i.e. the samples having a polluted continental profile.

The major organic components of particles emitted by biomass burning are mostly monosaccharide derivatives (polyols) from pyrolysis of cellulose, thus their $^1\text{H-NMR}$ spectra exhibit intense bands due to protons adjacent to hydroxyl and alcoxyl groups (H-C-O). Among these polyols, levoglucosan has been widely used as tracer for biomass smoke. The signals of levoglucosan have been clearly identified in the spectral profile attributed to biomass burning-impacted samples and the identification has been confirmed by comparison with the standard compound (fig. 33).

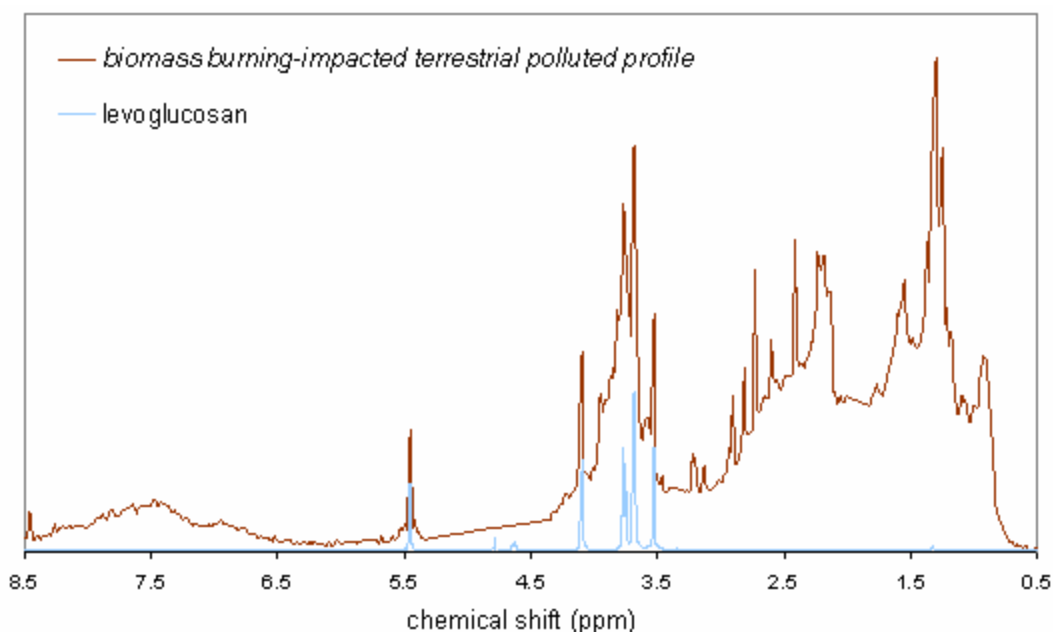


Figure 33. Cluster centroid spectral profile of biomass burning-impacted terrestrial polluted samples (brown line) and $^1\text{H-NMR}$ spectrum of levoglucosan (light blue line).

Our findings indicate that biomass burning accounts for a common organic aerosol type in rural continental areas, confirming previous studies which have suggested that this source can contribute up to 30 % (on annual basis) to the organic matter constituting the European aerosol background (Puxbaum et al., 2007).

3.3.3 Relationship between functional group distribution and WSOC sources

Functional group compositions of all the collected ambient samples have been calculated by the integration of the corresponding bands in the $^1\text{H-NMR}$ spectra in order to determine the functional group patterns characterizing each cluster of samples, distinguished above merely on the basis of their overall spectral profiles (fig. 30).

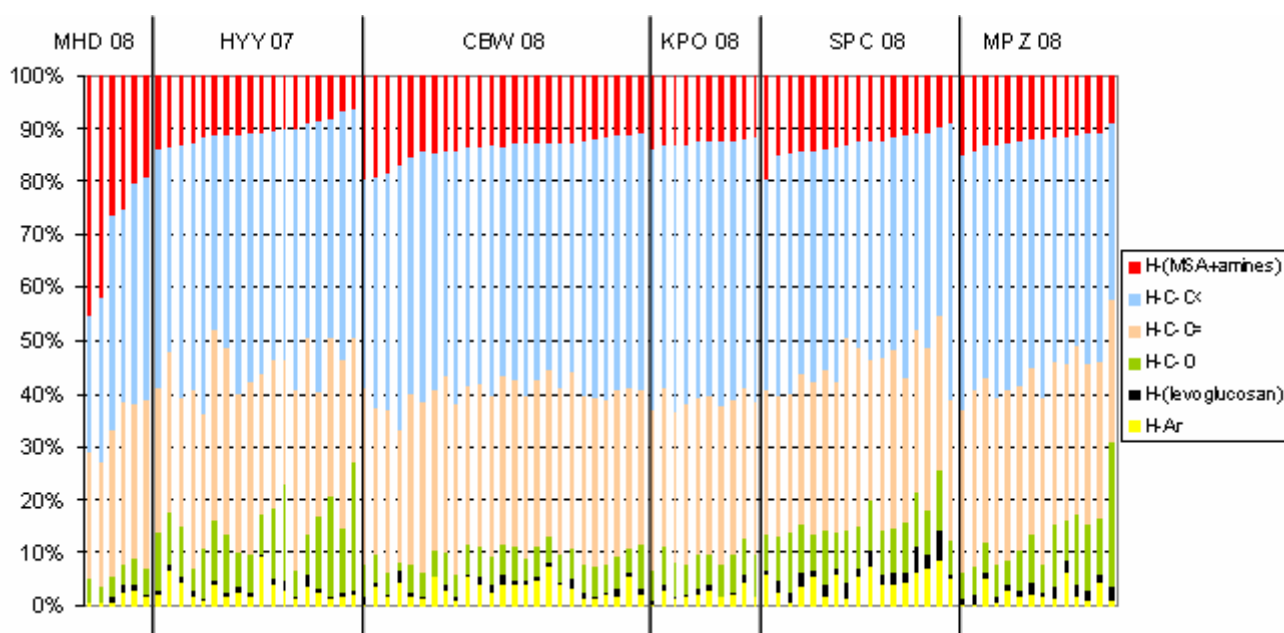


Figure 34. Relative abundances of the protons attributable to the main functional groups (or species) quantified in $^1\text{H-NMR}$ spectra of ambient WSOC and expressed as percentages of the total signal. In the horizontal axis are the series of samples lumped for the various sampling sites. Within each series, the samples are listed from the left to the right as decreasing “MSA + amines” content.

In figure 34 are reported the relative concentrations (in % of the total signal) of organic hydrogen corresponding to main functional groups of WSOC in the analyzed ambient aerosol samples. The samples in the graph are grouped together on the basis of the different sampling sites. and, within each series, they are listed from the left to the right side as the “MSA + amines” content decreases. The functional group composition of marine atmospheric particles is strongly dominated by the MSA signal, particularly in the case of the samples collected at Mace Head with air masses coming from the clean sector, where the signal corresponding to MSA and amines represents up to 45% of the total signal (first two samples starting from the left). Conversely, the samples collected in the other sites show a quite limited variability in the functional group composition.

Recently, the $^1\text{H-NMR}$ functional group compositions of WSOCs from different environments have been already explored, providing characteristic $^1\text{H-NMR}$ fingerprints for at least three major aerosol

sources: emission from the ocean, biomass burning and secondary formation from anthropogenic and biogenic emissions (Decesari et al., 2007). The analysis involved two indexes for the aliphatic functional group composition, i.e. the fraction of aliphatic carbon accounted for by hydroxyl groups ($\text{H-C-O} / \text{sum aliphatics}$) and the fraction of aliphatic carbon accounted for by carbonyls/carboxyls groups ($\text{H-C-C=O} / \text{sum aliphatics}$). A third index expressed the ratio of aromatic moieties to total aliphatic groups. The observed variability of the composition of few samples selected as representative for the above-mentioned sources allowed to assign for each source type specific areas of the scatter plot reporting these two indexes (fig. 35).

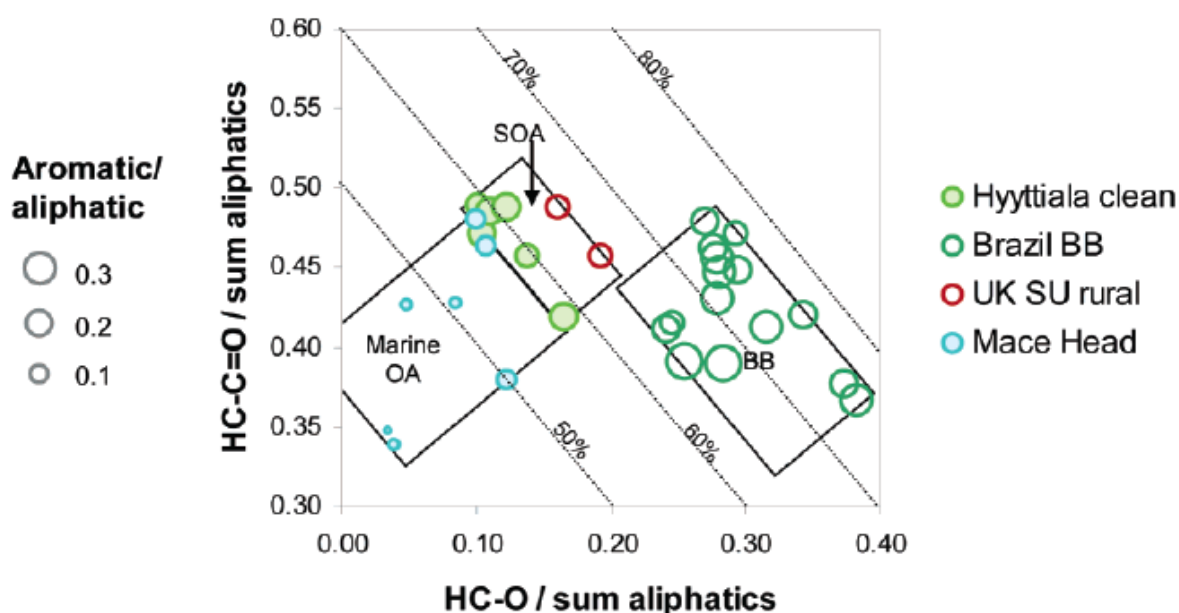


Figure 35. Functional group distribution of WSOCs samples of specific aerosol sources. Diagonal lines represent the percentage fraction of total oxygenated groups ($\text{H-C-O} + \text{H-C-C=O}$). The rectangular areas mark the regions assigned to marine OA, SOA, and biomass burning (BB) aerosols. Figure taken by Decesari et al. (2007).

The four sets of samples shown in the figure 35, for which a source apportionment had already been performed on the basis of the study of the back-trajectories, the analysis of chemical tracers and the emissions known to impact the sampling sites, fall in different areas in the diagram. As can be seen, biomass burning samples (Brazil BB) are characterized by the highest hydroxyls to alkyls ratio occupying the lower right corner of the diagram. Clean marine aerosol are characterized by the lowest fraction of total oxygenated groups appearing in the lower left corner. Anthropogenic and biogenic SOA are similarly characterized by a slightly higher content of carbonyls and form a crowded region in the middle of the scatter plot.

The two indexes related to the aliphatic composition have been calculated for the ambient samples collected within this thesis work in order to compare their functional group compositions with those characteristic of the three main WSOCs sources identified in the study of Decesari et al. (2007).

The measured hydrogen contents of the $^1\text{H-NMR}$ functional groups were converted into carbon contents using H/C molar ratios on the basis of the corresponding expected stoichiometry, i.e.:

	H-Ar	H-C-O	H-C-X	H-C-C=	H-C-C<
H/C expected molar ratio	0.4	1.1	2	2	2

Moreover the unsaturated carbon (H-C-C=) have been exploited to estimate the amount of the oxygenated unsaturated aliphatic groups (H-C-C=O) upon the subtraction of the fraction corresponding to the benzylic groups (H-C-Ar), assuming these groups to be proportional to the measured aromatic protons (specifically it has been considered one benzylic substituent per aromatic ring).

Functional group distributions for the whole set of ambient samples analyzed in this thesis work are plotted in the following figure (fig. 36), together with those obtained for SOA from the laboratory studies. The rectangular areas defining the functional group compositions of biomass burning OA, marine OA and secondary OA, based on the previous studies, are kept in this figure with the aim of comparison between the present and past data sets.

The Mace Head samples collected on May 2008 show a composition within the same range observed in the previous campaigns at the same site, while most of the samples collected at the continental polluted sites and in the forest site exhibit a functional group distribution which overlap with that previously assigned to SOA, although with a lower carbonyl/carboxyl content compared to past studies (Decesari et al., 2007). Finally, only a few samples from the Po Valley (San Pietro Capofoume, March-April 2008) show a compositions which appears to be partly affected by biomass burning aerosols. The samples collected in the Finnish forest station (HYY 07) appear partly included into the SOA sector, but showing scattered plots also in areas of the diagram of unexplained assignment.

The compositions of laboratory-generated SOA did not overlap with any of the areas characteristic of ambient oxidized aerosol samples. In particular, anthropogenic SOA, having been generated by a single VOC precursor (trimethylbenzene) show the most distinct functional group composition and are characterized by the lowest carbonyl/carboxyl content. Conversely, biogenic SOA generated from mixtures of monoterpenes (MT-SOA) show the highest amount of oxygenated unsaturated groups. Finally, both laboratory-SOA types are characterized by a lower content of hydroxyls groups with the majority of the continental ambient OA samples.

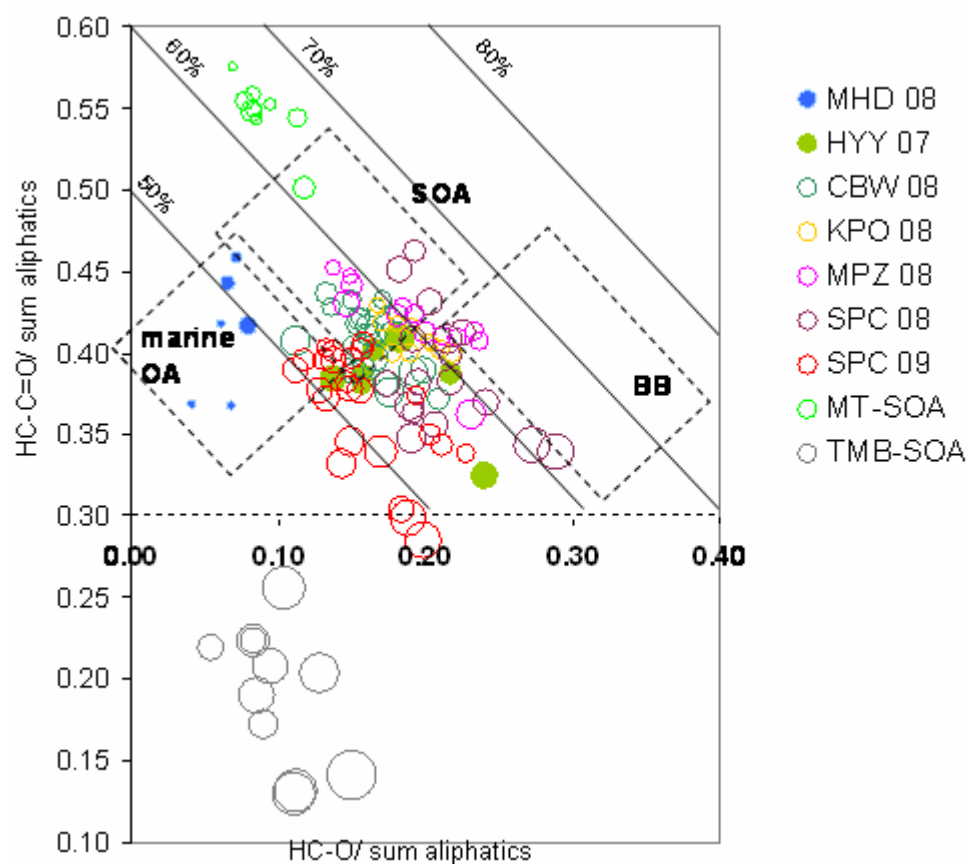


Figure 36. Functional group distribution of WSOCs samples analyzed within this thesis work, including those obtained in laboratory experiments starting from anthropogenic and biogenic precursors (TMB-SOA and MT-SOA). Distinguishing colours are used for ambient samples collected at different sites.

3.3.4 Identification of biogenic SOA based on NMR spectral signatures observed in chamber experiments and at pristine forest sites

The set of samples collected at Hyytiälä in spring 2007 was analysed with the main objective of deriving an NMR spectral fingerprint for biogenic SOA in an unperturbed, unpolluted, environment.

As already stated in the paragraph 3.3.1, the series of samples were preliminary classified on the basis of the back-trajectories analysis. The series of samples has been divided into “clean” or “polluted” subsets depending on the origin of the air masses reaching the forest station, and considering also the time spent over the land, and its population density encountered along the air mass transport (fig. 37). A similar approach was already tested for other measurement intensive campaigns held in Hyytiälä (Cavalli et al., 2006; altre referenze).

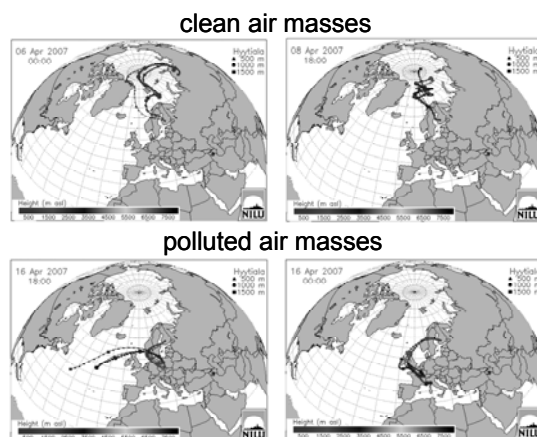


Figure 37. Air mass back trajectories arriving at Hyytiälä calculated by FLEXTRA model from the Norwegian Institute of Air Research (<http://www.nilu.no/trajectories/index.cfm>). Clean period – Arctic air masses; Polluted period – air masses from Eastern/Central Europe. (Figure taken by Alves et al.)

Further classification was provided by measurements performed in parallel to the filter sampling with an Aerodyne quadrupole aerosol mass spectrometer (Q-AMS). Q-AMS measures mass concentrations of non-refractory species including sulphate, nitrate, ammonium ions and organics from submicron particles, and can be used to trace the transport of polluted air masses with a sub-hourly time resolution.

Total carbon and water-soluble carbon concentrations determined for the filter samples collected in Hyytiälä, together with their classification, are listed in the table below (tab.6).

In summary, many samples were collected in very clean conditions, i.e. those with $TC < 1 \mu\text{gC}/\text{m}^3$ and labelled as background organic aerosol in the table. Moderately polluted air masses were

sampled between 15th and 17th of April and an intense pollution outbreak was also observed at the beginning of the period (30th March).

sample ID	sampling start	sampling stop	WSOC ($\mu\text{gC}/\text{m}^3$)	TC ($\mu\text{gC}/\text{m}^3$)	classification extracted from Q-AMS data
HYY_29_03_07_D	29/3/07 6:52	29/3/07 17:20		5.3	polluted
HYY_30_03_07_D	30/3/07 7:02	30/3/07 20:20	6.9	8.6	polluted
HYY_30_03_07_N	30/3/07 20:30	31/3/07 8:40	0.60	0.82	background
HYY_31_03_07_D	31/3/07 8:50	31/3/07 19:45	0.53	0.84	background
HYY_01_04_07_D	1/4/07 8:43	1/4/07 21:09	0.46	0.87	background
HYY_02_04_07_D	2/4/07 8:40	2/4/07 20:30	0.54	0.83	background
HYY_02_04_07_N	2/4/07 20:38	3/4/07 8:59	0.71	0.76	background
HYY_05_04_07_D	5/4/07 9:10	5/4/07 19:12	0.51	0.78	background
HYY_07_04_07_D	7/4/07 8:00	7/4/07 19:30		0.78	background
HYY_08_04_07_D	8/4/07 9:05	8/4/07 18:43	0.75	0.89	background
HYY_11_04_07_D	11/4/07 8:21	11/4/07 19:47	0.83	0.84	background
HYY_12_04_07_D	12/4/07 8:07	12/4/07 19:04	0.76	0.81	background
HYY_14_04_07_D	14/4/07 8:54	14/4/07 20:29	0.57	0.97	background
HYY_15_04_07_m	15/4/07 8:44	15/4/07 12:25	1.3	2.3	high OM, low SO ₄
HYY_15_04_07_a	15/4/07 12:29	15/4/07 20:00	1.0	2.0	high OM, low SO ₄
HYY_15_04_07_N	15/4/07 20:03	16/4/07 9:20	0.98	2.2	moderately polluted
HYY_16_04_07_m	16/4/07 9:26	16/4/07 12:00	1.5	3.7	moderately polluted
HYY_16_04_07_a	16/4/07 12:06	16/4/07 22:22	0.92	1.9	moderately polluted
HYY_17_04_07_N	17/4/07 21:04	18/4/07 7:05	0.51	1.2	high OM, low SO ₄

Table 6. Total carbon and water-soluble carbon values obtained for samples collected in Hyytiälä. Sample code: D = day, N = night, m = morning, a = afternoon.

With respect to samples showing low concentrations, the supposed clean samples, not many overlaps was found by the straight comparison of their ¹H-NMR spectral profiles with those of the laboratory biogenic SOA, due likely to the simultaneous presence other sources hindering the biogenic one.

Factor analysis has been applied to the whole collection of ¹H-NMR spectra obtained for the Finnish samples in order to discern the biogenic SOA contribution from those related to other

sources. The factor profiles resulting by applying positive matrix factorization (PMF, EPA 3.0v) on binned (low resolution) spectra using a 4-factor solution, are shown in figure 38. The analysis has been focused only on the aliphatic zone being the rest of the spectrum quite void of signals. The resulted factors have been interpreted as follows:

- 1) a first factor was attributed to polluted oxidized organic aerosol (pollution OOA) based on the similarity with the spectra recorded for samples collected in polluted conditions in the other continental sites. Such factor accounted for most of the signal in the 30th March sample and, to a lesser extent, it contributed to the moderately polluted samples collected in the final part of the campaign.
- 2) a second factor was attributed to unknown species, interpreted as possible contaminants, showing features similar to the spectrum of commercial butyl-glycols and occurring randomly in a subset of samples. These signals have not been found in blank filters but some sampling artefacts or contaminations could not be excluded.
- 3) a third factor included the signals of low-molecular weight amines and MSA and provided the largest contribution to the background aerosol samples, collected when clean arctic air masses reached the site.
- 4) a fourth factor with spectral features very close to those of the biogenic SOA generated in laboratory from the oxidation of terpenes (MT-SOA). The characteristic spectrum of this factor correlated well with the spectrum of aged MT-SOA generated in the SAPHIR chamber. This factor was then attributed to real biogenic oxidized organic aerosols (biogenic OOA).

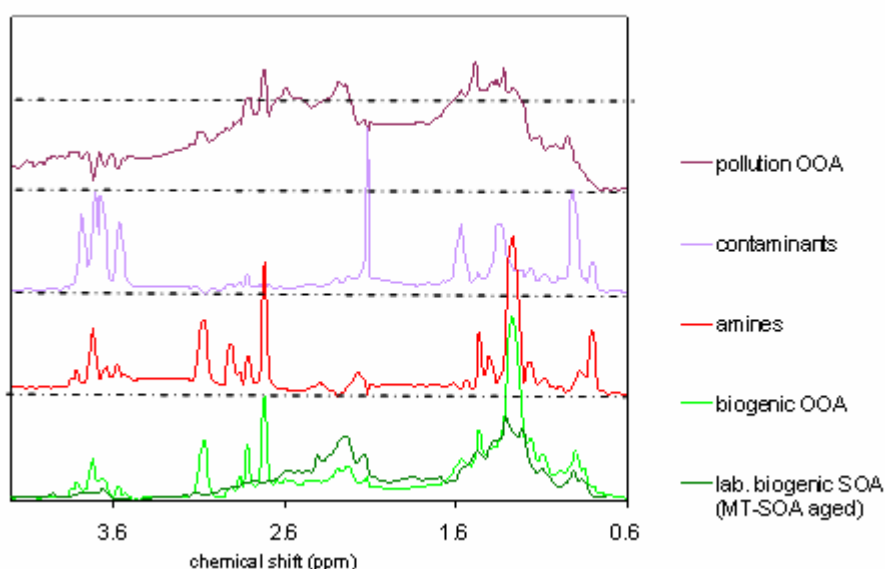


Figure 38. ¹H-NMR factors extracted by applying the factor analysis (PMF) to the Hyytiälä samples. The profile of the factor attributed to aged MT-SOA is also shown for comparison together with that related to biogenic OOA.

The apportionment of the water-soluble carbon based on the extracted four PMF factors is shown in the figure 39 together with the indication of the three identified regimes.

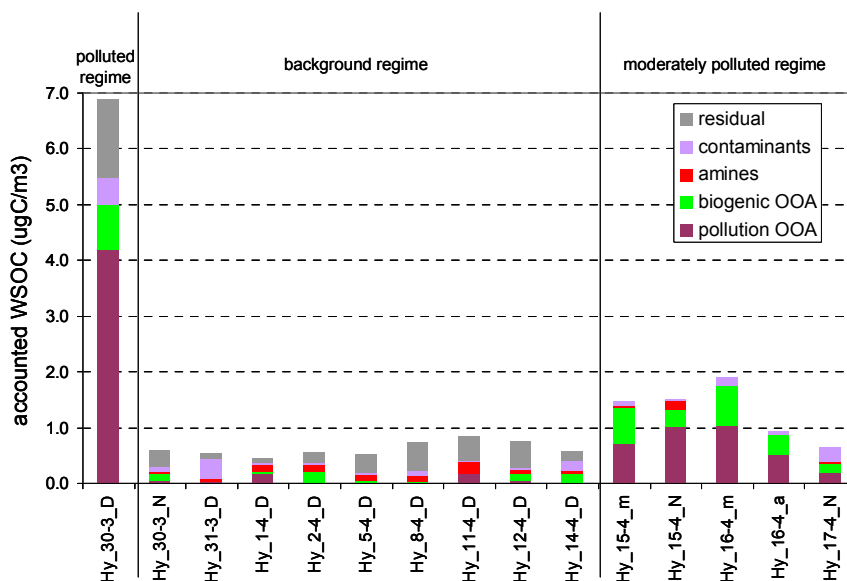


Figure 39. Apportionment of the WSOC based on the extracted ¹H-NMR factors with PMF. Absolute concentrations (µgC/m³). The three above-described regimes are also reported on the top of the figure. Few samples have been excluded from the factorization due to very low signal to noise ratios.

The relative contribution of each factors to the WSOC of the Hyttiälä samples are shown in the figure 40.

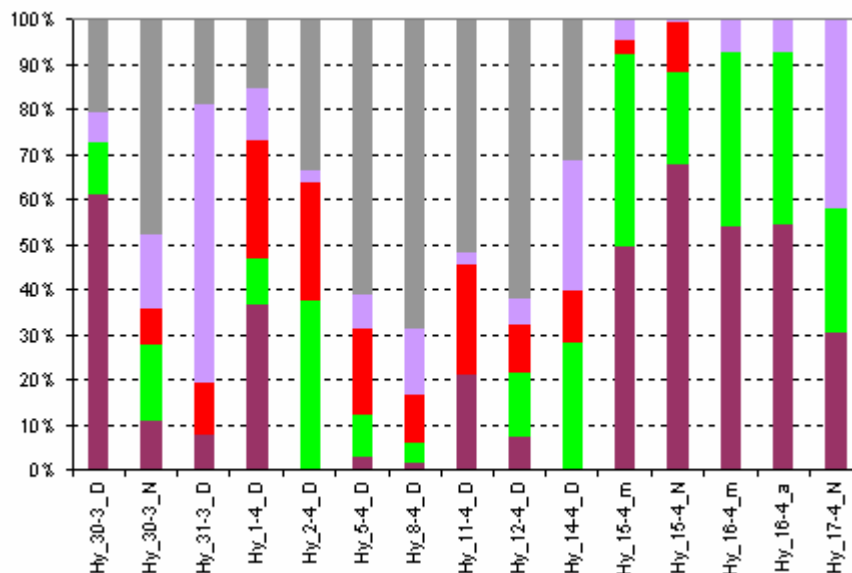


Figure 40. Relative contributions (%) of the PMF factors to the accounted WSOC for the Hyttiälä samples.

Noticeably, the factor associated to amines contributed to the WSOC of samples collected primarily during background conditions, while the relative importance of the factor attributed to biogenic SOA increased during moderately polluted conditions.

These findings suggest that biogenic organic aerosols in Hyytiälä originate from at least two independent sources: condensation of amines and the oxidation of reactive terpenes, with the first process relatively more important at low aerosol concentration regime. The larger fraction of MT-SOA under moderately polluted conditions may be explained by the higher level of atmospheric oxidants promoting the conversion of terpenes to SOA precursors, and also by the greater amount of pre-existing aerosol burden promoting the condensation of semivolatile organic compounds onto particles.

Independent measurements conducted at Hyytiälä during an other intensive observation period held in spring 2005 also indicated that factors related to the biogenic and polluted sources are frequently mixed and that background aerosol at this pristine forest station is not necessarily enriched in biogenic SOA (Raatikainen et al., 2009). In that study, the relative importance of biogenic SOA with respect to polluted OOA was deduced applying PMF to the Q-AMS spectra and following the $m_{44}/(m_{43}+m_{44})$ ratio.

In summary, the findings of that work are in good agreement with those obtained applying PMF analysis to $^1\text{H-NMR}$ spectra.

3.3.5 Ambient organic aerosol vs anthropogenic laboratory-SOA

In order to identify a spectral signature specific for anthropogenic SOA in ambient aerosol, multivariate statistical methods have been also applied to the $^1\text{H-NMR}$ spectra of the water-soluble organic aerosol samples collected in polluted continental sites such as those sampled in San Pietro Capofiume during the intensive field campaign carried out from 31st March to 20th April 2008 (SPC 08).

This set of samples has been chosen because during this observation period distinct conditions typical of continental atmospheric regimes developed. In particular, during the first days of the campaign, until 6th April, and in the middle of the sampling period, between 8th and 10th April, conditions were favourable for the accumulation of pollutants, while the last days were characterized by more ventilation, precipitation and hence removal of pollutants.

The adopted time resolution sampling was 12 hours, from 8:00 to 20:00 and from 20:00 to 8:00 (local times, UTC+2), with the aim to collect day and night samples (fig. 41).

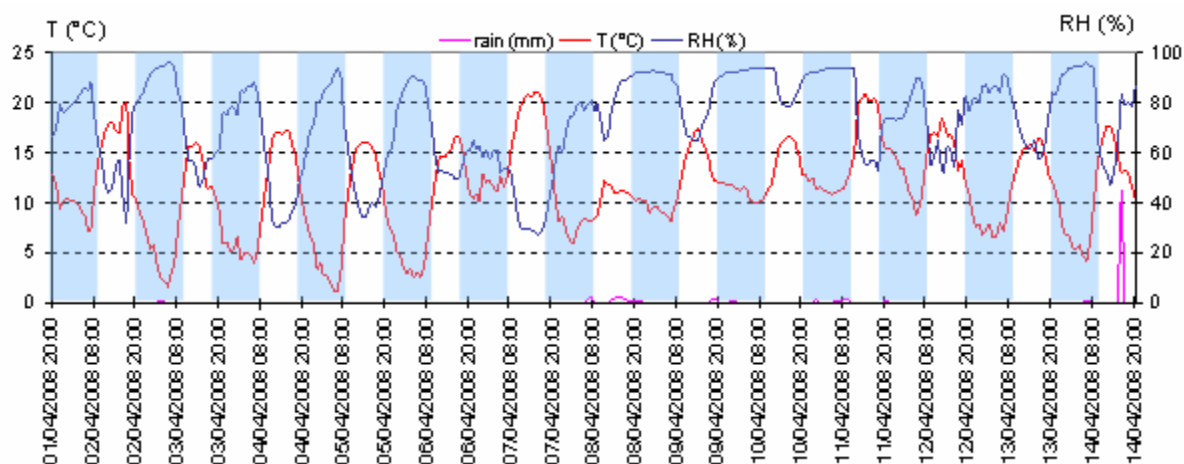


Figure 41. Ground temperature (°C) and relative humidity (percentage) trends measured in San Pietro Capofiume throughout the campaign held in spring 2008. Hourly data produced by the regional environmental agency (ARPA-Emilia Romagna). The light blue and white bars overlapped to the graph refer to night and day filter samples, respectively.

The concentrations trends for major submicron aerosol species including sulphate, nitrate, ammonium ions and organics as measured by an Aerodyne High Resolution ToF-AMS instrument running in parallel with filter sampling are also shown below (fig. 42).

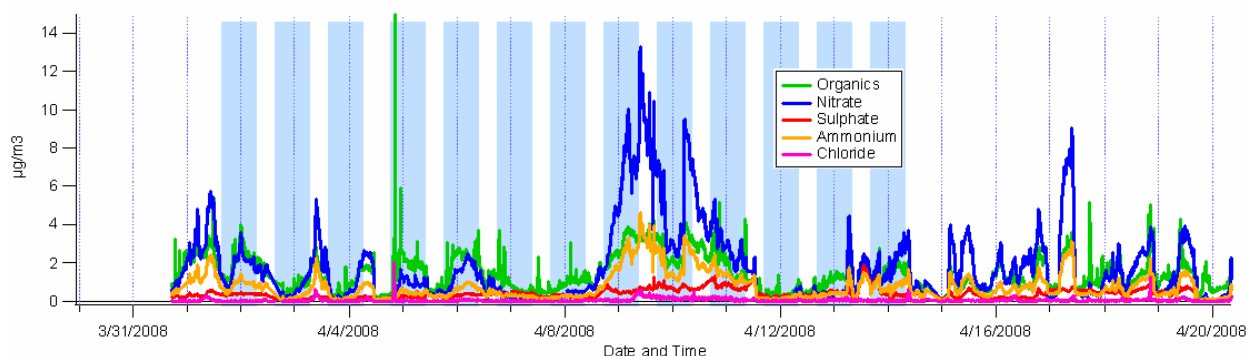


Figure 42. On-line aerosol measurements performed with an Aerodyne HR-ToF-AMS running in parallel with the filter sampling. The light blue and white bars overlapped to the graph refer to night and day filter samples, respectively.

Total carbon and water-soluble carbon concentrations determined for the analyzed filter samples are listed in the following table, where it is also reported the sample classification based on supporting data such as the aerosol chemical composition provided by the HR-ToF-AMS.

Sample ID	sampling start	sampling stop	WSOC ($\mu\text{gC}/\text{m}^3$)	TC ($\mu\text{gC}/\text{m}^3$)	Classification extracted from atmospheric conditions and AMS data
SPC_01_4_08_N	01/04/2008 20:00	02/04/2008 8:00	2.0	6.3	Polluted
SPC_02_4_08_N	02/04/2008 20:24	03/04/2008 7:58		1.4	Polluted
SPC_04_4_08_D	04/04/2008 8:17	04/04/2008 20:03	1.1	1.3	Polluted
SPC_04_4_08_N	04/04/2008 20:18	05/04/2008 8:01	2.2	4.9	Polluted
SPC_05_4_08_D	05/04/2008 8:21	05/04/2008 20:00	1.4	1.8	Polluted
SPC_05_4_08_N	05/04/2008 20:23	06/04/2008 8:00	2.1	4.2	Polluted
SPC_06_4_08_D	06/04/2008 8:21	06/04/2008 20:00		2.4	Polluted
SPC_06_4_08_N	06/04/2008 20:29	07/04/2008 8:00	0.92	0.97	
SPC_07_4_08_D	07/04/2008 8:21	07/04/2008 20:00		0.65	Clean (strong winds)
SPC_07_4_08_N	07/04/2008 20:28	08/04/2008 8:01		1.6	
SPC_08_4_08_D	08/04/2008 8:22	08/04/2008 20:00		2.9	(rain)
SPC_08_4_08_N	08/04/2008 20:21	09/04/2008 8:00		4.6	Polluted, high NO ₃
SPC_09_4_08_D	09/04/2008 8:31	09/04/2008 19:58	1.9	4.5	Polluted, high NO ₃
SPC_09_4_08_N	09/04/2008 20:19	10/04/2008 8:00	1.7	2.5	Polluted, high NO ₃
SPC_10_4_08_D	10/04/2008 8:20	10/04/2008 20:00	2.1	3.4	Polluted, high NO ₃
SPC_10_4_08_N	10/04/2008 20:22	11/04/2008 8:00	1.2	1.5	
SPC_11_4_08_D	11/04/2008 8:20	11/04/2008 19:35	0.66*	1.8	Clean
SPC_11_4_08_N	11/04/2008 20:00	12/04/2008 8:01	*	0.67	
SPC_12_4_08_D	12/04/2008 8:25	12/04/2008 19:58	*	1.0	
SPC_12_4_08_N	12/04/2008 20:22	13/04/2008 8:00	0.91*	2.9	
SPC_13_4_08_D	13/04/2008 8:26	13/04/2008 20:00	*	1.2	
SPC_13_4_08_N	13/04/2008 20:22	14/04/2008 8:00	0.82*	1.6	
SPC_14_4_08_D	14/04/2008 8:20	14/04/2008 20:00	*	1.4	

Table 7. Total carbon and water-soluble carbon concentrations ($\mu\text{gC}/\text{m}^3$). Diurnal and nocturnal samples are marked with N and D in sample labels. Asterisks mark samples extracts which were lumped in order to have enough material for NMR analysis.

Finally, we applied Positive Matrix Factorization (PMF, EPA 3.0v) to the set of ^1H -NMR spectra of samples collected at SPC. A simple three-factor solution provided a clear split between the following profiles:

- 1) a first factor containing significant signals from levoglucosan together with other polyols and abundant aromatic compounds. Such factor was attributed to biomass-burning products (BB)
- 2) a second factor containing sharp peaks assigned to low-molecular weight alkylammonium salts and methanesulphonate (MSA) mixed with other aliphatic compounds. Protonated alkylamines were speciated into monomethylamine (MMA), dimethylamine (DMA), trimethylamine (TMA) and triethylamine (TEA), and can be related to the emissions from landfills or incinerators or to those associated to animal husbandry.
- 3) a third factor showing NMR bands attributable to oxidized aliphatic moieties with a smaller contribution from aromatics, with “typical” features for continental pollution aerosols.

The resulted apportionment of WSOC based on the 3-factor solution and the factors profiles are shown in the following figures (fig. 43, 44, 45). Since the carbonaceous material collected in the samples was too low for NMR analysis, their extracts were lumped together. The three resulting combined samples are hereinafter labelled as 11D+11N+12D, 12N+13D and 13N+14D.

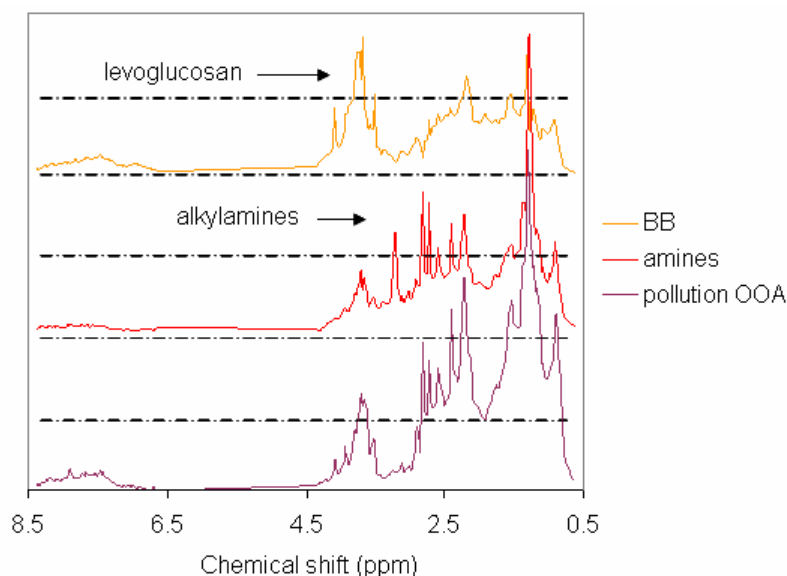


Figure 43. ^1H -NMR factors extracted by applying the factor analysis (PMF) to the SPC 08 samples.

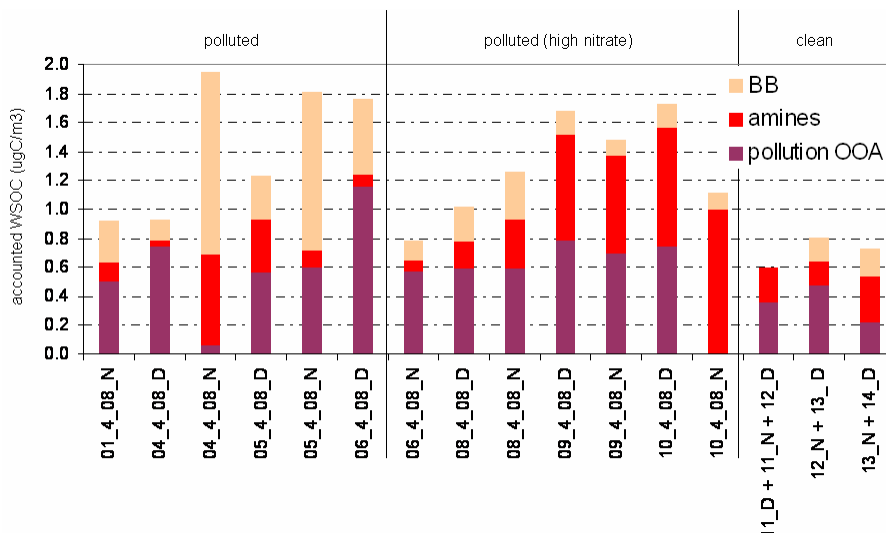


Figure 44. Apportionment of the WSOC based on the three extracted $^1\text{H-NMR}$ factors with PMF. Absolute concentrations ($\mu\text{gC}/\text{m}^3$). The above-described regimes are also reported on the top of the figure. Few samples have been excluded from the factorization due to very low signal to noise ratios.

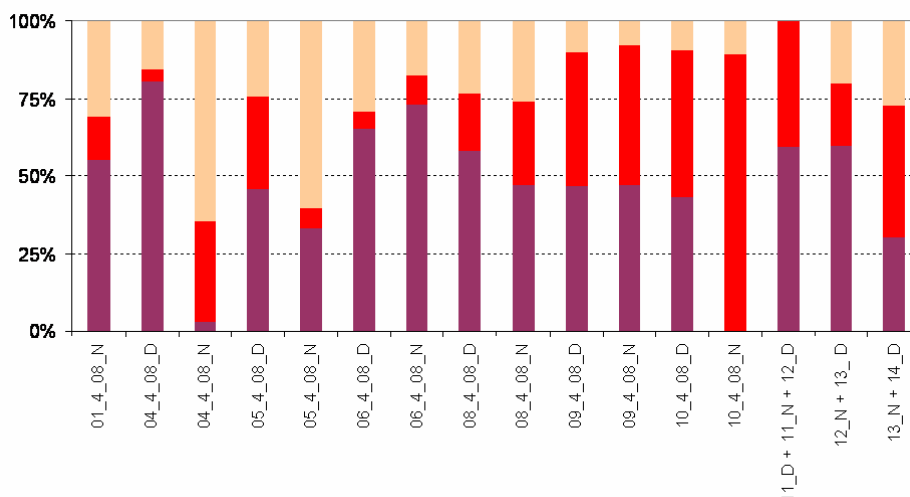


Figure 45. Relative contributions (%) of the PMF factors to the accounted WSOC for the SPC 08 samples

We can observe that the biomass burning (BB) factor contributed largely to the samples from the first (colder) period of the campaign and particularly to the nocturnal samples collected on 4th and 5th April, while the amines factor experienced an increase in the second part of the campaign, when high nitrate concentrations were observed, and reaching the highest values in the 10th April samples. The third factor did not show a clear temporal trend and characterized the WSOC composition in polluted as well as in background conditions. Such factor may result from transported aerosol particles from pollution sources distributed over a vast geographic area, compared to the previous two factors which appears to be related to more local sources in the rural sector of the Po Valley surrounding SPC.

Interestingly, the NMR biomass burning factor concentrations correlate well with those of levoglucosan as measured both by the integration of the $^1\text{H-NMR}$ signal and as well by ion chromatography (fig. 46).

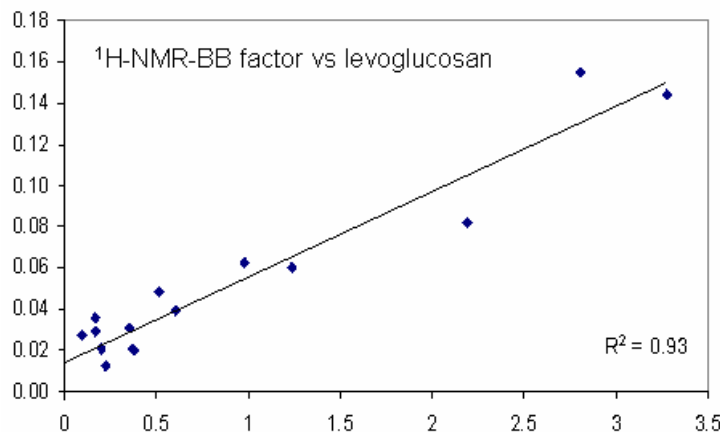


Figure 46. Correlation between measured levoglucosan concentrations and those corresponding to the biomass burning factor expressed in $\mu\text{g}/\text{m}^3$ (using $\text{OM}/\text{OC}=1.8$)

Several studies conducted in both laboratory and as well in areas with high biomass smoke impact have investigated the relationship between levoglucosan and fine particulate matter (Simoneit et al., 1999; Fine et al., 2001; Schmidl et al., 2005). On the basis of these data, conversion coefficients for estimating the contribution of wood combustion from levoglucosan concentrations were derived. The conversion coefficients for the conversion of levoglucosan mass concentration to biomass smoke differs depending on fuels and combustion type (Puxbaum et al., 2007). The organic matter accounted for by biomass burning products (OM_{BB}) in the set of the SPC 08 samples has been reconstructed using the $^1\text{H-NMR}$ biomass burning factor loadings. The adopted OM/OC ratio was 1.8 as suggested for highly oxygenated organics (Russell et al., 2003). Interestingly the OM_{BB} reconstructed via the NMR-BB factor resulted comprised in the range of OM_{BB} values obtained by applying literature conversion coefficients to the measured levoglucosan concentrations (fig. 47). A maximum of 13.5 and a minimum of 2.9 were chosen among the available literature $\text{OC}/\text{levoglucosan}$ ratios, on the basis of the expected fuel type for this site.

These results, indicating that the OM_{BB} is found and quantified similarly by NMR BB factor and by levoglucosan concentrations, suggest that the interpretation of the BB NMR factor can be considered quite robust. At the same time, NMR analysis provides a new quantitative way to estimate the PM fraction accounted for by biomass burning whenever there is significant uncertainty in the conversion coefficients to be applied to levoglucosan concentrations in retrieving OM_{BB} .

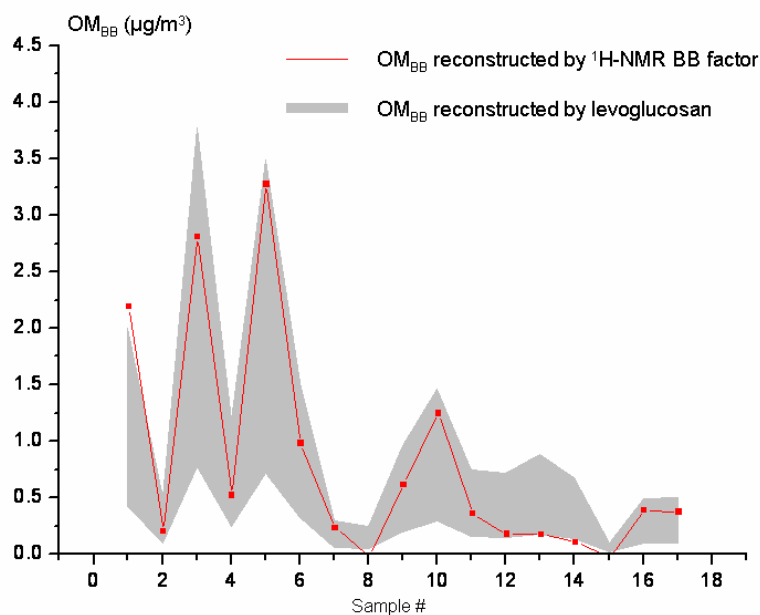


Figure 47. Organic matter accounted for by biomass burning products (OM_{BB}) in the SPC 08 samples. Red points refer to OM reconstructed from 1H -NMR-BB factor. The grey area limits the OM_{BB} range obtained by levoglucosan concentrations and applying literature OC/levoglucosan ratios between 2.9 and 13.5. The OM/OC ratio adopted in both cases was 1.8. Samples are marked with progressive numbers in the x-axis.

Since none of these three factors showed features resembling those characterizing laboratory-generated anthropogenic SOA, PMF solutions with increasing number of factors were tested with aim to discern new factors with a better correlation with the spectra of anthropogenic SOA formed by aromatic hydrocarbon oxidation.

A 4-factor solution provides an additional split of the former third factor into two OOA types, but also a partial refinement of the amine factor, whereas the biomass burning factor is little affected. The apportionment of WSOC based on 4-factor solutions of NMR PMF analysis is plotted in fig. 48. Nevertheless, none of the factors obtained applying PMF with increased solutions numbers resulted to overlap with those of TMB-SOA.

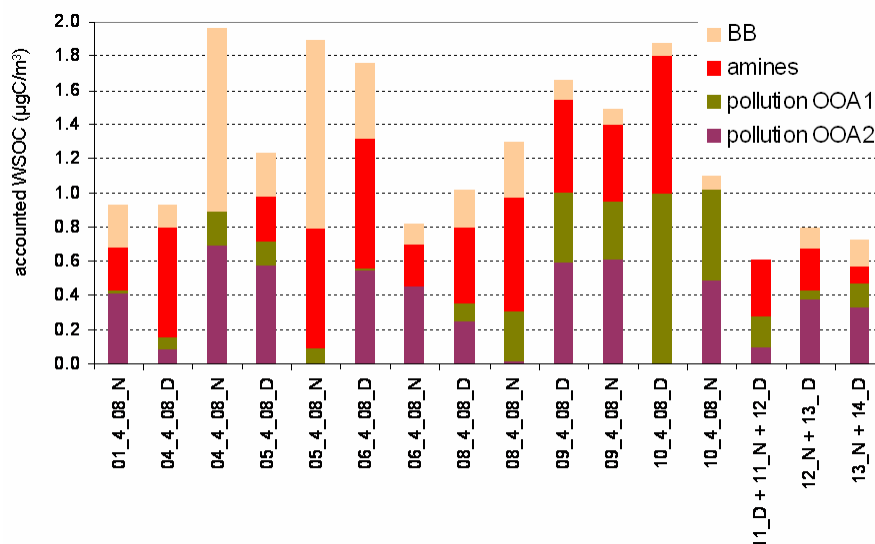


Figure 48. Apportionment of the WSOC based on the four extracted $^1\text{H-NMR}$ factors with PMF. Absolute concentrations ($\mu\text{gC}/\text{m}^3$).

In summary, significant differences in the overall spectral signature of TMB-SOA with respect to those of the factors extracted from ambient OOA strongly suggest that a single hydrocarbon precursor could be not sufficient to reproduce the complex chemistry of real environments.

3.3.6 Chemical classes of WSOCs

Water extracts of both laboratory-generated and selected ambient aerosol samples underwent to fractionation by an anion exchange chromatographic method which allowed to quantitatively resolve WSOC into few chemical classes according to their neutral/acidic nature. The employed HPLC method, already described in details in the experimental section, allowed to separate: basic/neutral compounds (N), mono-acidic compounds (MA), di-acidic compounds (DA) and poly-acidic compounds (PA), i.e. compounds bearing more than two carboxylic functionalities (fig. 49).

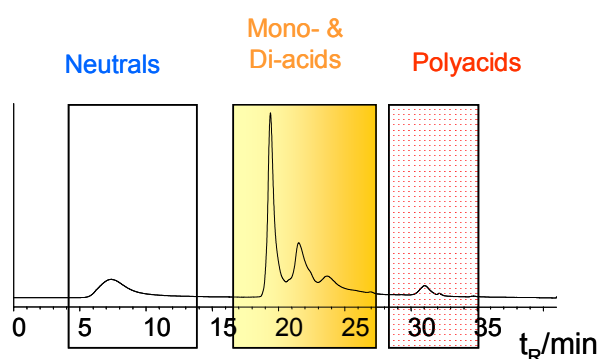


Figure 49. HPLC chromatogram resulting from the WSOC fractionation of a samples of MT-SOA as example.

In the following histogram, the relative abundances (%) of the chemical classes with respect to total fractionated WSOC are summarized two laboratory and two field sample sets (fig. 50).

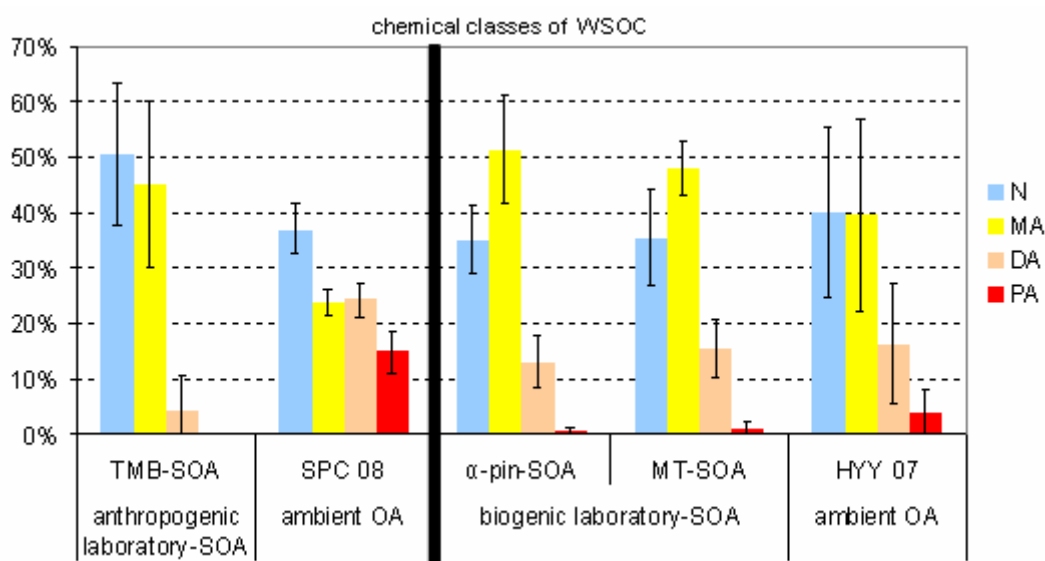


Figure 50. Chemical compositions, in terms of acidity classes, of water-soluble organics extracted from laboratory-generated SOA and selected ambient organic aerosols. The vertical black bar in the middle of the diagram separate anthropogenic from biogenic samples. N= neutral compounds, MA= mono-acids, DA= di-acids and PA= poly-acids. Bars represent the variability among the samples.

The laboratory-generated SOA, both anthropogenic (TMB-SOA) as well biogenic (α -pin-SOA and MT-SOA), are mainly composed by neutral and mono-acidic species, with di-acids contributing in much lesser extent, particularly in the TMB-SOA case. The latter were also characterized by very high concentrations of acetate as detected by NMR analyses. Thus TMB-SOA were actually constituted by neutral compounds (about 43%) and mono-acids (about 42%) which included about 4% of acetate as determined from NMR spectra.

The chemical class distributions in SOA generated by α -pinene as single VOC precursor or by mixtures of terpenes resulted very similar, confirming the findings of the NMR analyses, i.e. that spectral features varied mostly according to the chemical ageing of the particles over the course of each experiment, and to a lesser extent depending on the different biogenic VOCs mixtures employed.

If the overall chemical composition of WSOC of pristine boreal forest samples (HYY 07) resulted partly reproduced by those of biogenic laboratory SOA, fewer common features emerged from the comparison between the composition of polluted continental OA (SPC 08) and TMB-SOA. Compounds carrying more than two acidic (carboxylic) groups (PA) were generally found very close or below to the limit of detection in laboratory-SOA while they contributed in much more extent to the chemical composition of polluted continental samples. On the basis of their retention coefficient, PA correspond to atmospheric humic-like substances (HULIS). Since the presence of these high molecular weight compounds has been associated to biomass burning emissions in many studies, their occurrence in the HPLC composition of the analyzed ambient samples even suggests that residential burning for domestic heating and combustion of agricultural wastes impacted significantly the organic composition of the European background aerosols. This is also supported by the measurements of the levoglucosan concentrations as obtained by NMR spectroscopy.

A fraction between 15 and 30% of WSOC was unaccounted for by the employed HPLC method and that, among all analyzed samples, laboratory TMB-SOA samples showed the lowest recoveries. Unaccounted compounds include substances irreversibly absorbed to the stationary phase, possibly polymeric. The occurrence of polymeric material has been already observed in SOA generated by aromatic compounds such as trimethylbenzene (Karlberer et al., 2004). Furthermore measurements performed on TMB-SOA by laser desorption ionization-mass spectrometry (LDI-MS) have shown that a substantial fraction of TMB-SOA mass is composed of polymers. In that study an acetal polymerization mechanism with methylglyoxal as the main monomer unit has been proposed to explain the formation of these high molecular mass compounds in the particle phase.

As already described in the section about TMB-SOA, the NMR spectral profiles could be explained by the molecular structure of the suggested polymeric substances. The HPLC composition of TMB-

SOA, showing the predominance of compounds with neutral features, is as well in agreement with the assumed occurrence of such substances. Hence the low HPLC recovery observed in TMB-SOA could be interpreted as caused by such high molecular weight compounds trapped throughout the column by hydrophobic interactions.

4 Conclusions

The main objective of this thesis was the chemical characterization of synthetic secondary organic aerosol (SOA) produced from atmospherically relevant anthropogenic and biogenic VOCs during reaction chamber experiments. In parallel, the resulting chemical features of these laboratory-SOA were used to interpret the composition of ambient samples of atmospheric fine particulate matter collected at several sites in Europe, in order to determine the fraction of ambient aerosol organic mass accounted for by biogenic and anthropogenic SOA.

4.1 Terrestrial biogenic SOA

Biogenic SOA characterized in this thesis were generated from various mixtures of terpenes representative for VOCs emitted by conifer tree species, including α/β -pinene, limonene, Δ^3 -carene, ocimene, β -caryophyllene and α -farnesene. These samples showed similar chemical composition in terms of ^1H -NMR functional groups and HPLC fractions.

Results indicate that biogenic SOA are mainly formed by polar (water-soluble) organic compounds, mostly neutral or carrying one acidic group, although dicarboxylic acids can also contribute to a lesser extent. The overall chemical composition of WSOC, in terms of chemical classes, of ambient samples collected in pristine forested environments resulted reproduced by biogenic laboratory SOA.

The functional groups distribution of biogenic SOA shows a completely aliphatic composition which is consistent with the current knowledge about the terpenes oxidation. Specifically, the spectra of biogenic SOA show sharp peaks from individual compounds, including well-known species such as pinic and pinonic acids, superimposed to a broad background signal attributable to a more complex mixture of degradation products. Results of chamber experiments performed at different ranges of concentrations highlighted that laboratory loadings higher than those representative of the real atmosphere favour the partitioning of less oxidized species which would otherwise remain in gas phase under atmospheric conditions. Under low concentration regimes, the NMR spectra of biogenic SOA showed actually the best fit with those of SOA components isolated from pristine ambient samples.

Moreover, the dependence of SOA composition on ageing processes was also investigated collecting SOA samples in different time intervals during each experiment with the aim to compare

fresh and aged SOA. The NMR spectral features of biogenic SOA resulted to change substantially according to the chemical ageing of the particles over the course of each experiment.

Few ozonolysis experiments were also conducted together with the photo-oxidation ones in order to study the effect of the photochemistry on SOA composition. The SOA samples formed by ozonolysis show a higher proportion of pinic acid and of similar compounds retaining the original structure of α -pinene (two geminal methyls on a substituted cyclobutane ring) with respect to those formed during photo-oxidation experiments.

In summary, all these laboratory experiments provided spectral signatures that were helpful for the interpretation of field data. In fact, the series of NMR spectra recorded for submicron aerosol particles collected in the boreal forest was subjected to multivariate statistical (positive matrix factorization, PMF) and the resulting factors were compared to those obtained for laboratory biogenic SOA. The PMF analysis showed the occurrence of multiple factors, some of which tracing transported aerosols, or particles produced in situ by biogenic sources (amines) other than terpenes, but also one factor whose $^1\text{H-NMR}$ features unambiguously fitted those of aged biogenic SOA obtained in reaction chambers. Such factor accounted for up to 30% of the particle organic matter in the boreal forest during the experiment. Therefore, the contribution of biogenic SOA to total organic particulate matter could be estimated for this environment.

4.2 Anthropogenic SOA

A single aromatic hydrocarbon (1,3,5-trimethylbenzene, TMB), having a high SOA formation yield, was used as model anthropogenic SOA precursor in chamber experiments.

The analyses performed showed that TMB-SOA is mostly composed by water-soluble (polar) compounds but contain also a significant fraction of insoluble carbon, in particular in fresh TMB-SOA samples.

Results from HPLC analysis showed that TMB-SOA is mostly accounted for by neutral and mono-acidic compounds. Polyacids, also called humic-like substances (HULIS), were generally found only in trace amounts in laboratory TMB-SOA despite of their abundance in polluted ambient SOA. The occurrence of HULIS in the HPLC composition of the analyzed ambient samples has been associated to biomass burning emissions on the basis the $^1\text{H-NMR}$ data.

$^1\text{H-NMR}$ spectroscopy was also exploited for the functional group characterization of TMB-SOA. The TMB SOA present a chemical composition prevalently aliphatic, with most of the bands from the alkyl moieties falling in the range of methyls in beta position to oxygen atoms (1.1-1.8 ppm). Compounds known from previous studies that can be responsible for the observed $^1\text{H-NMR}$ spectral

bands of TMB SOA include peroxide bicyclic species and methylglyoxal oligomers. These findings confirmed the major routes of SOA formation from aromatic VOCs suggested recently by models. Contrary to biogenic SOA, the comparison of the spectral features of TMB-SOA with those of polluted ambient samples was inconclusive. In general, the functional group composition of ambient samples showed a larger complexity containing significant amounts of aromatic and hydroxyl units with respect to TMB-SOA, and suggesting a contribution from additional sources of oxidized organic aerosols in polluted areas. The series of NMR spectra obtained from polluted ambient samples were processed using a variety of multivariate statistical techniques and factor analysis (PCA, cluster analysis, PMF, NMF) aiming to identify recurrent spectral profiles to be compared with the reference spectra provided by chamber experiments with TMB and by field observations conducted close to sources. Our findings indicate that biomass burning accounts for a common organic aerosol type in rural continental areas, confirming previous studies which have suggested that this source can contribute up to 30 % (on annual basis) to the organic matter constituting the European aerosol background. The remaining ¹H-NMR factors correspond to spectral types commonly found throughout continental Europe, but that have not been reproduced by any laboratory experiments so far and thus their attribution to anthropogenic or natural sources remains unclear at the moment.

Recent modelling studies indicate that the SOA yield increases substantially in polluted environments when accounting for the oxidation of volatile organic compounds such as evaporated POA (like PAHs and alkanes), beside the simple alkyl-benzenes. This hypothesis awaits confirmation from field measurements, and the analytical techniques employed in this thesis work assisted by laboratory studies can profitably be used for investigating this new research topic.

Bibliography

- Allan, J. D., Alfarra, M. R., Bower, K. N., Williams, P. I., Gallagher, M. W., Jimenez, J. L., McDonald, A. G., Nemitz, E., Canagaratna, M. R., Jayne, J. T., Coe, H., and Worsnop, D. R.: Quantitative sampling using an Aerodyne aerosol mass spectrometer: 2. Measurements of fine particulate chemical composition in two UK cities, *J. Geophys. Res.*, 108, 4091, doi:10.1029/2002JD002359, 2003.
- Andreae, M.O. and Rosenfeld, D.: Aerosol-cloud-precipitation interactions. Part 1 . The nature and sources of cloud-active aerosols, *Earth-Science Reviews*, 2008, 89, 13-41.
- Atkinson, R. and Arey, J.: Gas-phase tropospheric chemistry of biogenic volatile organic compounds: a review, *Atmos. Environ.*, 37, Supplement, 2, S197-S219, 2003.
- Baltensperger, U. et al. Secondary organic aerosols from anthropogenic and biogenic precursors, *Faraday Discuss.*, 130, 265-278, 2005.
- Bloss, C., Wagner, V., Bonzanini, A., Jenkin, M.E., Wirtz, K., Martin-Reiejo, M., Pilling, M.J. Evaluation of detailed aromatic mechanisms (MCMv3 and MCMv3.1) against environmental chamber data. *Atmospheric Chemistry and Physics* 5, 623-639, 2005a.
- Bloss, C., Wagner, V., Jenkin, M.E., Volkamer, R., Bloss, W.J., Lee, J.D., Heard, D.E., Wirtz, K., Martin-Reviejo, M., Rea, G., Wenger, J.C., Pilling, M.J. Development of a detailed chemical mechanism (MCMv3.1) for the atmospheric oxidation of aromatic hydrocarbons. *Atmospheric Chemistry and Physics* 5, 641-644, 2005b.
- Braun S., Kolinowski H.-O. & Berber S. (1998): 150 and more basic NMR experiments. VCH, New York.
- Calvert, J. G. et al. *The Mechanisms of Atmospheric Oxidation of Aromatic Hydrocarbons*, Oxford University Press, New York, 2002.

- Canagaratna, M. R., Jayne, J. T., Jimenez, J. L., Allan, J. D., Alfarra, M. R., Zhang, Q., Onasch, T. B., Drewnick, F., Coe, H., Middlebrook, A., Delia, A., Williams, L. R., Trimborn, A. M., Northway, M. J., DeCarlo, P. F., Kolb, C. E., Davidovits, P., and Worsnop, D. R.: Chemical and microphysical characterization of ambient aerosols with the aerodyne aerosol mass spectrometer, *Mass Spectrom. Rev.*, 26, 185–222, 2007.
- Cao, G. and Jang, M.: Effects of particle acidity and UV light on secondary organic aerosol formation from oxidation of aromatics in the absence of NO_x, *Atmos. Environ.*, 35, 7603–30 7613, 2007.
- Cao, G. and Jang, M.: Secondary organic aerosol formation from toluene photooxidation under various NO_x conditions and particle acidity, *Atmos. Chem. Phys. Discuss.*, 8, 14467–14495, 2008.
- Castro, L. M., Pio, C. A., Harrison, R. M., and Smith, D. J. T.: Carbonaceous aerosol in urban and rural European atmospheres: estimation of secondary organic carbon concentrations, *Atmos. Environ.*, 33, 2771–2781, 1999.
- Cavalli F., Facchini M. C., Decesari S., Emblico L., Mircea M., Jensen N. R. and Fuzzi S. Size-segregated aerosol chemical composition at a boreal site in southern Finland, during the QUEST project. *ATMOSPHERIC CHEMISTRY AND PHYSICS*, 6, 993–1002, 2006.
- Coker III D. R. et al. The effect of water on gas–particle partitioning of secondary organic aerosol: II. m-xylene and 1,3,5-trimethylbenzene photooxidation systems. *Atmospheric Environment* 35 (2001) 6073–6085.
- DeCarlo, P. F., Kimmel, J. R., Trimborn, A., Northway, M. J., Jayne, J. T., Aiken, A. C., Gonin, M., Fuhrer, K., Horvath, T., Docherty, K. S., Worsnop, D. R., and Jimenez, J. L.: Field-deployable, high-resolution, time-of-flight aerosol mass spectrometer, *Anal. Chem.*, 78, 8281–8289, 2006.
- Decesari, S., Facchini, M. C., Matta, E., Lettini, F., Mircea, M., Fuzzi, S., Tagliavini, E., and Putaud, J. P.: Chemical features and seasonal variation of fine aerosol water-soluble organic compounds in the Po Valley, Italy, *Atmos. Environ.*, 35, 3691–3699, 2001.

- Decesari, S., Mircea, M., Cavalli, F., Fuzzi, S., Moretti, F., Tagliavini, E., and Facchini, M. C.: Source attribution of water-soluble organic aerosol by nuclear magnetic resonance spectroscopy, *Environ. Sci. Technol.*, 41, 2479-2484, 2007.
- Derome A.E. (1987): *Modern NMR techniques for chemistry research*. Pergamon, Tarrytown, New York.
- Derwent, R.G., Jenkin, M.E., Passant, N.R., Pilling, M.J., 2007. Reactivity-based strategies for photochemical ozone control in Europe. *Environmental Science and Policy* 10, 445-453.
- Derwent, R.G., Jenkin, M.E., Saunders, S.M., Pilling, M.J., 1998. Photochemical ozone creation potentials for organic compounds in northwest Europe calculated with a master chemical mechanism. *Atmospheric Environment* 32, 2429-2441.
- Docherty, K. S., Stone, E. A., Ulbrich, I. M., DeCarlo, P. F., Snyder, D. C., Schauer, J. J., Peltier, R. E. Weber, R. J., Murphy, S. M., Seinfeld, J. H., Eatough, D. J., Grover, B. D., and Jimenez, J. L.: Apportionment of Primary and Secondary Organic Aerosols in Southern California during the 2005 Study of Organic Aerosols in Riverside (SOAR). *Environ. Sci. Technol.*, 42, 7655–7662, 2008.
- Donahue, N.M., Robinson, A.L., Stanier, C.O., Pandis, S.N., 2006. Coupled partitioning, dilution, and chemical aging of semivolatile organics. *Environmental Science and Technology* 40, 2635-2643.
- Donald, A. G., Nemitz, E., Canagaratna, M. R., Jayne, J. T., Coe, H., and Worsnop, D. R.: Quantitative sampling using an Aerodyne aerosol mass spectrometer: 2. Measurements of fine particulate chemical composition in two UK cities, *J. Geophys. Res.*, 108, 4091, doi:10.1029/2002JD002359, 2003.
- Duplissy, J., Gysel, M., Alfarra, M. R., Dommen, J., Metzger, A., Prevot, A. S. H., Weingartner, E., Laaksonen, A., Raatikainen, T., Good, N., Turner, S. F., McFiggans, G., and Baltensperger, U., Cloud forming potential of secondary organic aerosol under near atmospheric conditions, *Geophys. Res. Lett.*, 35, L03818, doi:10.1029/2007GL031075, 2008.

- Edney, E. O., Kleindienst, T. E., Jaoui, M., Lewandowski, M., Offenberg, J. H., Wang, W., and Claeys, M.: Formation of 2-methyl tetrols and 2-methylglyceric acid in secondary organic aerosol from laboratory irradiated isoprene/NO_x/SO₂/air mixtures and their detection in ambient PM_{2.5} samples collected in the eastern United States, *Atmos. Environ.*, 39, 5281-5289, 2005.
- Facchini M. C., Fuzzi S., Zappoli S., Andracchio A., Gelencser A., Kiss G., Krivacsy Z., Hansonn H.C., Alsberg T. and Zebuhr Y. Partitioning of the organic aerosol component between fog droplets and interstitial air. *JOURNAL OF GEOPHYSICAL RESEARCH-ATMOSPHERES*, 104, D21, 26821-26832.
- Forstner, H.J.L., Flagan, R.C., Seinfeld, J.H. Molecular speciation of secondary organic aerosol from photooxidation of the higher alkenes: 1-octene and 1-decene. *Atmospheric Environment* 31, 1953-1964, 1997b
- Forstner, H.J.L., Flagan, R.C., Seinfeld, J.H. Secondary organic aerosol from the photooxidation of aromatic hydrocarbons: molecular composition. *Environmental Science and Technology* 31, 1345-1358, 1997a.
- Fuzzi S. et al.: Critical assessment of the current state of scientific knowledge, terminology, and research needs concerning the role of organic aerosols in the atmosphere, climate, and global change. *Atmos. Chem. Phys.*, 2006, 6, 2017-2038.
- Fuzzi, S., Decesari, S., Facchini, M. C., Matta, E., Mircea, M., and Tagliavini, E.: A simplified model of the water soluble organic component of atmospheric aerosols, *Geophys. Res. Lett.*, 28, 4079-4082, 2001.
- Gao, S., Keywood, M., Ng, N. L., Surratt, J. D., Varutbangkul, V., Bahreini, R., Flagan, R. C., and Seinfeld, J. H.: Low-molecular-weight and oligomeric components in secondary organic aerosol from the ozonolysis of cycloalkenes and alpha-pinene, *J. Phys. Chem. A*, 108, 10147-10164, 2004a.
- Goldstein, A. H. and Galbally, I. E.: Known and unexplored organic constituents in the earth's atmosphere, *Environ. Sci. Technol.*, 41, 1514-1521, 2007.

- Graber, E. R. and Rudich, Y.: Atmospheric HULIS: How humic-like are they? A comprehensive and critical review, *Atmos. Chem. Phys.*, 6, 729-753, 2006,
- Gross, D. S., Galli, M. E., Kalberer, M., Prevot, A. S. H., Dommen, J., Alfarra, M. R., Duplissy, J., Gaeggeler, K., Gascho, A., Metzger, A., and Baltensperger, U.: Real-time measurement of oligomeric species in secondary organic aerosol with the aerosol time-of-flight mass spectrometer, *Anal. Chem.*, 78, 2130-2137, 2006.
- Hallquist M. et al. The formation, properties and impact of secondary organic aerosol: current and emerging issues. *Atmos. Chem. Phys. Discuss.*, 9, 3555-3762, 2009
- Hamilton, J. F., Webb, P. J., Lewis, A. C., and Reviejo, M. M.: Quantifying small molecules in secondary organic aerosol formed during the photo-oxidation of toluene with hydroxyl radicals, *Atmos. Environ.*, 39, 7263-7275, 2005.
- Havers, N., Burba, P., Lambertm, J., and Klockow, D.: Spectroscopic characterization of humic like substances in airborne particulate matter, *J. Atmos. Chem.*, 29(1), 45-54, 1998.
- Healy R. M. et al. Gas/particle partitioning of carbonyls in the photooxidation of isoprene and 1,3,5-trimethylbenzene. *Atmos. Chem. Phys.*, 8, 3215–3230, 2008.
- Hoffer, A., Kiss, G., Blazso, M., and Gelencser, A.: Chemical characterization of humic-like substances (HULIS) formed from a lignin-type precursor in model cloud water, *Geophys. Res. Lett.*, 31, L06115, doi:10.1029/2003GL018962, 2004.
- Hoffmann, T. and Warnke, J.: Organic Aerosols, in *Volatile Organic Compounds in the Atmosphere*, edited by R. Koppmann, Blackwell Publishing Ltd., Oxford, UK., pp. 342-387, 2007.
- Iinuma, Y., Böge, O., Gnauk, T., and Herrmann, H.: Aerosol-chamber study of the α -pinene/O₃ reaction: Influence of particle acidity on aerosol yields and products, *Atmos. Environ.*, 38, 25 761-773, 2004.

IPCC 2007, Climate Change 2007: The Physical Science Basis, Summary for policy makers.

Jaenicke, R.: Abundance of cellular material and proteins in the atmosphere, *Science*, 2005, 73, 5718.

Jang, M. S., Czoschke, N. M., Lee, S., and Kamens, R. M.: Heterogeneous atmospheric aerosol production by acid-catalyzed particle-phase reactions, *Science*, 298, 814-817, 2002.

Jimenez, J. L., Jayne, J. T., Shi, Q., Kolb, C. E., Worsnop, D. R., Yourshaw, I., Seinfeld, J. H., Flagan, R. C., Zhang, X. F., Smith, K. A., Morris, J. W., and Davidovits, P.: Ambient aerosol sampling using the Aerodyne Aerosol Mass Spectrometer, *J. Geophys. Res.*, 108, 8425, doi:10.1029/2001JD001213, 2003.

Jimenez, J. L. et al. Evolution of organic aerosol in the atmosphere. *Science*, 326, 5959, 1525-1529, 2009.

Johnson, D., Jenkin, M.E., Wirtz, K., Martin-Reviejo, M. Simulating the formation of secondary organic aerosol from the photooxidation of aromatic hydrocarbons. *Environmental Chemistry* 2, 35-48, 2005.

Johnson, D., Jenkin, M.E., Wirtz, K., Martin-Reviejo, M., 2004. Simulating the formation of secondary organic aerosol from the photooxidation of toluene. *Environmental Chemistry* 1, 150-165.

Kalberer, M., Paulsen, D., Sax, M., Steinbacher, M., Dommen, J., Prevot, A. S. H., Fisseha, R., Weingartner, E., Frankevich, V., Zenobi, R., and Baltensperger, U.: Identification of polymers as major components of atmospheric organic aerosols, *Science*, 303, 1659-1662, 2004.

Kanakidou, M. et al.: Organic aerosol and global climate modelling: a review, *Atmos. Chem. Phys.*, 2005, 5, 1053-1123.

- Kiss, G., Tombacz, E., Varga, B., Alsberg, T., and Persson, L.: Estimation of the average molecular weight of humic-like substances isolated from fine atmospheric aerosol, *Atmos. Environ.*, 15 37, 3783-3794, 2003.
- Kleindienst, T. E., Jaoui, M., Lewandowski, M., Offenberg, J. H., Lewis, C. W., Bhave, P. V., and Edney, E. O.: Estimates of the contributions of biogenic and anthropogenic hydrocarbons to secondary organic aerosol at a southeastern US location, *Atmos. Environ.*, 41, 8288-8300, 2007.
- Kroll, J. H. and Seinfeld, J. H.: Chemistry of secondary organic aerosol: Formation and evolution of low-volatility organics in the atmosphere, *Atmos. Environ.*, 42, 3593-3624, 2008.
- Lanz V. A. et al. Source apportionment of submicron organic aerosols at an urban site by factor analytical modelling of aerosol mass spectra, *Atmos. Chem. Phys.*, 7, 1503-1522, 2007,
- Lanz, V. A., Alfarra, M. R., Baltensperger, U., Buchmann, B., Hueglin, C., Szidat, S., Wehrli, M. N., Wacker, L., Weimer, S., Caseiro, A., Puxbaum, H., and Prevot, A. S. H.: Source attribution of submicron organic aerosols during wintertime inversions by advanced factor analysis of aerosol mass spectra, *Environ. Sci. Technol.*, 42, 214-220, 2008.
- Lewis, A. C. et al. A larger pool of ozone-forming carbon compounds in urban atmospheres, *Nature*, 405(6), 778-781, 2000.
- Limbeck, A., Kulmala, M., and Puxbaum, H.: Secondary organic aerosol formation in the atmosphere via heterogeneous reaction of gaseous isoprene on acidic particles, *Geophys. Res. Lett.*, 30, 1996, doi:10.1029/2003GL017738, 2003.
- Mancinelli V., Rinaldi M., Finessi E., Emblico L., Mircea M., Fuzzi S., Facchini M.C. & Decesari S. (2007): An improved anion exchange chromatographic method for water-soluble organic carbon analysis in atmospheric samples. *Journal of Chromatography A*, 1149, 385-389.
- McMurry, P. H.: A review of atmospheric aerosol measurements, *Atmos. Environ.*, 34, 1959- 1999, 2000.

- Metzger, A., Dommen, J., Gaeggeler, K., Duplissy, J., Prevot, A. S. H., Kleffmann, J., Elshorbany, Y., Wisthaler, A., and Baltensperger, U.: Evaluation of 1,3,5 trimethylbenzene degradation in the detailed tropospheric chemistry mechanism, MCMv3.1, using environmental chamber data, *Atmos. Chem. Phys.*, 8, 6453-6468, 2008.
- Molina, M.J., Ivanov, A.V., Trakhtenberg, S., Molina, L.T., 2004. Atmospheric evolution of organic aerosol. *Geophysical Research Letters* 31, L22104.
- Moretti F., Tagliavini E., Decesari S., Facchini M. C., Rinaldi M., Fuzzi, S. NMR determination of total carbonyls and carboxyls: A tool for tracing the evolution of atmospheric oxidized organic aerosols. *ENVIRONMENTAL SCIENCE & TECHNOLOGY*, 42, 13, 4844-4849, 2008.
- Murphy, D. M., Cziczo, D. J., Hudson, P. K., and Thomson, D. S.: Carbonaceous material in aerosol particles in the lower stratosphere and tropopause region, *J. Geophys. Res.*, 112, D04203, doi:10.1029/2006JD007297, 2007.
- Ng, N. L., Kroll, J. H., Chan, A. W. H., Chhabra, P. S., Flagan, R. C., and Seinfeld, J. H.: Secondary organic aerosol formation from m-xylene, toluene, and benzene, *Atmos. Chem. Phys.*, 7, 3909-3922, 2007a, <http://www.atmos-chem-phys.net/7/3909/2007/>.
- O'Dowd C.D., Facchini M.C., Cavalli F., Ceburnis D., Mircea M., Decesari S., Fuzzi S., Yoon Y.J. & Putaud J.-P. (2004): Biogenically driven organic contribution to marine aerosol. *Nature*, 431, 676– 680.
- Pankow, J. F. An absorption model of the gas/aerosol partitioning involved in the formation of secondary organic aerosol, *Atmos. Environ.*, 28, 185-188, 1994a.
- Pankow, J.F. An absorption-model of gas-particle partitioning of organic compounds in the atmosphere. *Atmospheric Environment* 28, 185-188,1994a.
- Pankow, J.F. An absorption-model of the gas aerosol partitioning involved in the formation of secondary organic aerosol. *Atmospheric Environment* 28, 189-193, 1994b.

- Pankow, J.F. An absorption-model of the gas aerosol partitioning involved in the formation of secondary organic aerosol. *Atmospheric Environment* 28, 189-193, 1994b
- Pathak, R.K., Stanier, C.O., Donahue, N.M., Pandis, S.N., 2007. Ozonolysis of α -pinene at atmospherically relevant concentrations: temperature dependence of aerosol mass fractions (yields). *Journal of Geophysical Research-Atmospheres* 112, D03201.
- Paulsen, D., Dommen, J., Kalberer, M., Prevot, A. S. H., Richter, R., Sax, M., Steinbacher, M., Weingartner, E., and Baltensperger, U.: Secondary organic aerosol formation by irradiation of 1,3,5-trimethylbenzene-NO_x-H₂O in a new reaction chamber for atmospheric chemistry and physics, *Environ. Sci. Technol.*, 39, 2668–2678, 2005.
- Poschl, U.: Atmospheric aerosols: composition, transformation, climate and health effects, *Angew. Chem. Int. Ed.*, 44, 7520-7540, 2005.
- Presto, A.A., Donahue, N.M., 2006. Investigation of α -pinene+ ozone secondary organic aerosol formation at low total aerosol mass. *Environmental Science and Technology* 40, 3536-3543.
- Putaud J.P. et al.: A European aerosol phenomenology-2: chemical characteristics of particulate matter at kerbside, urban, rural and background sites in Europe, *Atmos. Environ.*, 2004, 38, 2579-2595.
- Puxbaum et al. Levoglucosan levels at background sites in Europe for assessing the impact of biomass combustion on the European aerosol background. *JOURNAL OF GEOPHYSICAL RESEARCH-ATMOSPHERES*, 112, D23, 2007.
- Raatikainen et al. Physicochemical properties and origin of organic groups detected in boreal forest using an aerosol mass spectrometer. *Atmos. Chem. Phys. Discuss.*, 9, 21847–21889, 2009.
- Ravishankara A.R. Chemistry-climate coupling: the importance of chemistry in climate issues. *Faraday Discuss.*, 130, 9-26, 2005. DOI: 10.1039/b509603k.

- Reinhardt, A., Emmenegger, C., Gerrits, B., Panse, C., Dommen, J., Baltensperger, U., Zenobi, R., and Kalberer, M.: Ultrahigh mass resolution and accurate mass measurements as a tool to characterize oligomers in secondary organic aerosols, *Anal. Chem.*, **79**, 4074- 4082, 2007
- Rickard, A.R., et al., Gas phase precursors to anthropogenic secondary organic aerosol: Using the Master Chemical Mechanism to probe detailed observations of 1,3,5-trimethylbenzene photo-oxidation, *Atmospheric Environment* (2009), doi:10.1016/j.atmosenv.2009.09.043
- Rinaldi, M; Emblico, L.; Decesari, S.; Fuzzi, S.; Facchini, M. C.; Librando, V.: Chemical characterization and source apportionment of size-segregated aerosol collected at an urban site in Sicily, *Water Air Soil Pollut.*, 2007, **185**, 311-321. DOI 10.1007/s11270-007-9455-4.
- Robinson, A.L., Donahue, N.M., Shrivastava, M.K., Weitkamp, E.A., Sage, A.M., Grieshop, A.P., Lane, T.E., Pierce, J.R., Pandis, S.N., 2007. Rethinking organic aerosols: semivolatile emissions and photochemical aging. *Science* **315**, 1259-1262.
- Rudich, Y., Donahue, N. M. and Mentel, Th. F.: Aging of organic aerosol: Bridging the gap between laboratory and field studies, *Ann. Rev. Phys. Chem.*, **58**, 321-352, 2007.
- Sax, M., Zenobi, R., Baltensperger, U., Kalberer, M., 2005. Time resolved infrared spectroscopic analysis of aerosol formed by photo-oxidation of 1,3,5-trimethylbenzene and a-pinene. *Aerosol Science and Technology* **39**, 822-830.
- Schauer, J. J., Rogge, W. F., Hildemann, L. M., Mazurek, M. A., and Cass, G. R.: Source apportionment of airborne particulate matter using organic compounds as tracers, *Atmos. Environ.*, **30**, 3837–3855, 1996.
- Seinfeld, J. H. and Pankow, J. F.: Organic atmospheric particulate material, *Annu. Rev. Phys. Chem.*, **54**, 121-140, 2003.
- Seinfeld, J. H.; and Pandis, S. N.: *Atmospheric chemistry and physics-from air pollution to climate change*. New York, Wiley Interscience, 1998.

- Song, C., Zaveri, R. A., Alexander, M. L., Thornton, J. A., Madronich, S., Ortega, J. V. Zelenyuk, A., Yu, X. Y. Laskin, A., and Maughan, D. A.: Effect of hydrophobic primary organic aerosols on secondary organic aerosol formation from ozonolysis of α -pinene, *Geophys. Res. Lett.*, 34, L20803, doi:10.1029/2007GL030720, 2007.
- Sullivan, A. P., Weber, R. J., Clements, A. L., Turner, J. R., Bae, M. S., and Schauer, J. J.: A method for on-line measurement of water-soluble organic carbon in ambient aerosol particles: Results from an urban site, *Geophys. Res. Lett.*, 31, L13105, doi:10.1029/2004GL019681, 2004.
- Surratt, J. D., Murphy, S. M., Kroll, J. H., Ng, N. L., Hildebrandt, L., Sorooshian, A., Szmigielski, R., Vermeylen, R., Maenhaut, W., Claeys, M., Flagan, R. C., and Seinfeld, J. H.: Chemical composition of secondary organic aerosol formed from the photooxidation of isoprene, *J. Phys. Chem. A*, 110, 9665-9690, 2006.
- Szidat, S., Jenk, T. M., Synal, H.-A., Kalberer, M., Wacker, L., Hajdas, I., Kasper-Giebl, A., and Baltensperger, U.: Contributions of fossil fuel, biomass burning, and biogenic emissions to carbonaceous aerosols in Zurich as traced by ^{14}C , *J. Geophys. Res.*, 111, D07206, doi:10.1029/2005JD006590, 2006.
- Tagliavini, E., Moretti, F., Decesari, S., Facchini, M. C., Fuzzi, S., and Maenhaut, W.: Functional group analysis by ^1H NMR/chemical derivatization for the characterization of organic aerosol from the SMOCC field campaign, *Atmos. Chem. Phys.*, 6, 1003-1019, 2006, <http://www.atmos-chem-phys.net/6/1003/2006/>
- Tolocka, M. P., Jang, M., Ginter, J. M., Cox, F. J., Kamens, R. M., and Johnston, M. V.: Formation of oligomers in secondary organic aerosol, *Environ. Sci. Technol.*, 38, 1428-1434, 2004.
- Turpin, B. J. and Huntzicker, J. J.: Identification of secondary organic aerosol episodes and quantitation of primary and secondary organic aerosol concentrations during SCAQS, *Atmos. Environ.*, 29, 3527-3544. 1995.
- Ulbrich, I. M., Canagaratna, M. R., Zhang, Q., Worsnop, D. R., and Jimenez, J. L.: Interpretation of organic components from positive matrix factorization of aerosol mass spectrometric data,

Atmos. Chem. Phys. Discuss., 8, 6729–6791, 2008, <http://www.atmos-chem-phys-discuss.net/8/6729/2008/>.

Van Dingenen et al. A European aerosol phenomenology-1: physical characteristics of particulate matter at kerbside, urban, rural and background sites in Europe. *ATMOSPHERIC ENVIRONMENT*, 38, 16, 2561-2577, 2004.

Zappoli, S. et al.: Inorganic, organic and macromolecular components of fine aerosol in different areas of Europe in relation to their water solubility, *Atmos. Environ.*, 1999, 33, 2733-2743.

Zhang, Q., Alfarra, M. R., Worsnop, D. R., Allan, J. D., Coe, H., Canagaratna, M. R., and Jimenez, J. L.: Deconvolution and quantification of hydrocarbon-like and oxygenated organic aerosols based on aerosol mass spectrometry, *Environ. Sci. Technol.*, 39, 4938-4952, 2005a.

Zhang, Q., Worsnop, D. R., Canagaratna, M. R., and Jimenez, J. L.: Hydrocarbon-like and oxygenated organic aerosols in Pittsburgh: insights into sources and processes of organic aerosols, *Atmos. Chem. Phys.*, 5, 3289-3311, 2005b <http://www.atmos-chem-phys.net/5/3289/2005/>.

List of frequently used abbreviations

AMS = Aerosol Mass Spectrometer
BB = Biomass Burning
CBW = Cabauw
CCN = Cloud Condensation Nuclei
CPC = Condensation Particle Counter
 D_p = Particle diameter
DEA⁺ = Diethylammonium
DMA⁺ = Dimethylammonium
DMPS = Differential Mobility Particle Sizer
EC = Elemental Carbon
HYY = Hyytiälä
KPO = K-Pusztá
MBL = Marine Boundary Layer
MHD = Mace Head
MPZ = Melpitz
MSA = MethaneSulfonic Acid
MT = monoterpenes
NMF = Non-negative Matrix Factorization
PCA = Principal Component Analysis
PMF = Positive Matrix Factorization
POA = Primary Organic Aerosol
SMPS = Scanning Mobility Particle Sizer
SOA = Secondary Organic Aerosol
SPC = San Pietro Capofiume
SQT = sesquiterpenes
TC = Total Carbon
TOC = Total Organic Carbon
TMB = Trimethylbenzene
VOC = Volatile Organic Compound
WIOC = Water Insoluble Organic Carbon
WIOM = Water Insoluble Organic Matter (= WIOC * 1.4)

WSOC = Water Soluble Organic Carbon

WSOM = Water Soluble Organic Matter (= WSOC * 1.8)

WSON = Water Soluble Organic Nitrogen